Pb-Pb ZIRCON DATING BY DIRECT EVAPORATION:

METHOD DEVELOPMENT AND SELECTED GEOLOGICAL APPLICATIONS.

by

EDNA LYDIA MUELLER, B. Sc. (Hon.)

A Thesis

Submitted to the School of Graduate Studies

in Partial Fulfilment of the Requirements

for the Degree

Master of Science

McMaster University

September, 1991

MASTER OF SCIENCE (1991)   McMASTER UNIVERSITY
(Geology)   Hamilton, Ontario

TITLE: Pb-Pb Zircon Dating by Direct

        Evaporation: Method Developement and

        Selected Geological Applications.

AUTHOR: EDNA LYDIA MUELLER

        B. Sc. Honours (University of Toronto)

SUPERVISORS: Dr. A. P. Dickin

        Dr. R. H. McNutt

NUMBER OF PAGES: xii, 158

Abstract

The zircon evaporation method requires no chemical treatment of the zircon grain in the form of acid dissolution or isotopic spiking. In a test of this method, the derived Pb-Pb age is consistent with conventional U-Pb age of zircons from the Battersea Pluton.

Zircons from the Britt Domain reveal a variety of ages from a complete isotopic resetting to the time of the Grenville orogeny (approx. 1100 Ma) to ages of plutons at approx. 1330 Ma and 1450 Ma. An orthoquartzite, CBQ, contained zircons from a Penokean aged terrain and an Archean aged terrain. This may be evidence for a collision of a Penokean aged island arc onto the Superior Province. The age of the Pine Cove Pluton constrains minimum age of the Penokean suture. Its minimum age of approx. 1330 Ma constrains the time of last movement of the French River suture line.

Zircons from the Cedar Lake and Lac Seul gneiss from the Winnipeg River Belt of the Superior Province show evidence of the last major metamorphic event, the Kenoran orogeny at 2700 Ma, and its age of crystallization at 3170 Ma. One zircon from the Cedar Lake tonalite results an age of 3391±2 Ma. This may be a xenocryst from older crust mixed into the tonalite.

The zircon evaporation technique is ideal for reconnaissance work due to the ease of sample preparation and the large number of zircons that can be tested quickly.

ACKNOWLEDGEMENTS

TABLE OF CONTENTS

LIST OF FIGURES

LIST OF TABLES

LIST OF PLATES

CHAPTER 1

THE ZIRCON EVAPORATION METHOD

Zircon geochronology has undergone rapid evolution over the last ten years, to the point where U-Pb dating is only considered reliable when applied to very small populations of abraded grains using ultra-low blank chemistry with a ^{205}Pb spike (Parrish, 1990).

This procedure is very labour intensive and therefore not well suited to reconnaisance studies of sediments with mixed provenance or in polymetamophic rocks, where the analysis of several single zircons is needed to get an adequate picture of the geological history of the sample.

In this situation a more rapid reconnaisance method of zircon dating would have particular advantages in supplementing Sm/Nd geochronology. Such a method is provided by direct Pb evaporation of the zircon grain.

1.1 Previous Work

The zircon crystal ($ZrSiO_4$) acts as a natural Pb emitter at high temperatures (Chukhonin, 1979). Nonetheless, the zircon evaporation technique described in this study was only a recently developed method.

Roubault *et al.* (1967) studied single zircons mounted upon a flat filament. The zircons were attached to the filament by H_3PO_4 and attacked by HF. This made the zircon a spongy mass and allowed the Pb to escape the crystal more easily. Gentry *et al.* (1982) introduced the concept of a trough-shaped filament in which the zircon was wrapped.

Kober (1987) improved the efficiency of the method by introducing a multiple filament, two-step method, by which Pb from the zircon is deposited onto another filament for subsequent thermal ionization. The double filament method is more efficient and provides a more stable ion beam than a single filament. The chemical treatment of the zircon grain is limited to washings with distilled water.

In comparison to conventional U-Pb dating of zircons, the evaporation method needs none of the clean lab chemistry, strong acid dissolution of the zircon or isotopic spiking ususally employed.

1.2 The U-Pb Dating Method

Zircon does not readily incorporate Pb into its lattice during crystallization. Usually the only Pb present is due to Pb found in inclusions during formation and Pb from the decay of U and Th. The only stable, non-radiogenic isotope of Pb is ^{204}Pb. Thus, the Pb ratios with respect to ^{204}Pb are a good indicator of the Pb (a.k.a. common Pb) included during

crystallization. The presence of common Pb makes the zircon appear older than it actually is. From the decay law, the age can be calculated by:

$$t_{^{207}Pb/^{235}U} = \frac{1}{\lambda_{235}}\ln\left(\frac{^{207}Pb}{^{235}U}+1\right) \tag{1}$$

and

$$t_{^{206}Pb/^{238}U} = \frac{1}{\lambda_{238}}\ln\left(\frac{^{206}Pb}{^{238}U}+1\right) \tag{2}$$

where [207]Pb and [206]Pb have been corrected for common Pb at the time of crystallization. The ages are calculated using the decay constants of $\lambda_{238}=1.55125\times10^{-10}$ a^{-1} and $\lambda_{235}=9.8485\times10^{-10}$ a^{-1}. The locus of points $(^{207}Pb/^{238}U, ^{206}Pb/^{235}U)$, calucated from equations (1) and (2) for various ages (t), define a line known as concordia (solid line) (Figure 1.1). Samples that define a closed system (i.e. no loss or gain of U or Pb) would lie on this line since their ages, $t_{^{207}Pb/^{238}U}$ and $t_{^{206}Pb/^{235}U}$, would be equal. Zircons that are found to be almost concordant are those that are non-magnetic, abraded (Krogh, 1982 and Krogh, 1982) and are of magmatic origin rather than metamorphic. In thin section, magmatic zircons can be recognized by their euhedral shape and internal euhedral zoning. Metamorphic zircons tend to be rounded or irregularly-shaped and may contain an older core (Parrish and Roddick, 1985) (Figure 1.2). Most zircons, magmatic or metamorphic, do suffer from a certain degree of episodic or continual Pb loss. Pb is not

4

Figure 1.1 Concordia diagram for U-Pb dating. Concordia is shown as a solid line, discordia as a long dashed line, and "apparent ages" as short dashed lines.

$t_{207Pb/206Pb} = t_c$

concordia

t_c

$t_m < t_{207Pb/206Pb} < t_c$

t_c

discordia

$t_{207Pb/206Pb} = t_m$

isochron

t_m

$^{207}Pb/^{238}U$

$^{206}Pb/^{235}U$
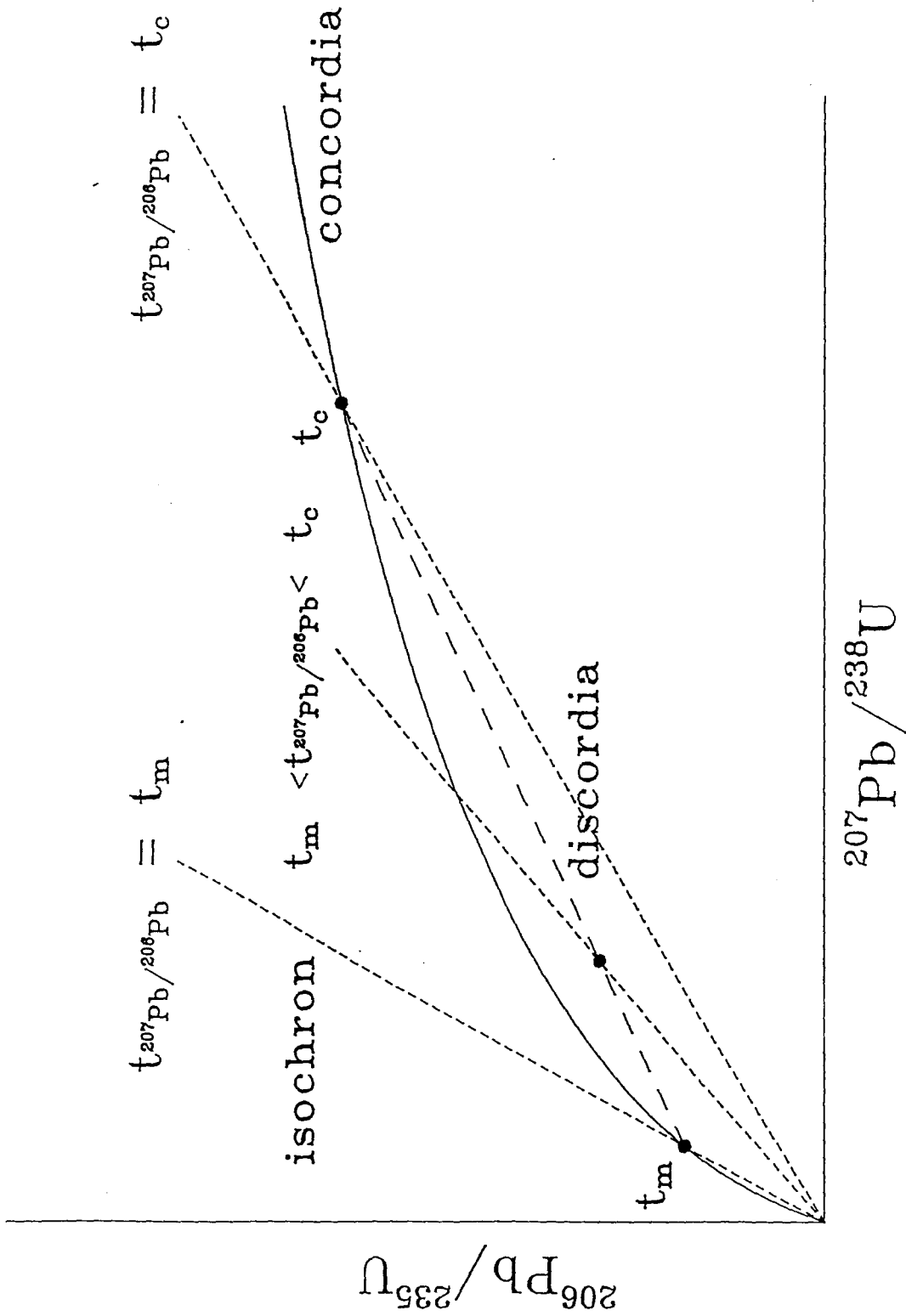
Figure 1.2 Internal structure of a) Magmatic zircons and b) Metamorphic zircons.

Magmatic Rims
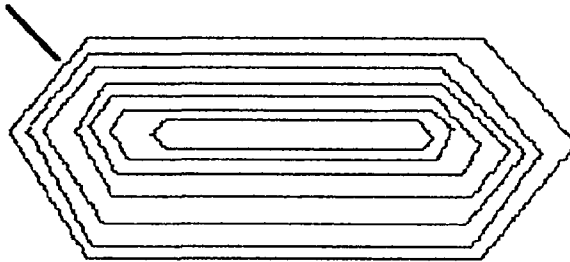
Older Core
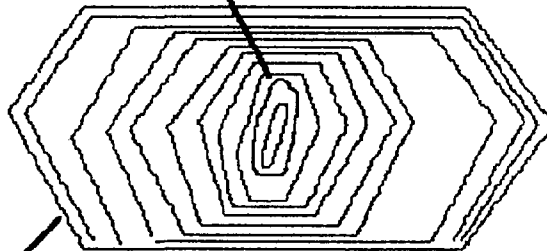
Metamorphic Rims

tightly bound in the crystal lattice, as opposed to U and Th. Thus, Pb may be free to diffuse out of the crystal. Techniques such as air abrasion are used to remove outer layers of the zircon where such diffusion occurs.

Zircons that have undergone a polymetamorphic history contain growths from the time of crystallization (t_c) and the time of metamorphism (t_m). The locus of points from these zircons lie on a mixing line between the concordant ages of t_c and t_m is known as the discordia (long dashes) (Figure 1.1). If there has been more than one time of metamorphism, there will be more than one discordia. The discordia represents an open system, but only between t_c and t_m. The position of the zircon on this discordia is dependent upon the relative amounts of mixing of U and Pb between the two endpoints. Samples that lie on the discordia can be extrapolated to an upper and lower intercept ages of t_c and t_m, respectively, on the concordia. Zircons that have had continuous Pb loss, also an open system, will have a lower intercept with a meaningless age near the origin of the graph (i.e. t≈0 Ma). Thus, U-Pb dating will result in an age for each event as well as the relative mixing between these points.

1.3 The Pb-Pb Dating Method

The method of direct Pb-Pb dating (no analyses of U are taken) loses one degree of freedom with respect to U-Pb

dating. The derived ages from the equation:

$$\frac{^{207}Pb}{^{206}Pb} = \left(\frac{^{235}U}{^{238}U}\right)_{t_o} \left(\frac{e^{\lambda_{235}t}-1}{e^{\lambda_{238}t}-1}\right) \qquad (3)$$

(where t_0 is the present day U ratio equal to 137.88^{-1}) are known as "apparent ages". For magmatic zircons the $t_{207Pb/206Pb}$ isochron (short dashes) (Figure 1.1) only coincides with concordant ages when there has been no Pb loss. Metamorphic zircons, however, have a spread of $t_{207Pb/206Pb}$ "apparent ages" from t_c to t_m. Each zircon in the rock will be affected by the metamorphism, but each to a different degree. Some zircons will have old cores surrounded by younger rims. Some zircons may have been completely formed at the time of metamorphism. Others will have little or no younger rims due to sparse growth or the younger rims were abraded off during crushing. Thus, by sampling a variety of zircons from the same rock, a distribution of ages will be derived with the age extrema ranging from t_c and t_m.

An assumption that is made is that the Pb evaporated from the zircon is an accurate reflection of the internal mixing of two concordant phases. Many authors (Kober, 1986, Kober, 1987, and Kröner *et al.*, 1989) believe that the different phases of the metamorphic zircon have different activation energies. It is argued that the Pb with the highest activation energies resides in the part of the zircon crystal that is undamaged and inferred to be concordant. Thus, the Pb will be released from older parts of the zircon with

progressively higher evaporating temperatures. This temperature range is found to be restricted to 1600 to 1650 K (Kober, 1987). This method is analogous to the step heating of biotite, feldspar and hornblende minerals for $^{40}Ar/^{39}Ar$ dating. Recent scanning electron microscope pictures of heated zircons (O'Hanley *et al.*, 1991) reveal that the Pb, along with Si, is released first from the rim and then gradually towards its centre. The manner of release does not appear to coincide with the internal structure of the zircon. Thus, the apparent lack of zones with higher activation energies would make it difficult to sample specific parts of the zircon.

In this study the temperature of evaporation could not be accurately controlled and repeated evaporations of the same zircon were not successful. Thus, temperatures were inferred to be high enough that the Pb from all phases of the zircon were evaporated at once and mixed as a deposit on the 'cold' filament.

Chapter 2

2.1   The Zircon Evaporation Technique

2.1.1   Sample Preparation

The samples studied in this work were received in different states of preparation from chip size to grain size crushed rock.   Rock sample sizes ranged from 1 to 3 kg.   The process by which the zircons were separated from the rest of the rock is illustrated in Figure 2.1.   Chip sizes were approximately 0.3 cm^3.   The chips were sieved to remove any zircon cross sample contamination due to the crushing process. Only chips larger than 24 mesh were further crushed.   The chips were crushed using a ring mill to obtain a grain size between 24 and 100 mesh.

The following steps were conducted to separate the heavier zircon grains from the remainder of the rock.   A shaking table removed the bulk of the lighter part of the rock.   The amount of shaking and flow of water was adjusted to collect the heavier minerals such as biotite, amphibole and magnetite.   The light fraction was passed at least twice through the shaking process to ensure that as much as possible of the heavy minerals were separated.   The remaining lighter minerals consisted mainly of quartz and feldspar.

The heavy liquid sodium polytungstate was used in the

Figure 2.1 Flowchart of sample preparation from whole rock to zircon grains.

Whole Rock

↓ jaw crusher

Chips

↓   ↓ ring mill

24<grains<100 mesh   grains>100 mesh

↓   ↓ shaking table

Light   Heavy

↓   ↓ heavy liquid

Light   Heavy

↓   ↓ magnetic separator

Magnetic   Non-magnetic

↓ hand picking

Zircon grains
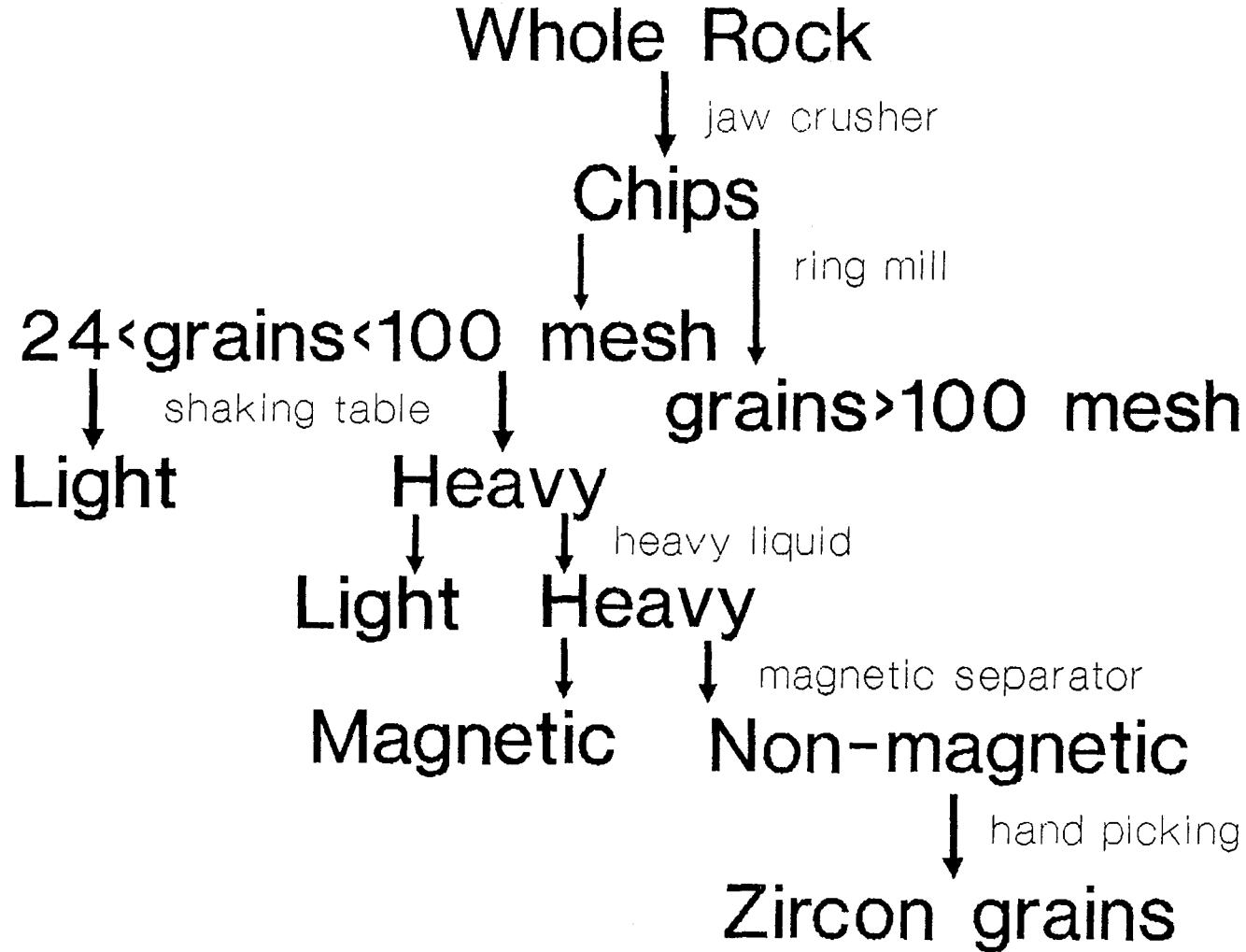
final heavy mineral separation step. Approximately 50 ml of crushed rock was added to 150 to 200 ml of heavy liquid in a 250 ml separatory flask. The density of the liquid could be adjusted up to 3.1 g/cm^3. This step was mainly used to remove any surplus quartz (specific gravity approximately 2.65 g/cm^3). The exact density of the heavy liquid was not critical, but was maintained at about 2.9 to 3.1 g/cm^3. The heavy mineral fraction was bled off and repeatedly washed in distilled water to remove any traces of the heavy liquid, then allowed to dry in air.

The remaining sample was put through a Franz magnetic separator. Progressive steps of magnetic current of 0, 0.2, 0.4, 0.8, 1.7 Amps were used to acquire the non-magnetic fraction. A stepwise increase is required to prevent the separator from being clogged with magnetic grains. The slope and side tilt were 25 and 15 degrees, respectively.

Finally, the zircons were hand-picked under a microscope. A pin and magnet were used to pick zircons that were nonmagnetic. It has been found by Krogh (1982) that discordant grains tend to be magnetic due to alteration which introduces hematite into the zircon's fractures. Grains that appeared inclusion free and the least fractured were chosen, if possible.

2.1.2 Filament Preparation

The beads used were standard filament beads used for Sm-Nd or Rb-Sr work. The filament, however, was wider (.05"x.001") than the standard filament. The wider rhenium was needed to securely wrap around the zircon grain. The rhenium was zone refined so that no Pb was present. This has been demonstrated by blank runs.

The preparation of the beads was a two-step process. First, the filament was welded to one pair of the two side posts. This filament would hold the zircon grain. The filament must be bent into a trough-like form. This was achieved by scoring the length of the filament down its centre with a pair of tweezers. Thus, when the filament was bent into shape it would tend to bend along the crease and into a symmetrical trough (Plate 2.1). An opening was left so that the zircon could be placed inside. Early tests used epoxy or water in the trough so that the zircon would stick to the filament and not be dislodged when the opening was closed. Epoxy could cause Pb contamination so its use was discontinued. All zircons analyzed in this study were mounted dry. The trough was squeezed closed along the length of the filament. Care must be taken to avoid crushing the zircon.

The final step was the addition of the second filament onto the centre pair of posts (Figure 2.2 A and B). This filament would have the Pb evaporated onto it from the side

13

Plate 2.1 The doulbe filament design. A) shows the trough-shaped side filament used to hold the zircon, and B) the finished bead with a centre flat filament used to catch the Pb deposit.

14
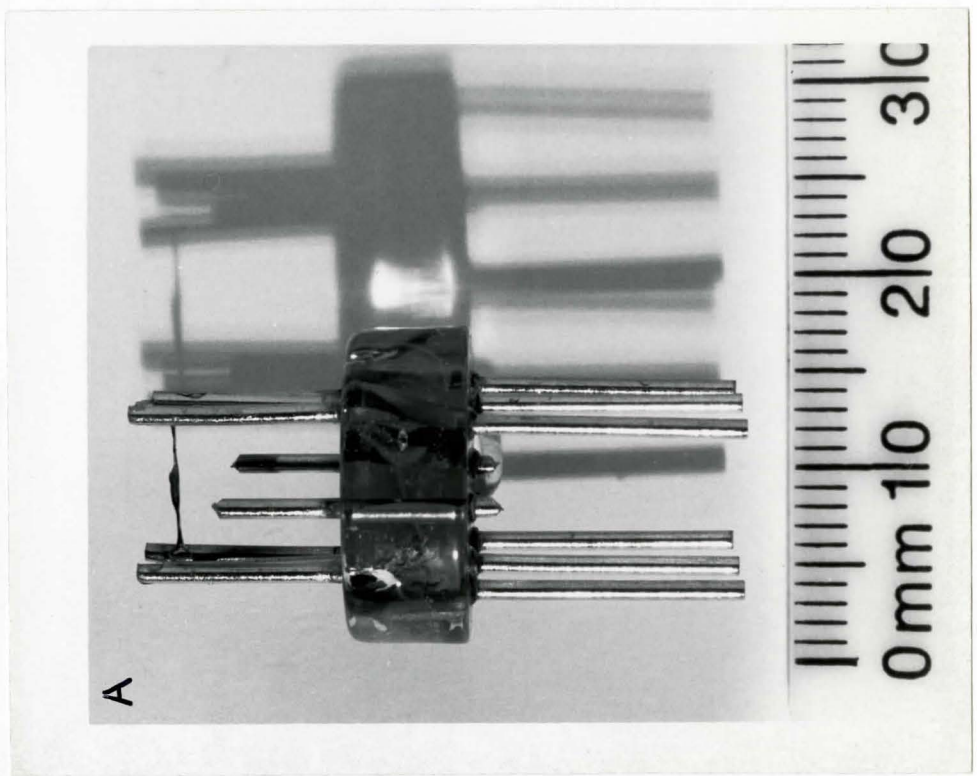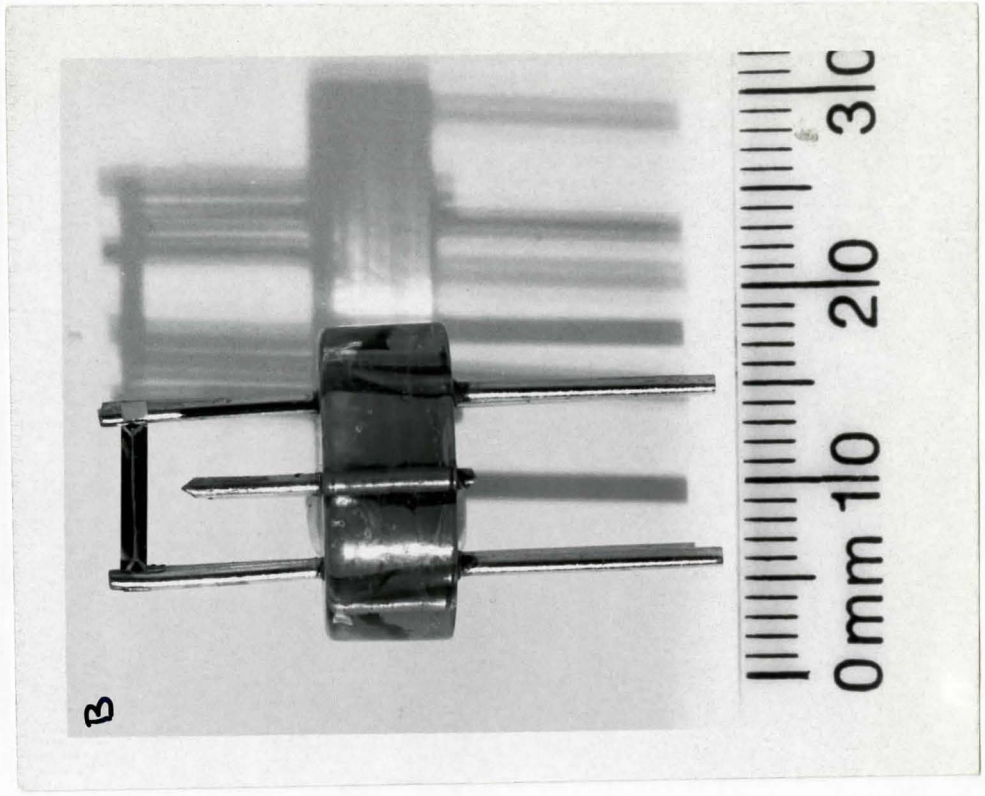
Figure 2.2 Orientation of the side and centre filaments of the bead in A) side view, and B) plan view.

a)

b)

0.5-1mm

10 mm
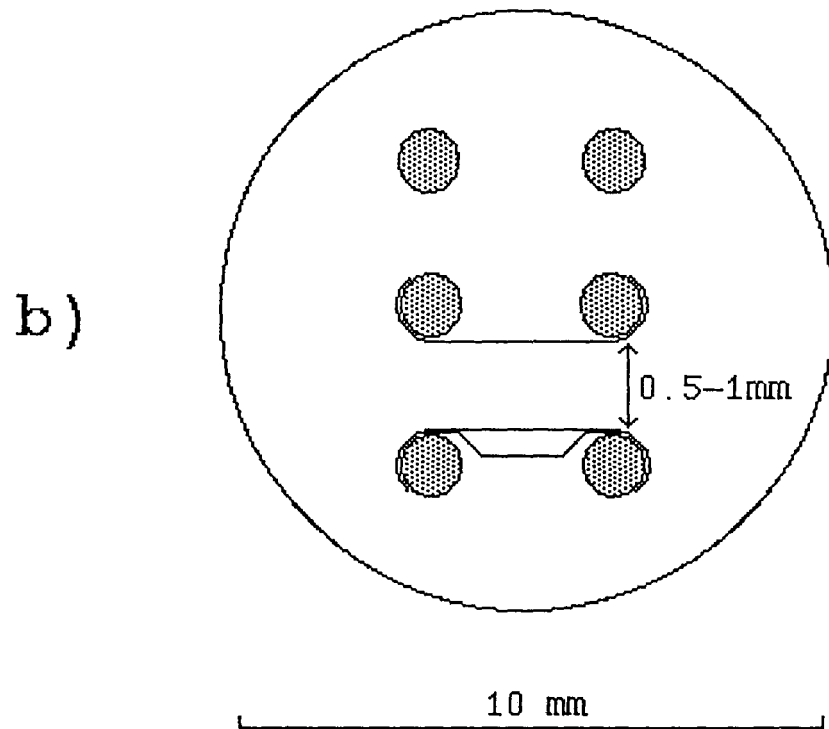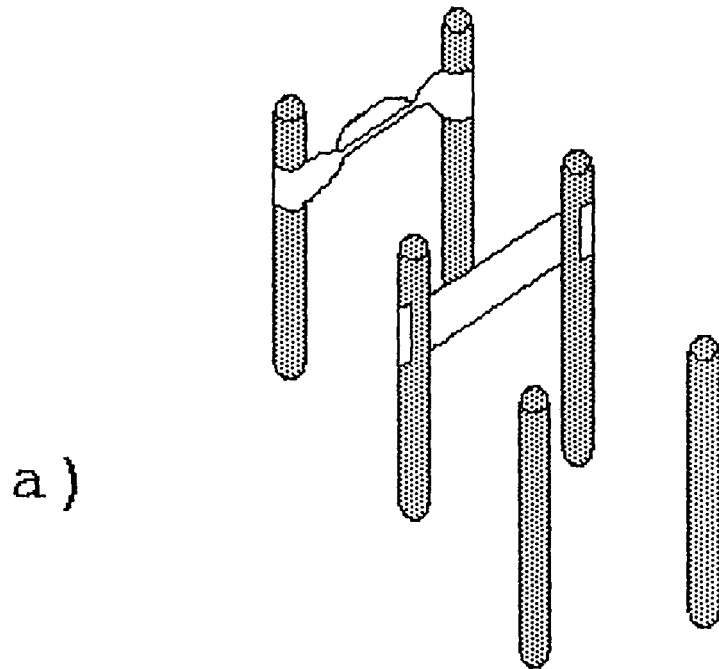
filament. It was simply a piece of wide zone refined rhenium orientated vertically. This ensures that the centre filament would catch as much Pb from the side filament as possible. Also, as shown in Figure 2.2, the filaments were wrapped around the sides of the posts so that the filaments were as close together as possible. The resultant filaments were approximately 0.5 to 1 mm apart.

The surface of the centre filament was etched with 1 μl of 0.3 N H_3PO_4. This produced a rougher surface on which the evaporated Pb would adhere. Not all samples were etched with acid. Those that were treated with phosphoric acid are denoted by the letter P after their sample name, i.e. PE11E1P.

2.1.3 Operation Procedure

The zircons were analyzed on a VG 354 solid source mass spectrometer with a 27cm radius and 90^0 magnet sector and a Daly detector in analogue mode at the Geology department of McMaster University.

The analysis of each zircon proceeds as follows:

1. Cleaning procedure for centre filament

2. Evaporation of zircon from side filament onto centre filament

3. Ionization of deposit and data collection.

The centre filament was the source of Pb for the

collection of data. Thus, it was important that this filament was clean to prevent contamination. This is done by heating the centre filament to a current higher than at which the data is taken, i.e. 4.5 to 6.0 A. During the cleaning step the mass spectrometer focuses on the resultant rhenium beam. Since the eventual Pb beam would also originate from the centre filament this first step does a coarse focusing of the source plate, extract plate, z bias, etc. During the cleaning of the centre filament the temperature was high enough to drive off any discordent Pb from the surface or fractures of the zircon in the side filament.

The zircon evaporation was achieved by a 10 to 15 minute heating of the side filament. During this time the computer was put on pause to prevent the collection of data. The current for evaporation ranged between 4.0 and 4.5 Amps. The temperature which these currents represent is unknown since no pyrometer was used. No Pb beam was found for evaporation currents below 4.0 Amps. Higher currents in excess of 5.0 Amps were not used to avoid heating the centre filament more than necessary during the deposition.

Once the evaporation step was complete, the side filament was turned off and the temperature of the centre filament was gradually increased. If there was any appreciable Pb deposit upon the centre filament it usually became apparent at a current of 3.6 to 3.8 Amps. At this current the program was allowed to continue and it began to scan and focus upon Pb.

The mass order of Pb analyses was 203.5, 204, 204.5, 206, 207, and 208. 203.5 and 204.5 were measured to detect the level of background. Ten mass scans of this range were taken and the ratios of $^{207}Pb/^{206}Pb$, $^{204}Pb/^{207}Pb$, $^{204}Pb/^{206}Pb$, and $^{204}Pb/^{208}Pb$ were calculated for the last eight scans. These ratios were calculated since the value of ^{204}Pb was very small and may have been zero in some cases. Thus, $^{206}Pb/^{204}Pb$, $^{207}Pb/^{204}Pb$, and $^{208}Pb/^{204}Pb$ could have resulted in undefined values and would cause the data collection program to crash. The eight sets of ratios were averaged and a standard error (in %) was calculated. Thus, for each block of data consisting of ten mass scans the result was one value and error for each of the $^{207}Pb/^{206}Pb$, $^{204}Pb/^{207}Pb$, $^{204}Pb/^{206}Pb$, and $^{204}Pb/^{208}Pb$ ratios.

The number of blocks of data acquired varied from zircon to zircon. It depended upon the amount of Pb evaporated onto the centre filament and the rate at which the Pb was evaporated off from it. The number of blocks of data in this study varied from 1 to 23. For each zircon, the blocks of data were considered separate points and so no grand average of all the mass scans were taken. This was done since the ratios often vary during the data acquisition. The variation in Pb ratios was usually due to a very low value of ^{204}Pb. ^{204}Pb was usually a few orders of magnitudes smaller than the ^{206}Pb, and very close to the background level. The size of the Pb ion beam may grow or decay during a block of data, but usually at a rate so that the ratios were constant. Thus, the

time interpolation was valid. A change in the ionization current was ususally accompanied a change in the beam size. The current was only altered during the focusing steps between the data blocks.

Other methods for analyzing the zircon were also used, but were not successful. One method consisted of heating the side and centre filaments concurrently in the previously described setup. Kober (1987) postulates that the deposit of evaporated zircon consists of a $Pb/Hf/SiO_2$ compound. Thus, evaporation and ionization would occur at the same time and not just Pb would be ionized, but a combination of elements.

The other method, electron bombardment consisted of both side filaments being heated to a high temperature to release electrons which would ionize the sample on the centre filament. Both of these methods resulted in a very high apparent value of ^{204}Pb which almost rivalled ^{206}Pb in size. This, however, did not reflect a zircon with a large amount of ^{204}Pb, but isobaric interference of compounds such as $HfSi^+$.

2.1.4 Age Determination and Error Statistics

The method by which the age of the zircon was calculated was dependent upon the value and quality of the Pb ratio data. The most important criteria was the value of the $^{206}Pb/^{204}Pb$ for a particular zircon. A value of $^{206}Pb/^{204}Pb$ greater than 10,000 is considered by many authors (Compston and Kröner, 1988 and

Kober *et al.*, 1989) to be sufficient so that a common Pb correction is not necessary.

If the ratio of $^{206}Pb/^{204}Pb$ was greater than 10,000 then the age may be determined directly from the $^{207}Pb/^{206}Pb$ ratio. The average of the $^{207}Pb/^{206}Pb$ ratio of each block was calculated and any blocks that were outside 2 population standard deviations (95% confidence) were eliminated from the data set. The standard deviation is defined as:

$$\sigma = \sqrt{\frac{\sum_{i=1}^{n} (x_i - \overline{x})^2}{n-1}} \quad (4)$$

where n is the number of blocks in the data set. The error in the average of $^{207}Pb/^{206}Pb$ was quoted as ±2 standard errors. Standard error was used since the data set is considered to be a random sampling of a larger population (Box, Hunter, and Hunter, 1978). Standard error is defined as:

$$standard\ error = \frac{\sigma}{\sqrt{n}} \quad (5)$$

The $^{207}Pb/^{206}Pb$ of each block has a different standard error. Initially, some attempts were made to weigh the final $^{207}Pb/^{206}Pb$ average in favour of blocks that had a small standard error. Such a weight was defined as 1/(standard error). The error was calculated as a ±2σ distribution about

the weighted average. The resultant weighted average was within 2σ of the simple average described previously. Thus, the simple average was kept and the weighted average was discarded. Also, there was no guarantee that the block with the smallest standard error would also be the most accurate indicator of the true $^{207}Pb/^{206}Pb$ ratio of the zircon.

If the $^{206}Pb/^{204}Pb$ was less than 10,000 then there must be a correction made for Pb that is non-radiogenic and present in the zircon when it formed. The age was determined using a York Fit program (York, 1969) which produces a best fit linear regression through data that have correlated errors in the x and y coordinates. x (i.e. $^{206}Pb/^{204}Pb$) and y (i.e. $^{207}Pb/^{204}Pb$) have correlated errors since they both have errors in ^{204}Pb as well as errors in ^{206}Pb and ^{207}Pb. The best fit line has two types of error associated with it. First, the apparent error is the error in the line due solely to the errors in each data point. Second, the scatter error is the scatter of all the data points around the best fit line. The resultant error of the best fit line was taken as twice the larger of either the apparent error or the scatter error to result in a $\pm 2\sigma$ error.

Linear regressions can be used in two ways to determine the age of the zircon. The data of $^{206}Pb/^{204}Pb$ versus $^{207}Pb/^{204}Pb$ may be plotted (slope method) with the resultant slope being $^{207}Pb/^{206}Pb$. The age is then calculated using equation (3). The error in age was due to the error in the slope. Also, the data of $^{204}Pb/^{206}Pb$ versus $^{207}Pb/^{206}Pb$ can also be plotted

(intercept method) and the resultant intercept of the $^{207}Pb/^{206}Pb$ axis would give the age. The appropriate age error would be due to the error in the intercept.

In the case of zircons in which the $^{206}Pb/^{204}Pb$ versus $^{207}Pb/^{204}Pb$ age was calculable the $^{204}Pb/^{206}Pb$ versus $^{207}Pb/^{206}Pb$ age was usually also possible to determine. The ages calculated by this method were comparable within 2σ error with that of the $^{206}Pb/^{204}Pb$ versus $^{207}Pb/^{204}Pb$ slope ages. This was expected since the data used to calculate the intercept age was not completely independent from that of the slope age. In many cases even the error in age was comparable. Thus, this intercept method could be used to reaffirm the age from the slope method.

In both methods, slope and intercept York fit regressions, the age was initially determined using the blocks of data from each zircon only. Since there was common Pb in these zircons, it must also be taken into account. The value of common Pb was derived from Stacey and Kramers' (1975) Pb evolution curve. The common Pb for the initial age was added to the data set. The slope and/or intercept was then recalculated with this point. Further adjustments were made to the value of the common Pb point till there was no more change in the value of age. The addition of the common Pb point must often be used since the data derived from the zircon evaporations alone were often in a tight cluster to which it was difficult to fit an isochron. Similarly, the

common Pb value could be subtracted from every point and the best fit line forced through the origin to achieve the same result.

The intercepts and slopes were both corrected by a mass fractionation correction of 0.5% for the Daly detector (Li *et al.*, 1989). The correction was determined by an analysis of a Pb standard using both the Daly and Faraday detectors. This was due to the preference for light Pb isotopes in the detector.

2.1.5 Graphical Presentation

Each zircon analysis results in an age and a $\pm 2\sigma$ error. This value can be plotted on an age histogram (Figure 2.3). The error in age for each zircon vary, therefore, a weighting factor was used so that zircons with a small error were more prominent than those that have a large error.

Statistically, each age and error represent a normal distribution given by:

$$f(x) = \frac{1}{\sigma\sqrt{2\pi}} e^{-\frac{(x-\mu)^2}{2\sigma^2}} \tag{6}$$

where μ is the mean of the distribution, i.e. the age. The first term is a normalizing or weighting factor so that:

Figure 2.3   Age histogram of zircons as a normalized distribution with various 2σ errors. Normalized frequency is $1/(\sigma\sqrt{(2\pi)})$.
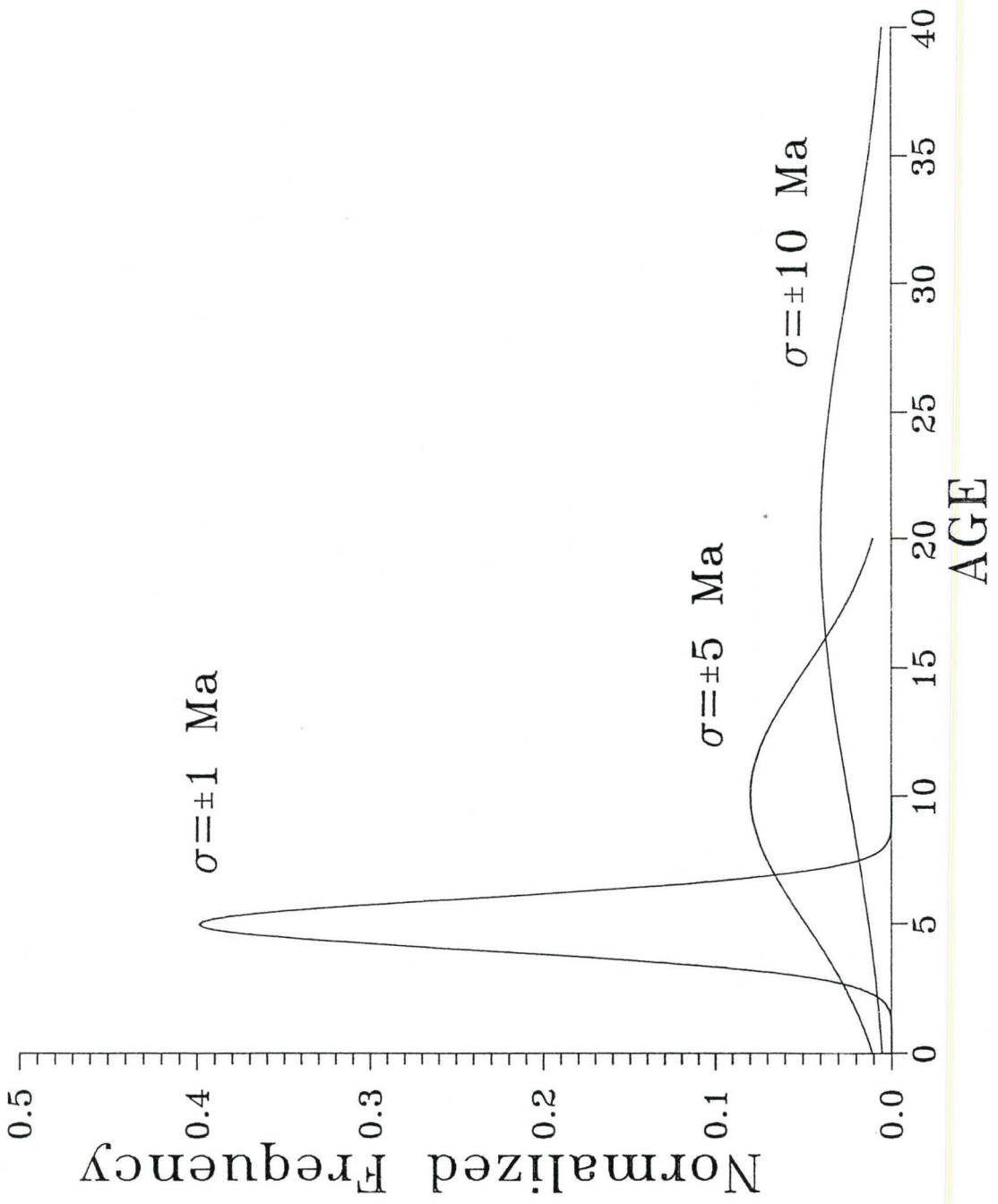
$$\int\limits_{-\infty}^{\infty} f(x)\ dx = 1 \qquad\qquad (7)$$

That is, the area under each normal distribution curve is equal to one. Therefore, ages with large errors will be represented as short broad peaks. Likewise, ages with small errors will have tall narrow peaks.

2.2 Experimental Testing of the Evaporation Method

The validity of the zircon evaporation method was
investigated by analyzing zircons of known age. The zircons
from the Battersea pluton have been dated by conventional U-Pb
methods by Marcantonio (1989). A supply of zircons from the
same rock sample were made available for the zircon evporation
method.

2.2.1 General Geology

The Battersea pluton is located in an area of exposed
Grenvillian rocks known as the Frontenac Axis in the Central
Metasedimentary Belt (CMB) (Figure 1.6). The Grenville
Province consists of gneissic, metasedimentary, and granulitic
terrains which vary in metamorphic grade from amphibolite to
granulite facies (Wynne-Edwards, 1972). These variations in
terrains are the basis for the subdivisions of the Grenville
Province into the Grenville Front (GF), Grenville Front
Tectonic Zone (GFTZ), Central Gneiss Belt (CGB), Central
Metasedimentary Belt (CMB) and others. The CMB is composed of
a supracrustal succession (Wynne-Edwards, 1972) known as the
Grenville Supergroup which consists of carbonates, calc-
silicates, quartzites, paragneisses, amphibolite and
metavolcanic rocks. The metamorphic grade varies from low
amphibolite to granulite facies. Locally, the area around the

26

Figure 2.4   Location map of the Battersea Pluton (after
Marcantonio, 1989).

A

Map A labels: SUPERIOR PROVINCE, GRENVILLE PROVINCE, 47N, METASEDIMENTARY BELT, CENTRAL, Bancroft, 45N, MONTREAL, OTTAWA - HULL, St. Lawrence R., L. Champlain, KINGSTON, B, 0 50 Km, 76W, 74W

B

Map B labels: Wolfe Lake Pluton, Westport Pluton, Rideau Lake Pluton, Westport, Rideau Lake Fault, SAMPLE LOCATION MAP, Crow Lake Pluton, Lyndhurst Pluton, Perth Road Pluton, Battersea Pluton, South Lake Pluton, Gananoque Pluton, Gananoque, km

Battersea Pluton is in the granulite facies. A whole rock isotopic and geochronological study was conducted by Marcantonio (1989). The Battersea pluton is a granite (sensu stricto) with no evidence of inherited zircons. Nonetheless, these within-plate granitoids were probably formed by mixing with a crustal component. The absence of xenocrysts is probably due to the high temperature of melting (Marcantonio *et al.*, 1990).

2.2.2   Zircon Description

The Battersea zircons (Plate 2.2) are transparent and colourless, but have a slight pinkish colour along some fractures and edges. They are prismatic crystals with very sharp faces and a length to width ratio of 3:1. Typical zircon sizes are up to 0.5mm in length. All zircons contain inclusions, both black and colourless. They have no obvious cores or zoning. The zircons appear magmatic in origin.

2.2.3   Results and Conclusions

Previous U-Pb work of various magnetic fractions of zircons of the Battersea Pluton (Marcantonio, 1989) have found it to be almost concordant. Thus, the best estimate of the age is the average of the $^{207}Pb/^{206}Pb$ ratios of the different fractions. This results in an age of 1165±4 Ma (2σ).

Plate 2.2 Typical zircons from the Battersea Pluton.

0.5 mm
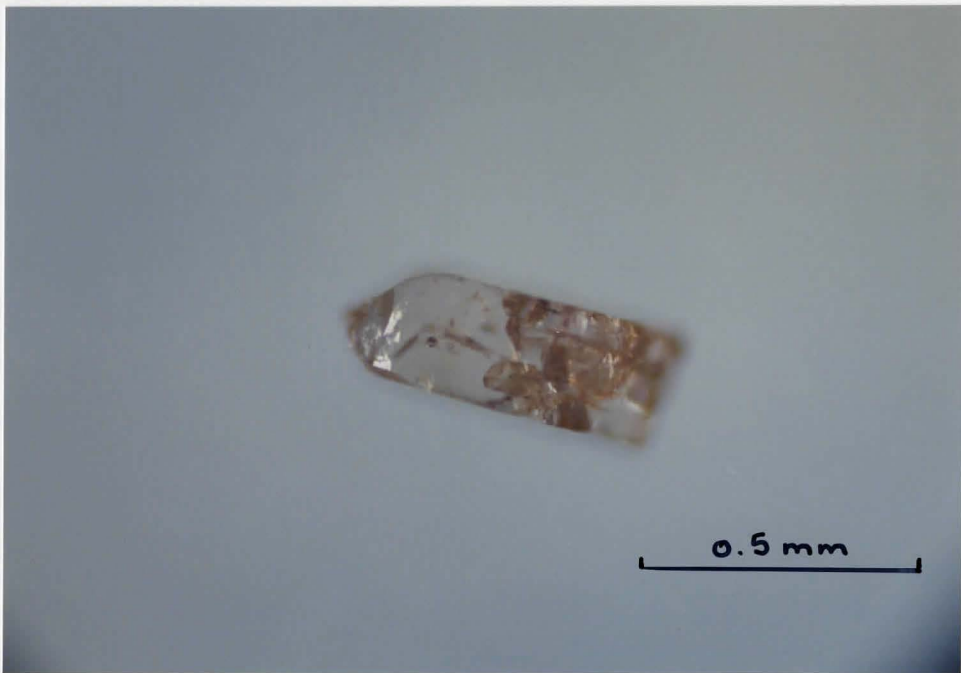
The data derived from zircon evaporation in this study is shown in Table 2.1. In total, 72 zircons from the Battersea pluton were tested and only nine provided data of high enough quality. The remaining zircons were rejected due to an absence of a Pb ion beam or a beam that was unstable so that the standard error of the block of data was greater than 10%. Most zircons have large amounts of ^{204}Pb and the amount varies from one zircon to another. This probably reflects the amount of Pb found in the inclusions, as well as the amount of inclusions. Each zircon, in itself, varied little in the ^{206}Pb/^{204}Pb and ^{207}Pb/^{204}Pb ratios. Thus, for each zircon it was difficult to fit an isochron to such a small spread. The data from all nine zircons was combined to give a greater range in ^{206}Pb/^{204}Pb and ^{207}Pb/^{204}Pb. Thus, an isochron could be fitted to allow a statistical analysis of the data. A York fit linear regression (York, 1969) was calculated for both the ^{206}Pb/^{204}Pb versus ^{207}Pb/^{204}Pb and ^{204}Pb/^{206}Pb versus ^{207}Pb/^{206}Pb data (Figure 2.5 and 2.6). The resultant ages are 1167±8 Ma (2σ) and 1167±7 Ma (2σ), respectively. These ages are identical, within error, to the age derived from U-Pb dating. The mean squared standard deviation (MSWD) of each age is 0.83 and 0.84, respectively. If the MSWD=1, then errors input into the regression calculation adequately describe the scatter in the data. If the MSWD<1, then the scatter of the data is less than predicted by the input errors. Therefore, the errors quoted for the ages is considered to be an overestimation of

Table 2.1 Raw data from the Battersea Pluton.

Name	Run	207/206	St. Err. (%)	207/204	St. Err. (%)	206/204	204/206	St. Err. (%)
ZT3	1	0.0838070	0.068	217.396	2.918	2673.797	0.000374	3.733
	2	0.0843053	0.095	204.073	1.880	2420.721	0.000413	1.808
	3	0.0852403	0.127	168.722	5.460	1991.239	0.000502	5.137
	4	0.0845994	0.118	193.510	3.674	2285.714	0.000438	3.790
	5	0.0848830	0.195	198.377	4.752	2350.729	0.000425	1.872
	6	0.0848230	0.199	191.894	2.355	2261.420	0.000442	2.139
	7	0.0845490	0.251	214.110	7.969	2524.615	0.000396	7.706
CQM8	3			137.114	5.802	1561.037		6.192
	4			77.546	4.138	800.897		4.326
	5			53.016	2.254	507.382		2.410
	6			48.053	2.047	438.135		1.889
	7			40.098	2.108	356.646		1.941
	8			44.387	2.965	393.298		2.836
	9			41.822	7.532	370.686		7.231
	10			40.661	6.466	386.952		3.007
CMQ2	1			38.875	2.500	305.736		3.069
	2			43.053	1.775	362.384		1.660
	3			47.898	5.919	402.139		5.966
CMQ1	1	0.0949667	0.167	83.793	8.687	881.290	0.001135	8.521
	2	0.0946730	0.112	81.725	3.596	862.887	0.001159	3.392
	3	0.0951838	0.292	81.841	3.438	860.067	0.001163	3.146
CMQB2	1	0.0877275	0.157	131.413	6.796	1502.178	0.000666	5.554
	2	0.0883862	0.282	132.892	2.740	1509.662	0.000662	2.478
BTSA3	1	0.0886000	0.226	153.179	6.620	1730.403	0.000578	6.541
	2			44.173	4.061	491.087		3.913
	4	0.0830958	0.133	237.372	4.931	2808.989	0.000356	4.677
BTSA4	1	0.0811406	0.156	436.034	7.938	5370.569	0.000186	7.687
BTSA8	1	0.1880890	0.263	24.485	1.205	130.080	0.007688	1.306
	2	0.1811387	0.183	24.928	1.490	137.448	0.007276	1.396
	3			26.959	2.228	153.591		1.589
BTSE5	5	0.0803559	0.076	764.701	3.372	9505.703	0.000105	3.220
	6	0.0802955	0.042	553.067	2.772	6896.552	0.000145	2.719
	7	0.0797145	0.182	784.314	5.240	9775.171	0.000102	4.621
Commom Pb point for 1170 Ma		0.0923219		15.475		16.762	0.059659	

Figure 2.5 York fit of Battersea Pluton data as calculated from the slope of $^{206}Pb/^{204}Pb$ versus $^{207}Pb/^{204}Pb$. The data set is a combination of data from 9 zircons.

Age = 1167 ± 8 Ma (±2σ)
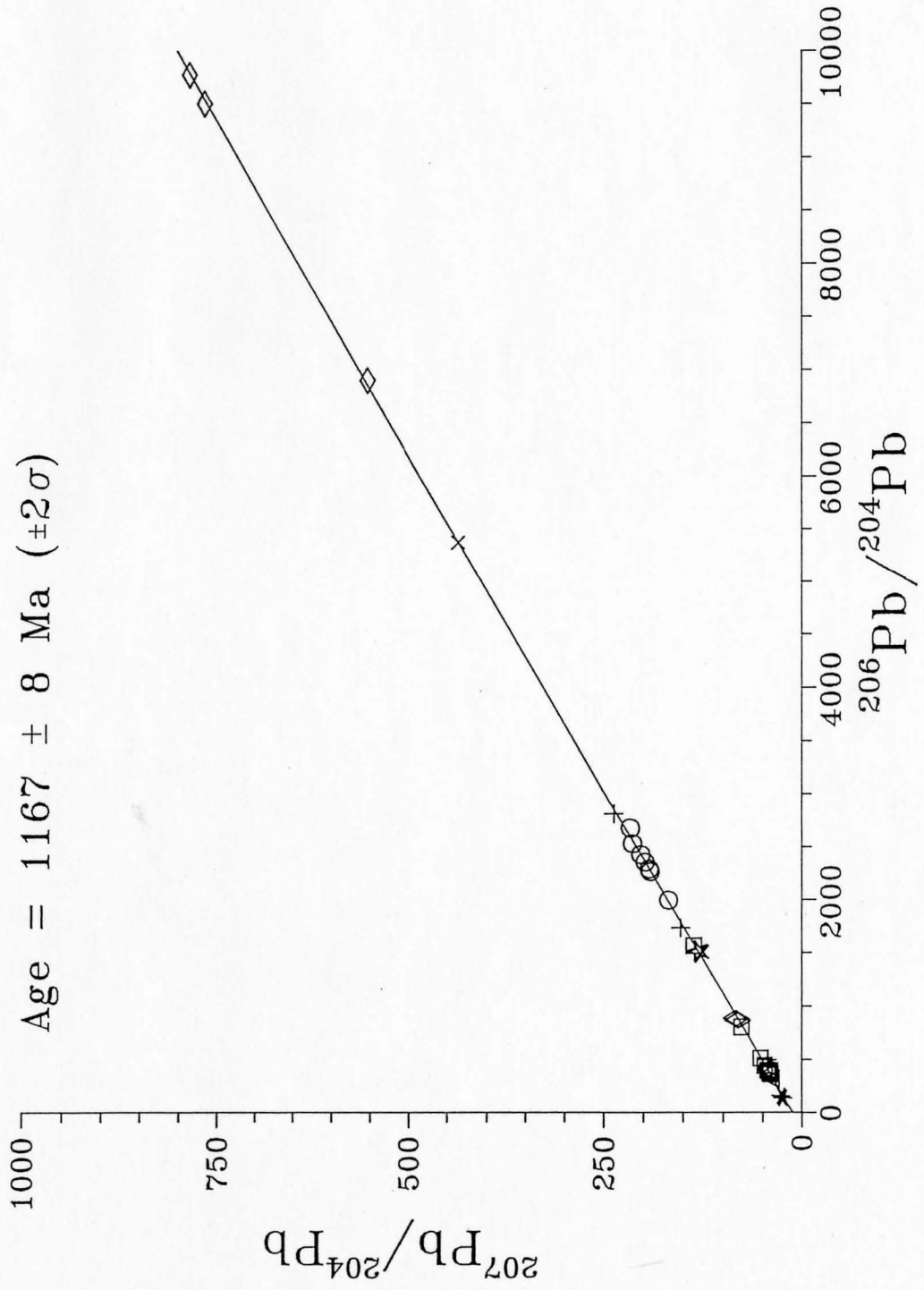
Figure 2.6 York fit of Battersea Pluton data as calculated from the the y axis intercept of ^{204}Pb/^{206}Pb versus ^{207}Pb/^{206}Pb. The data set is a combination of data from 7 zircons.

Age = 1167 ± 7 Ma (±2σ)

the true error.   This agreement also lends support to the assumption that the zircon evaporation technique is a viable alternative to convential U-Pb geochronology.   The precision of the evaporation technique is also comparable to that of the U-Pb method.

Chapter 3

3.1 The Britt Domain

3.1.1 General Geology

The Grenville Province is the youngest part of the Canadian Shield (Figure 3.1) (Moore, 1986). The Grenville Province is a combination of gneissic, metasedimentary, and granulitic terrains which vary in metamorphic grade from amphibolite to granulite facies (Wynne-Edwards, 1972). The area in the Grenville Province from which the zircons in this study were collected is located in the Britt Domain of the Central Gneiss Belt. It is in the western end of the Grenville Province, south of the Grenville Front and the Grenville Front Tectonic Zone.

The Grenville Front is the northerly boundary of the Grenville Province. At its southwest end it separates supracrustal rocks of the Southern Province from the gneissic terrain of the Grenville Province. There is a change in isotopic age of the rocks as well as a difference in metamorphic grade. The main characteristic that defines the position of the Grenville Front, though, is a structural one, i. e., a major fault.

The Grenville Province is a polymetamorphic terrain spanning more than 1500 Ma. It has undergone three

Figure 3.1 The subdivisions of the Grenville Province (after Wynne-Edwards, 1972).

Tectonic Framework of the Grenville Province map showing: Churchill Province, Nain Province, Superior Province, Eastern Grenville Province, Baie Comeau Segment, Central Granulite Terrain, Southern Province, GFTZ, GF, Central Gneiss Belt, CMB, Adirondack Segment, Figure 3.2

TECTONIC FRAMEWORK
OF THE
GRENVILLE PROVICE

0 100 200 300 400 500 600
km
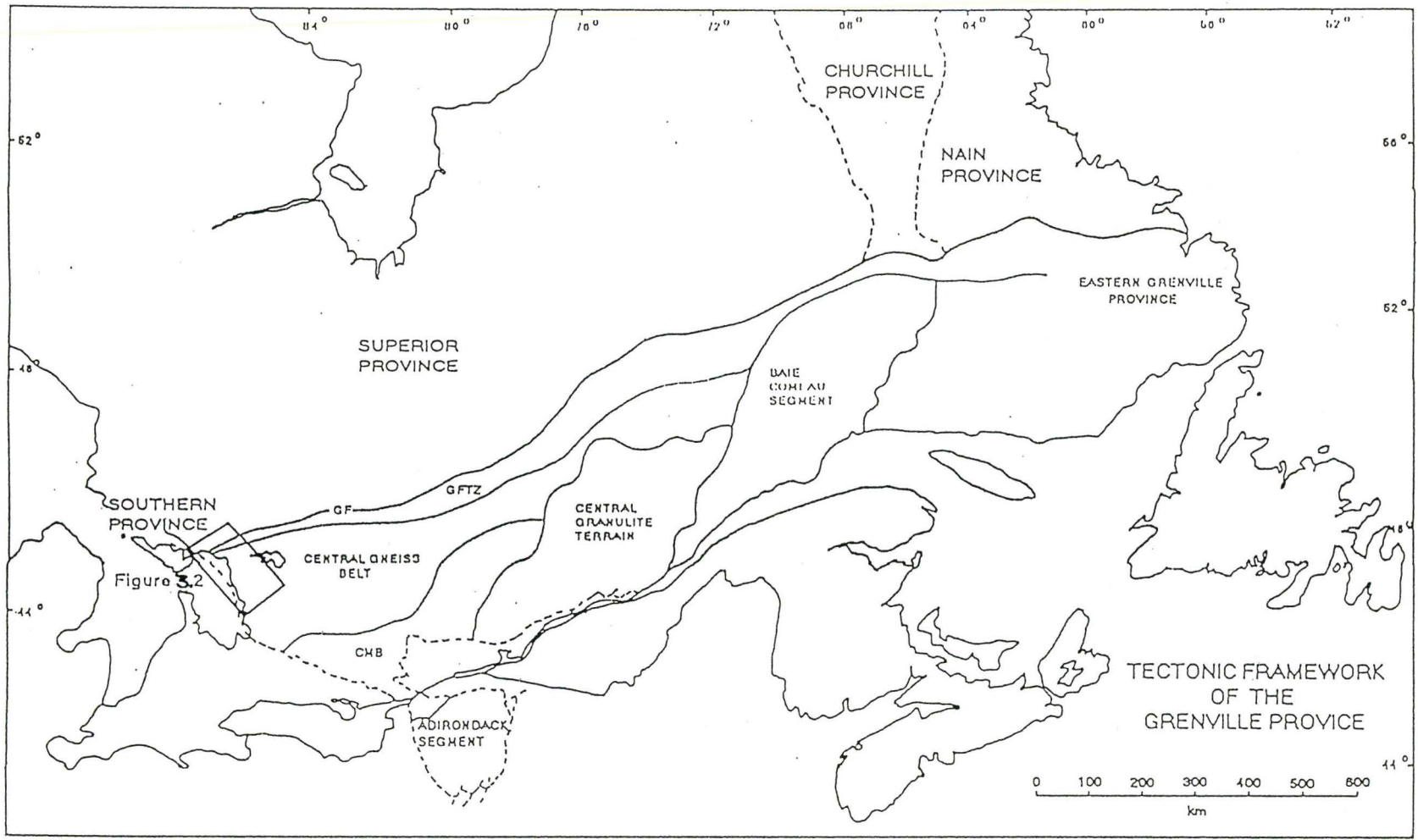
metamorphic events as well as periods of syntectonic and anorogenic plutonism (Condie, 1989). Archean aged folding is represented in the western Grenville. Another possible orogenic event (the Penokean orogeny) may have occurred in this area at 1.75-1.85 Ga. The events described as the Grenville orogeny occurred between 1.2 and 1.0 Ga. The sequence of tectonic events in this province is not well known due to overprinting by later metamorphic events, but it is believed that the Grenville Province is the result of continent-arc and continent-continent collisions (Condie, 1989).

A Penokean aged suture has recently been proposed in the western part of the Grenville Province (Dickin and McNutt, 1989). A suture is the boundary between two continents or a continent and an arc that have collided with one another. This suture in the Grenville Province is not obvious due to the high grade polymetamorphic history that it has undergone. The location of the suture has been defined by Dickin and McNutt (1989) and Dickin *et al.* (1990) by Sm-Nd model ages. This work has shown the presence of 1.9 Ga basement as well as the expected Archean crust.

The Central Gneiss Belt is characterized by quartzofeldspathic gneisses, but also marble, quartzite and paragneisses are present (Wynne-Edwards, 1972). The grade of metamorphism is in the upper amphibolite facies dates from the Grenvillian orogeny. The age of many plutons within the

Central Gneiss Belt are Proterozoic and therefore, predate the metamorphism. The Central Gneiss Belt is divided into areas of similar character such as distinctive rock assemblages, metamorphic grade and/or structures (Davidson, 1986). These areas are known as domains and are separated from one another by zones of high strain. The domains are thought to represent different pieces of stacked crust (Davidson, 1986). The Britt Domain (Figure 3.2) is located in the western part of the Grenville Province in the Central Gneiss Belt. It is exposed along the eastern shore of Georgian Bay from the Grenville Front Tectonic Zone in the north to the Parry Sound Domain in the south.

The zircons examined in this study are from a variety of rock types in the Britt Domain as well as from different sides of the proposed suture. Samples PSK0.6 and PE10.2 are both from granitoid plutons. PE10.2 appears to be a finer grained equivalent of PSK0.6. PINE is from a granitic gneiss. PE11.3 is a feldspathic gneiss collected near the Britt pluton. The final sample, CBQ, is a metasedimentary quartzite containing detrital zircons. All samples were collected by Dr. A. P. Dickin in the summer of 1988 as part of a Sm-Nd study of the French River area.

38

Figure 3.2 Sample locations and general geology of the Britt Domain. Granitic plutons are denoted by red and quartzite by yellow. The Grenville Front (GF) (heavy solid line) divides the Superior Province to the north from the Grenville Province in the south. The hatched line indicated the southern extent of the Grenville Front Tectonic Zone (GFTZ). The position of the Grenville suture (dashed line) and Domain boundaries (triangular hatched line) are also shown. Highways are denoted by solid lines with the appropriate Highway number. (Complied from Lumbers, 1975, Davidson and Morgan, 1980, Davidson *et al.*, 1982, Davidson and Bethune, 1988, and Dickin and McNutt, 1989).
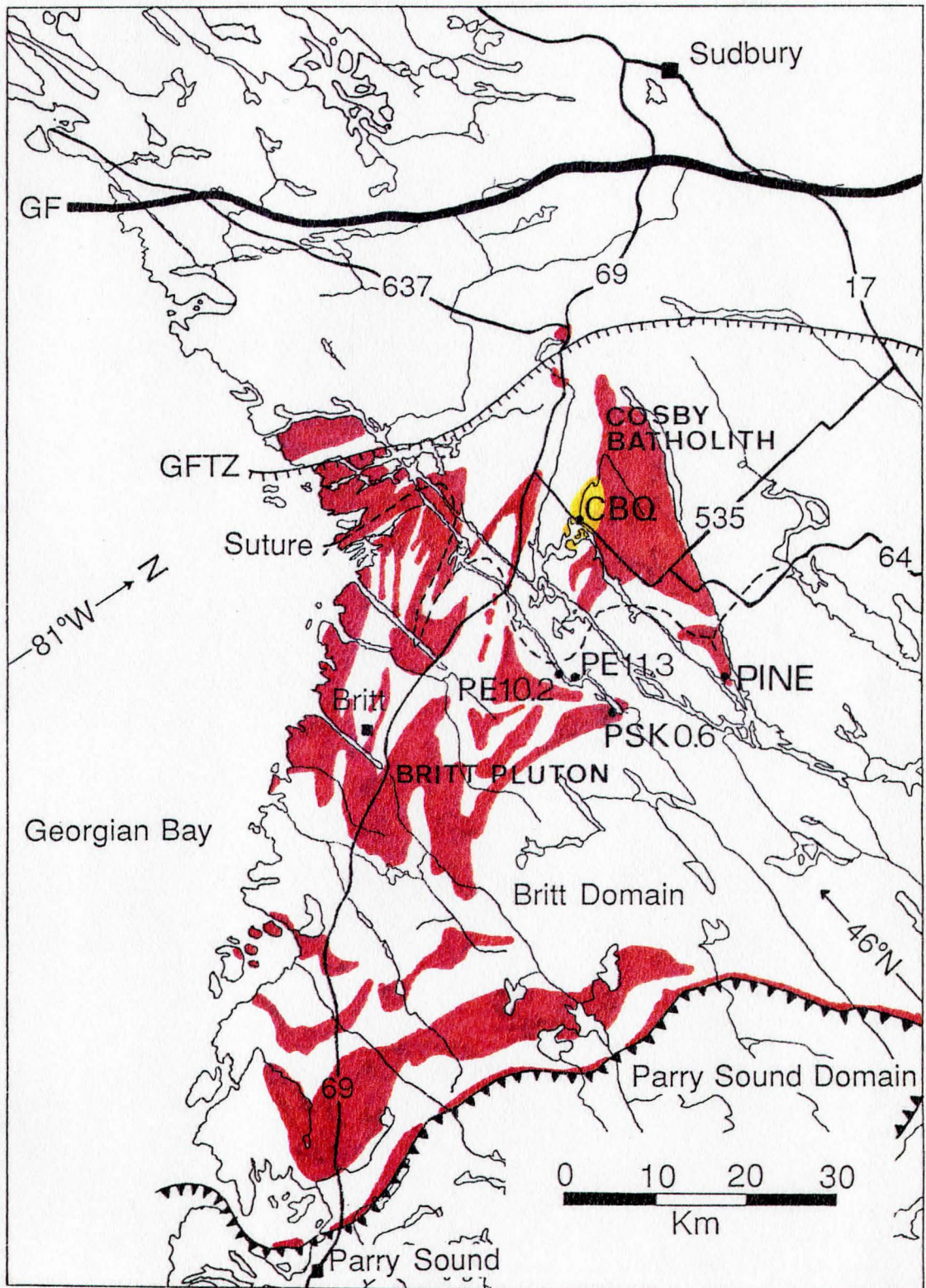
3.2 The Britt Pluton

3.2.1 General Geology

PSK0.6 is located in the Britt Pluton and PE10.2 is from a granitoid pluton located north of the Britt Pluton (Figure 3.2). The Britt Pluton has been described as a hornblende-garnet-biotite granitoid orthogneiss (Van Breeman *et al.*, 1986). It has been intruded into the surrounding country rock and folded by later metamorphism.

In thin section, the Britt Pluton contains approximately 50% quartz, 30% plagioclase, and minor alkali feldspar (Dickin *et al.*, 1990). The biotite is aligned parallel to gneissosity. Apatite, sphene and epidote are accessory minerals. Mineralogically, PE10.2 appears to be a finer grained equivalent to PSK0.6.

The zircons sampled from PSK0.6 (Plate 3.1) ranged in size from 0.25 to 0.5 mm in length. Their length to width ratio varies from 2:1 to 3:1. Almost all were heavily fractured so that they appeared translucent to opaque. In thin section (Plate 3.2) the zircons show no obvious zoning or cores, but contain black spherical and colourless rod-shaped inclusions. The shape of the zircons as grains and in thin section is euhedral but with varying amounts of roundedness. Transparent zircons tend to be euhedral and fractured zircons are more rounded. Thus, the roundedness may be due to their

Plate 3.1 Typical zircon grains from PSK0.6.

Plate 3.2 PSK0.6 zircons (Z) in thin section (plane polarized light).

1.0 mm

0.15 mm
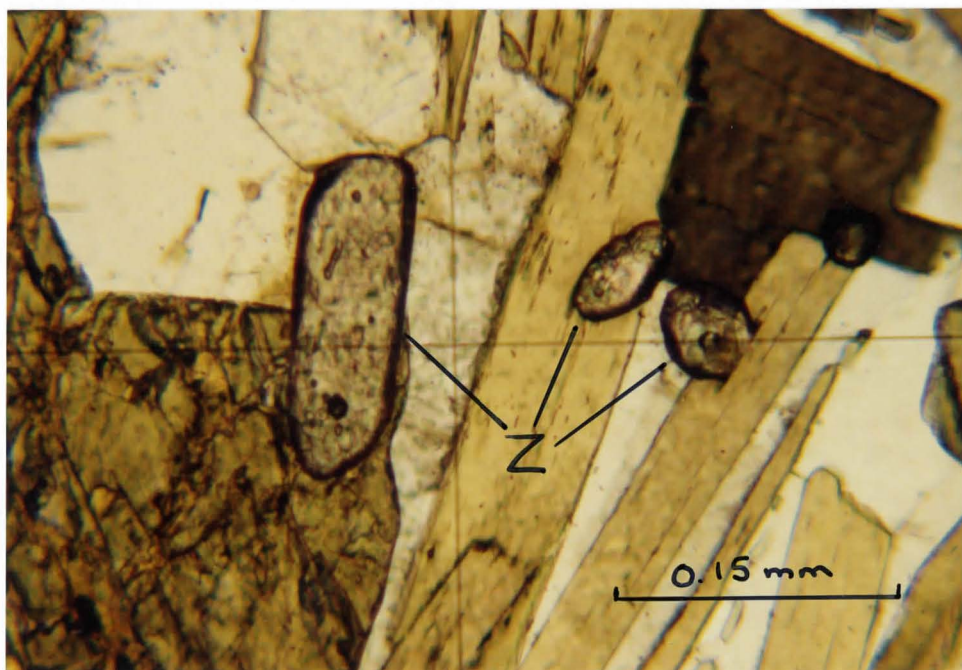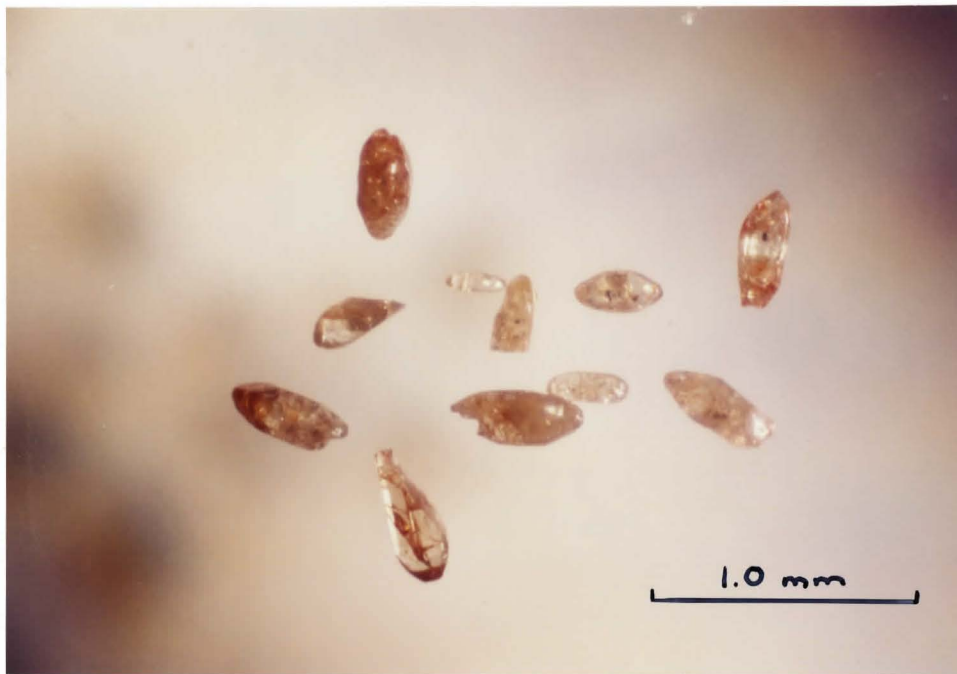
weakened structure caused by metamorphism rather than having been abraded by sediment transport. The reddish colour of some may be due to trace amounts of hematite along the fractures, though all zircons were non-magnetic. Thus, these zircons appear to have undergone some degree of alteration. The lack of unaltered zircons made it difficult to choose zircons that were unfractured and inclusion-free to ensure as much concordancy as possible.

The zircons from PE10.2 are similar in appearance to those of PSK0.6. The grains (Plate 3.3) seem to be less fractured, but contain many inclusions. Their shapes are similar to PSK0.6, i.e. euhedral to slightly rounded. In thin section (Plate 3.4), there seem to be no cores or metamorphic zoning.

3.2.2 Previous Isotopic Work

The Britt Pluton has been studied by many authors and by a variety of methods. Van Breeman *et al*. (1986) have dated the pluton with an U-Pb upper intercept age of 1456.5 +8.5/-5.9 Ma (2σ). This is interpreted as the age of crystallization. The lower U-Pb intercept of 726 +73/-61 Ma does not correspond to any known geological event, but is probably due to a combination of episodic (Grenvillian) and continuous Pb loss. In their work, a variety of zircons were tested ranging in size up to 0.18 mm in length. Some were

42

Plate 3.3 Zircon grains from PE10.2: A) PE10G4, B) PE10B3, and C) PE10C1.

Plate 3.4 PE10.2 zircon (Z) in thin section (plane polarized light).

0.5mm
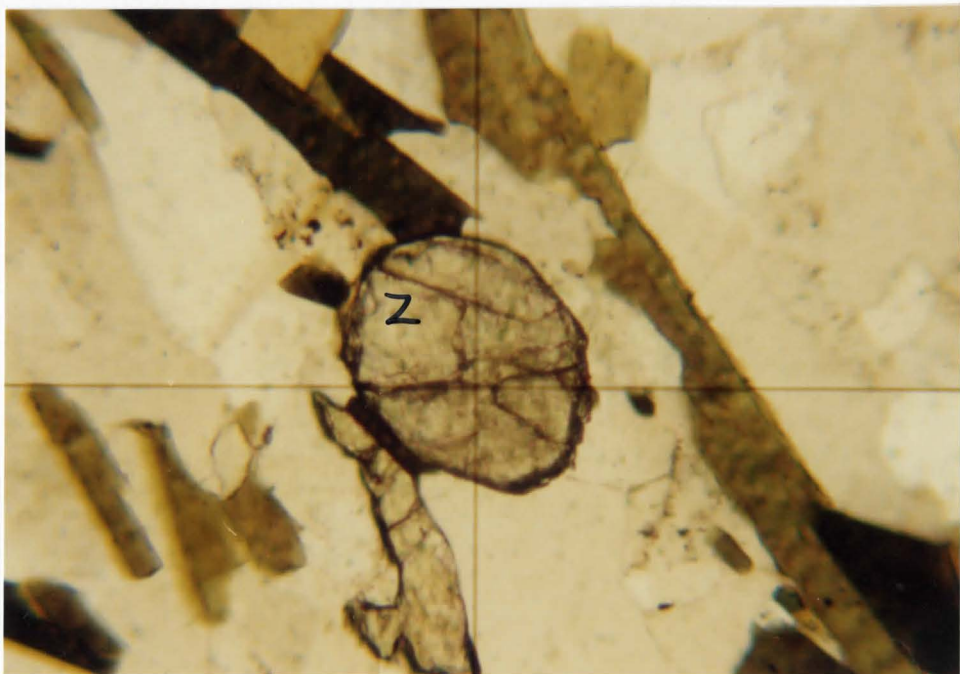
abraded and some were not. Their ^{207}Pb/^{206}Pb ages ranged from 1437.4 to 1409.8 Ma. With abrasion the zircons were still discordant by approximately 7%.

Work by Dickin and McNutt (1989) and Dickin *et al.*, (1990) examined the Sm-Nd model ages, Rb-Sr ratios, and major element composition of various plutons in the Britt Domain. The Sm-Nd model age of the Britt Pluton and other plutons south of the suture range in value from 1770 to 1950 Ma. The model ages of PSK0.6 (Dickin *et al.*, 1990) and PE10.2 (Dickin, unpublished data) are 1.82 and 1.89 Ga, respectively. This, combined with the U-Pb age by Van Breeman *et al.* (1986) implies the pluton was probably formed by crustal melting of a 1900 Ma old mobile belt which accreted onto the Superior Province.

3.2.3 Results

The resultant ages for PSK0.6 and PE10.2 are shown in Table 3.1. Most ages were derived from the slope of ^{206}Pb/^{204}Pb versus ^{207}Pb/^{204}Pb data (Figure 3.3 and 3.6) or the intercept of ^{204}Pb/^{206}Pb versus ^{207}Pb/^{206}Pb data (Figure 3.4 and 3.7). Only in a few rare cases was the amount of common Pb low enough that the age could be derived from the ^{207}Pb/^{206}Pb data directly (Figure 3.5 and 3.8). In most cases, ages derived by both methods were within 2σ of each other. The raw data from which these ages were calculated is given in Table 3.2 and 3.3. The

44

Table 3.1 Ages of zircons from PSK0.6 and PE10.2 from the Britt Domain. Ages derived by a York fit of ^{206}Pb/^{204}Pb vs. ^{207}Pb/^{204}Pb data and/or ^{204}Pb/^{206}Pb vs. ^{207}Pb/^{206}Pb data or an average of ^{207}Pb/^{206}Pb data.

Sample	York Fit of 206/204 vs. 207/204		Age (Ma)	Error	York Fit of 204/206 vs. 207/206		Age (Ma)	Error	Average of 207/206		Age (Ma)	Error
	slope w. mfc	2 sigma		2 sigma	intercept w. mfc	2 sigma		2 sigma	average w. mfc	2 sigma /sqrt(n) n=#runs		2 sigma /sqrt(n)
BRITT DOMAIN												
PSKA1									0.089782	0.001740	1420	37
PSKA4	0.090147	0.000398	1429	+82/-87	0.092274	0.000848	1473	17				
PSKC4	0.088694	0.000366	1398	8	0.089313	0.000668	1411	19				
PSKE2	0.089776	0.000428	1421	9	0.089961	0.000416	1425	9				
PSKE5	0.088708	0.002320	1398	+49/-51	0.089451	0.001462	1414	31				
PSKE6	0.096204	0.002350	1590	+44/-45	0.096704	0.000958	1562	19				
PE10B3	0.091707	0.001198	1461	25	0.091529	0.017092	1458	336				
PE10C1									0.090363	0.000664	1433	14
PE10D1	0.093117	0.009710	1490	+185/-212	0.092154	0.001708	1471	35				
PE10D3	0.086560	0.008240	1351	+173/-196	0.088354	0.006104	1390	130				
PE10E1A									0.089610	0.000121	1417	3
PE10E2A	0.089477	0.000590	1414	13	0.089789	0.000846	1421	18				
PE10G4	0.087142	0.000390	1364	9	0.088639	0.000666	1396	14				

mfc=mass fractionation correction of 0.5%

Table 3.2   Raw data from PSK0.6.

Name	Run	207Pb/206Pb	St.Err. (%)	207Pb/204Pb	St.Err. (%)	206Pb/204Pb	204Pb/206 Pb	St.Err. (%)
PSKA1	1	0.0888031	0.132	2128.565	40.670	23809.524	0.000042	36.335
	2	0.0888686	0.260	-2740.477	99.990	-31645.570	-0.000032	99.990
	3	0.0903354	0.525	1567.398	99.990	21834.061	0.000046	99.990
Common Pb for 1400 Ma		0.9436896		15.418		16.338	0.061207	
PSKA4	3	0.0924708	0.098				0.000056	42.189
	4	0.0932287	0.246	1154.068	14.023	12391.574	0.000081	13.107
	7	0.0928802	0.251				0.000082	30.621
	8	0.0947813	0.606	371.195	19.219	4008.016	0.000250	19.321
	11	0.0940633	0.280	207.331	14.857	2209.456	0.000453	14.655
Common Pb for 1430 Ma		0.9463825		15.409		16.282	0.061418	
PSKC4	1	0.0911188	0.043	545.732	3.845	5995.204	0.000167	3.417
	2	0.0903546	0.055	614.968	7.428	6830.601	0.000146	8.428
	3	0.0906183	0.081	741.125	6.446	8169.935	0.000122	6.204
	4	0.0906451	0.110	615.498	6.083	6816.633	0.000147	5.746
	5	0.0912600	0.181	790.514	8.409	8635.579	0.000116	7.940
Common Pb for 1410 Ma		0.9446044		15.415		16.319	0.061278	
PSKE2	1	0.0912106	0.164	718.597	10.408	7886.435	0.000127	9.891
	2	0.0913386	0.100	743.660	10.120	8169.935	0.000122	9.717
Common Pb for 1420 Ma		0.9454635		15.412		16.301	0.061346	
PSKE5	1	0.0909185	0.110	1076.310	36.494	11820.331	0.000085	35.273
	2	0.0900032	0.361	550.388	10.032	6093.845	0.000164	9.047
	3	0.0900288	0.235	1396.258	75.248	15847.861	0.000063	69.046
	4	0.0905856	0.313	852.878	42.282	9960.159	0.000100	49.489
Common Pb for 1390 Ma		0.9427768		15.421		16.357	0.061136	
PSKE6	2	0.1007752	0.167	322.664	1.216	3147.624	0.000318	2.009
	3	0.1001627	0.417	355.809	12.044	3511.236	0.000285	11.413
Common Pb for 1600 Ma		0.9623989		15.357		15.957	0.062668	

Figure 3.3 York fit ^{206}Pb/^{204}Pb vs. ^{207}Pb/^{204}Pb data from PSK0.6.

Legend (appears within the figure):

○ PSKA4 — 1429+82/−87 Ma (2σ)
□ PSKC4 — 1398±8 Ma (2σ)
△ PSKE2 — 1421±9 Ma (2σ)
◇ PSKE5 — 1398+49/−51 Ma (2σ)
☆ PSKE6 — 1590+44/−45 Ma (2σ)

47
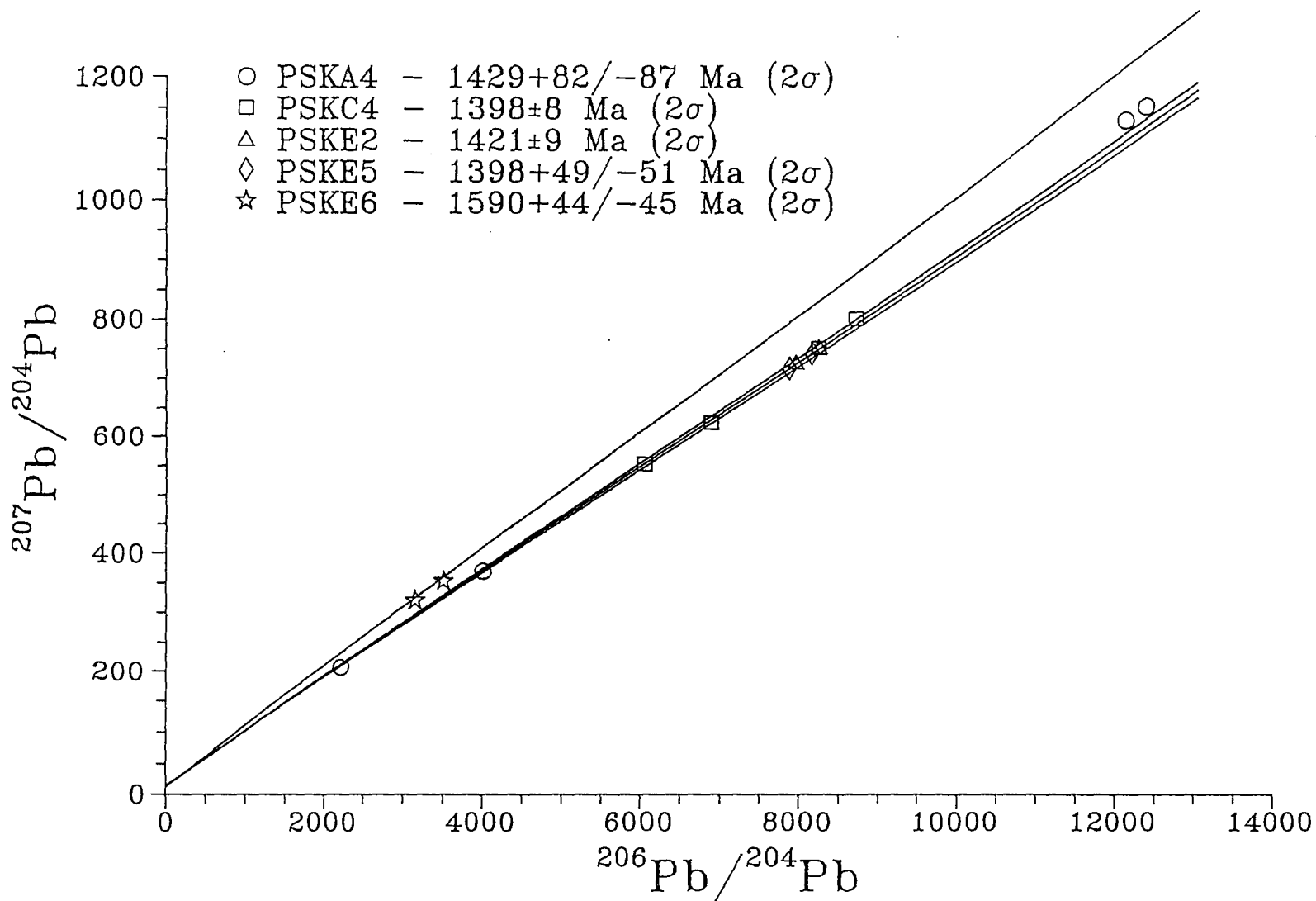
Figure 3.4   York fit of ^{204}Pb/^{206}Pb vs. ^{207}Pb/^{206}Pb data from PSK0.6.

PSKA4 — 1473±17 Ma (2σ)
PSKC4 — 1411±19 Ma (2σ)
PSKE2 — 1425±9 Ma (2σ)
PSKE5 — 1414±31 Ma (2σ)
PSKE6 — 1562±19 Ma (2σ)

Figure 3.5 ^{207}Pb/^{206}Pb histogram of data from PSK0.6.

Age (Ma)

PSKA1 — 1420±37 Ma (2 St. Err.)

49
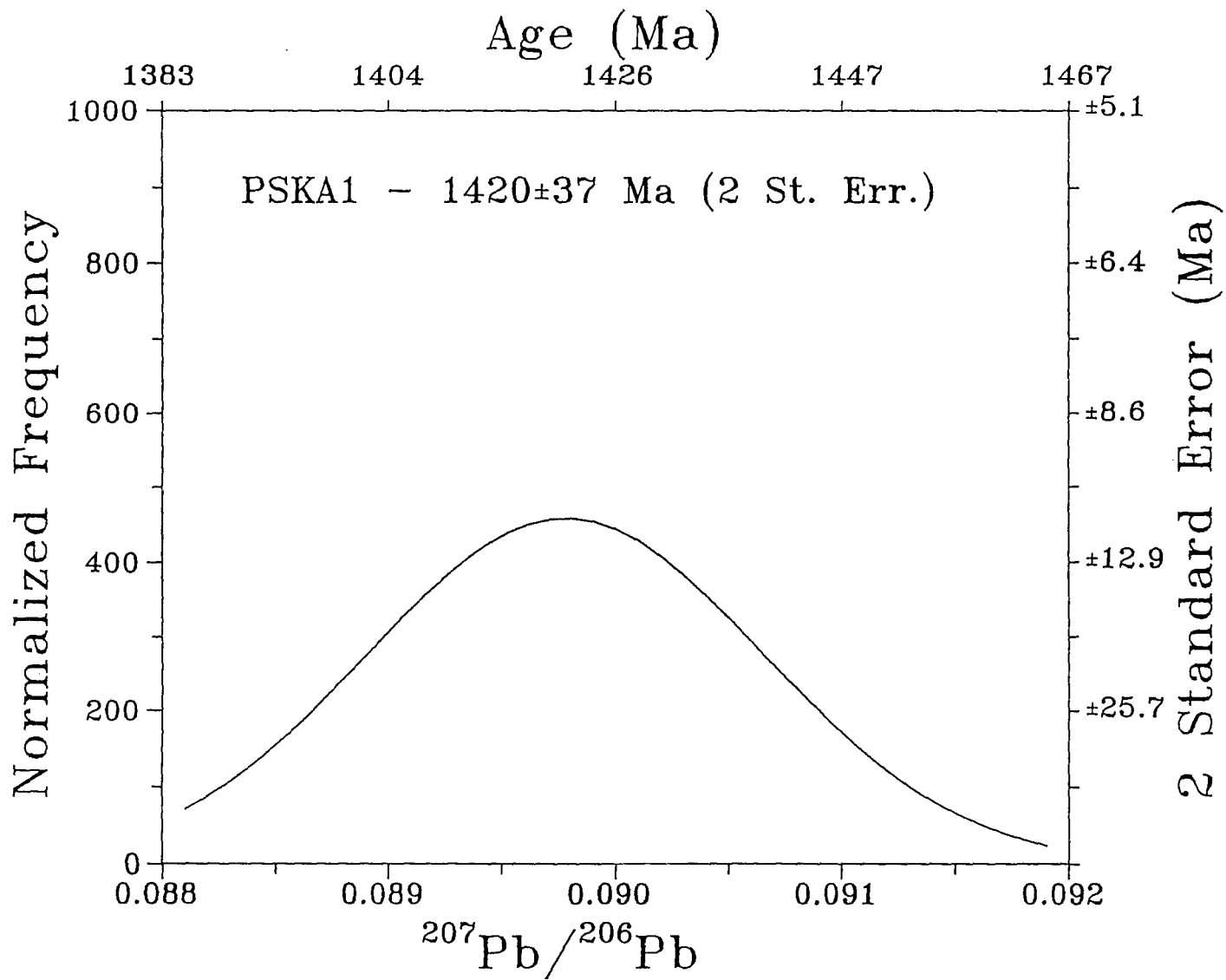
Table 3.3 Raw data from PE10.2.

Name	Run	207/206	St.Err. (%)	207/204	St.Err. (%)	206/204	204/206	St.Err. (%)
PE10B3	1	0.1069869	1.189	129.329	18.947	1203.225	0.000831	17.152
	2	0.1032296	1.075	79.787	20.251	756.144	0.001323	17.808
Common Pb for 1440 Ma		0.9720213		15.407		16.263	0.061489	
PE10C1	1	0.0905707	0.549	234.368	40.120	2511.932	0.000398	38.214
	2	0.0896704	0.234	5367.687	99.990	62500.000	0.000016	99.990
	3	0.0894984	0.428	2402.114	99.990	28011.204	0.000036	99.990
Common Pb for 1420 Ma		0.9454635		15.412		16.301	0.061346	
PE10D1	1	0.0933901	0.295	834.655	29.744	8417.508	0.000119	32.797
	2	0.0955754	0.472	202.786	18.219	2143.163	0.000467	17.340
Common Pb for 1530 Ma		0.9557544		15.380		16.092	0.062143	
PE10D3	1	0.1070212	1.182	55.929	13.409	528.150	0.001893	15.513
	2	0.1065281	0.403				0.001413	19.336
	3	0.1064944	0.506	83.682	15.976	772.141	0.001295	15.074
	4	0.1056431	0.643	88.784	6.700	850.774	0.001175	6.735
	5	0.1049480	0.762	77.751	9.901	746.770	0.001339	8.676
	6	0.1025606	0.462				0.000995	23.722
Common Pb for 1440 Ma		0.9427768		15.421		16.357	0.061136	
PE10E1A	1	0.0900436	1.789	525.928	99.990	5425.936	0.000184	99.990
	3	0.0894585	0.199	-1758.396	54.152	-20491.803	-0.000049	51.200
	4	0.0894785	0.151	4199.211	74.548	45248.869	0.000022	68.256
	5	0.0890585	0.138	7980.846	99.990	93457.944	0.000011	99.990
	6	0.0893520	0.133	3101.737	57.630	34246.575	0.000029	52.657
	7	0.0888624	0.128	1877.582	44.756	20833.333	0.000048	41.310
	8	0.0891893	0.195	13123.360	99.990	135135.135	0.000007	99.990
	9	0.0892007	0.109	26595.745	99.990	555555.556	0.000002	99.990
	10	0.0888655	0.188	4773.270	61.195	54347.826	0.000018	55.410
	11	0.0890035	0.099	5288.207	99.990	55248.619	0.000018	99.990
	12	0.0891818	0.364	1817.191	57.955	20533.881	0.000049	56.431
	13	0.0891560	0.185	2029.633	60.341	23866.348	0.000042	58.042
Common Pb for 1440 Ma		0.9446044		15.415		16.319	0.061278	

Name	Run	207/206	St.Err. (%)	207/204	St.Err. (%)	206/204	204/206	St.Err. (%)
PE10E2A	1	0.0940933	0.099	347.790	1.628	3675.119	0.000272	1.470
	2	0.0935131	0.112	403.372	4.434	4308.488	0.000232	3.936
	3	0.0935659	0.044	318.107	5.174	3404.835	0.000294	4.900
	4	0.0943037	0.111	270.687	3.148	2865.330	0.000349	2.790
	5	0.0939451	0.088	271.496	3.603	2888.504	0.000346	3.373
	6	0.0932715	0.070	288.784	2.061	3096.934	0.000323	1.761
	7	0.0934327	0.167	311.925	2.921	3513.703	0.000285	5.425
	8	0.0932928	0.101	333.700	2.480	3575.259	0.000280	2.232
	9	0.0931462	0.148	311.284	3.128	3346.720	0.000299	2.915
	10	0.0930911	0.115	363.438	3.575	3900.156	0.000256	3.450
	11	0.0926448	0.014	378.544	4.773	4088.307	0.000245	4.592
	12	0.0923794	0.099	387.988	2.287	4201.681	0.000238	2.058
Common Pb for 1440 Ma		0.9529383		15.409		16.282	0.061418	
PE10G4	1	0.0925226	0.204	240.292	9.145	2600.104	0.000385	8.710
	3	0.0919454	0.587	295.622	39.623	3192.848	0.000313	38.649
	4	0.0913074	0.305	325.977	11.703	3586.801	0.000279	11.312
	5	0.0902218	0.396	446.748	9.264	4960.317	0.000202	8.543
	6	0.0893274	0.180	943.396	17.103	10729.614	0.000093	17.107
	7	0.0895841	0.180	805.348	9.292	9041.591	0.000111	8.464
Common Pb for 1440 Ma		0.9447853		15.400		16.300	0.061350	

50

Figure 3.6   York fit of ^{206}Pb/^{204}Pb vs. ^{207}Pb/^{204}Pb data from PE10.2.
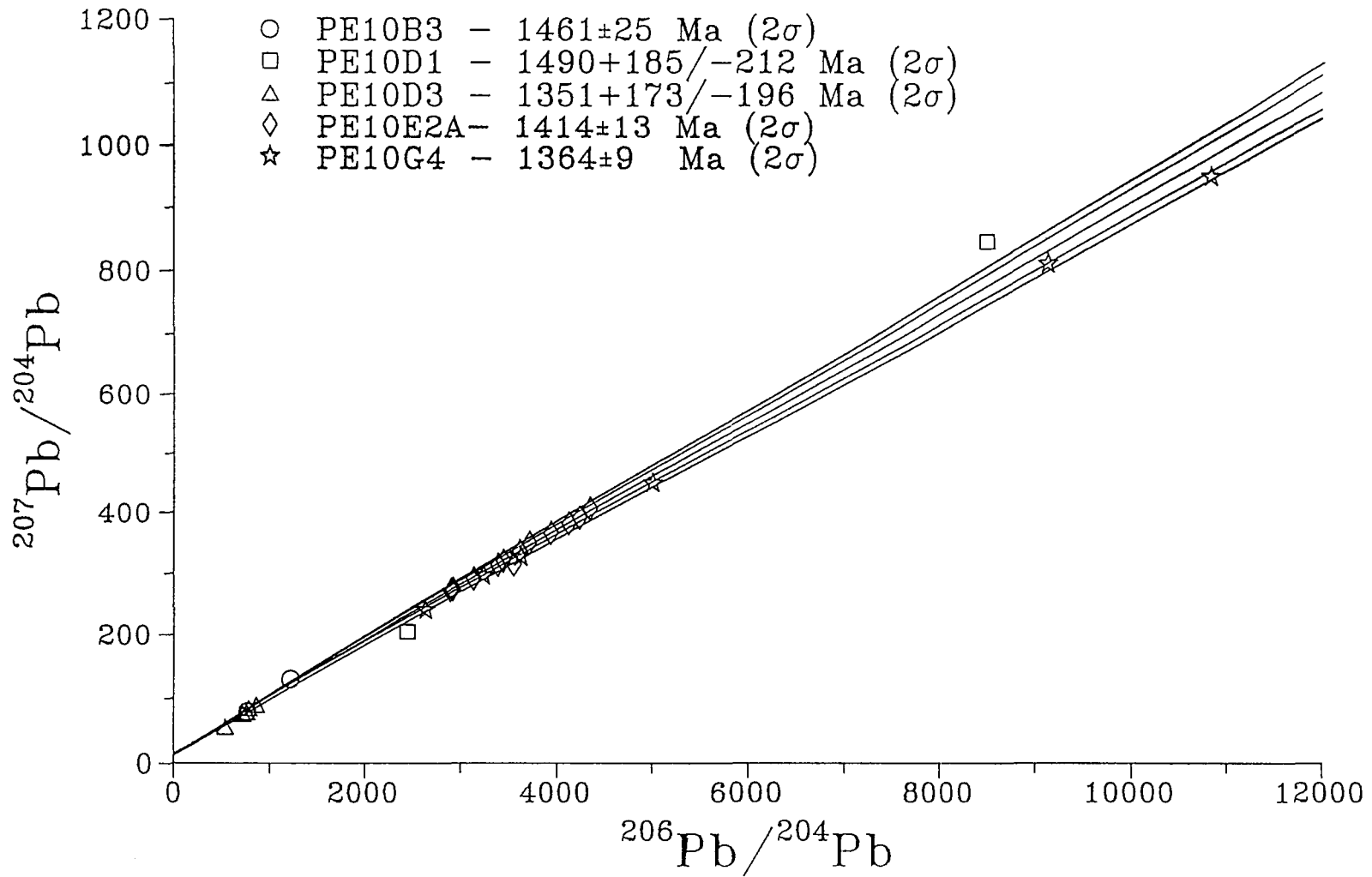
Figure 3.7   York fit of ^{204}Pb/^{206}Pb vs. ^{207}Pb/^{206}Pb data from PE10.2.

52
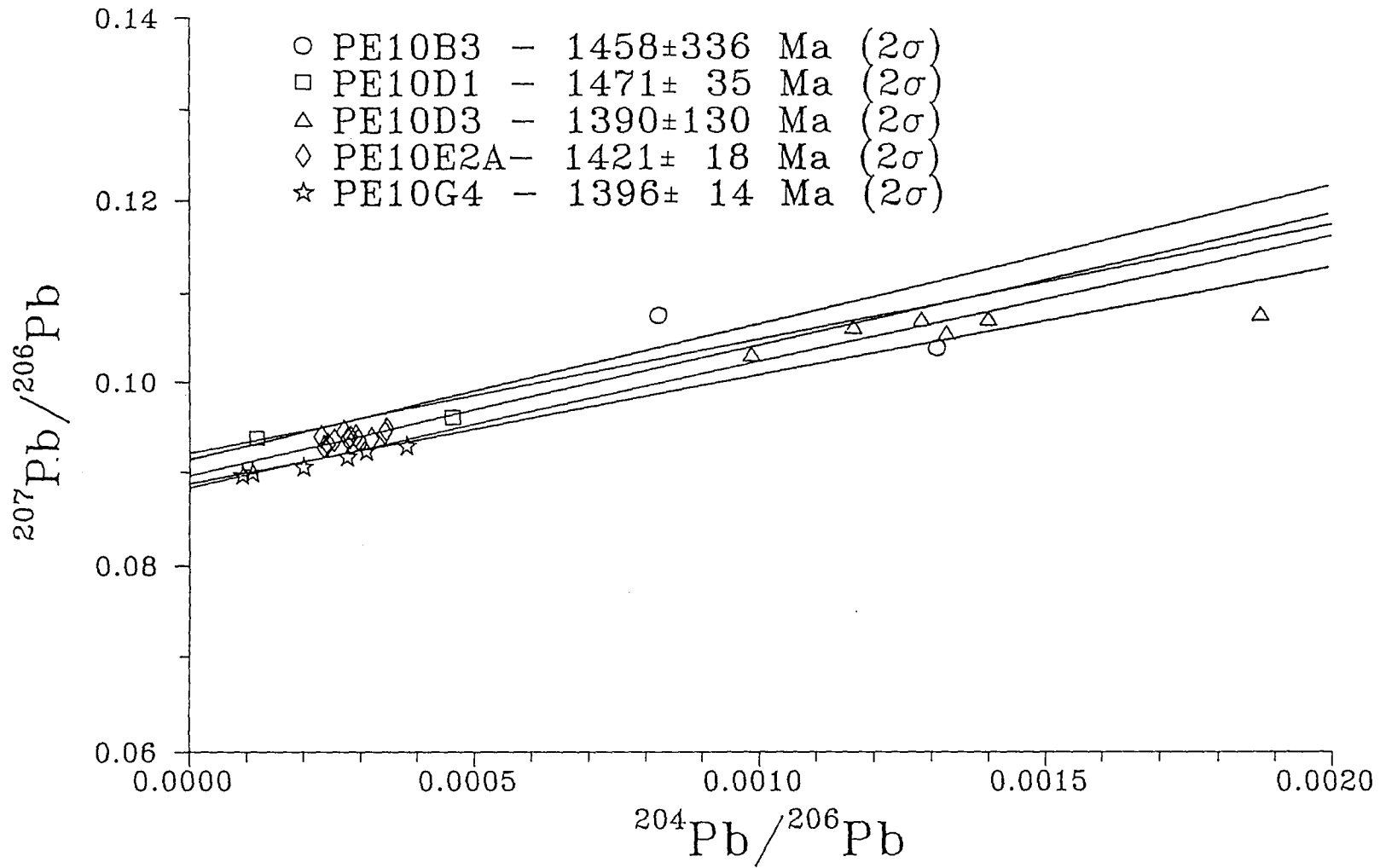
Figure 3.8 $^{207}Pb/^{206}Pb$ histogram of data from PE10.2.
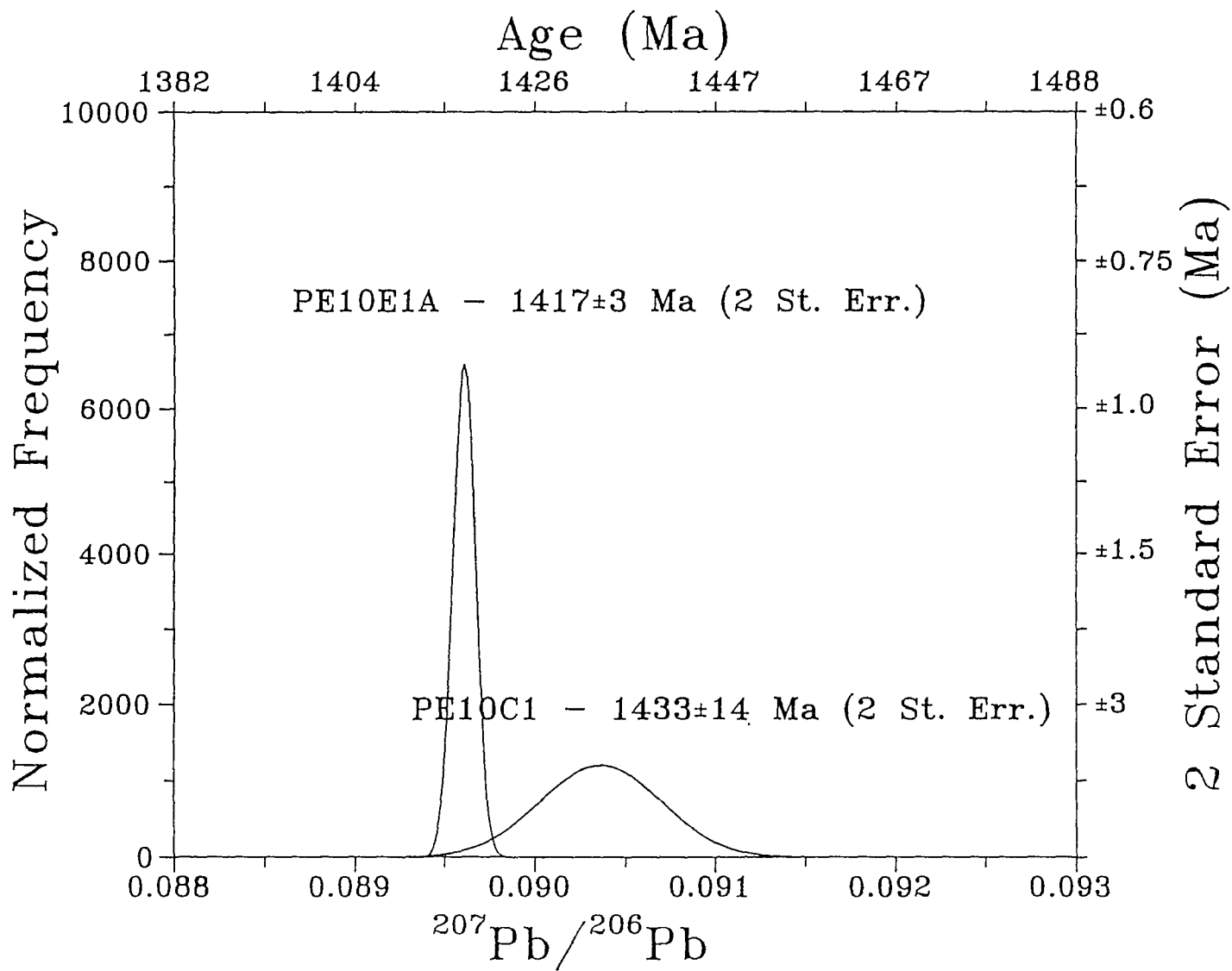
number of zircons sampled for PSK0.6 and PE10.2 were 27 and 22, of which 6 and 7 zircons were able to provide age data, respectively. The remaining 36 zircons either produced no Pb ion beam or produced low quality data. For 12 of 13 zircons, resultant ages were less than or equal to the age (within 2σ error) derived by Van Breeman *et al.* (1986). A pseudo-concordia diagram (Figure 3.9) was derived from the apparent ages and known concordia age. The amount of discordance for these 12 zircons varied from 28 to -6 % (error in apparent ages are not taken into account for this calculation). Positive discordance (values that lie below the concordia) can be due to Pb loss. This amount of discordance is reasonable due to the fractured appearance of the zircons which probably resulted in continual Pb loss. PE10.2 zircons appeared less fractured than PSK0.6, this is also reflected by the fact that the ages of PE10.2 zircons were more concordant than those of PSK0.6. Generally, in a given analysis, apparent age increases with decreasing common Pb. This implies that the most reliable age is the one with minimum common Pb. Finally, the one zircon from PSK0.6, known as PSKE6, had an apparent age of 1562 +44/-45 Ma which translates into an amount of discordance of -51%. It probably represents a mixing of an older xenolithic core with a younger rim formed at the time of plutonism. Unfortunately, no photographs of this zircon were made and age derived from the raw data (Table 3.2) is based upon two data points and one common Pb point. This is the

54

Figure 3.9 Pseudo-concordia of $^{207}Pb/^{206}Pb$ ages derived from PSK0.6 and PE10.2. Dashed line represents the discordia (as derived by Van Breeman *et al.*, 1986).

PSK0.6 and PE10.2
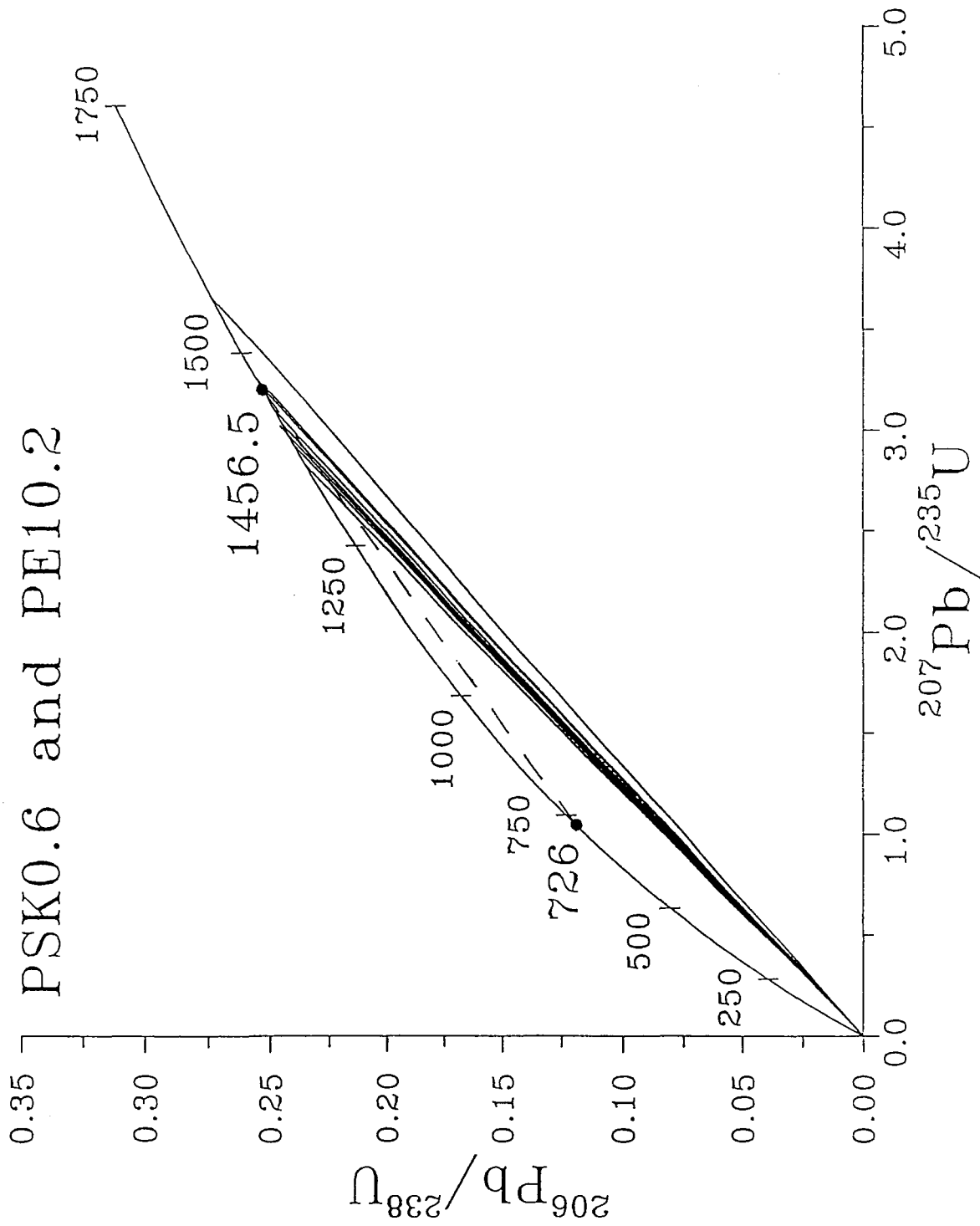
minimum amount of data that can be used to construct an isochron. Therefore, this age could be a construct of unsatisfactory data, i.e. large errors due to an unstable Pb beam.

3.2.4 Conclusions

The aim in studying the samples from these plutons was to discover if a granite that had undergone a high degree of metamorphism was possible to date accurately with the Pb evaporation method. The variation in ages of PSK0.6 and PE10.2 in Table 3.1 indicate that only a minimum age can be derived from a single zircon. Therefore, more than one zircon must be tested to take into account the variable amount of discordance caused by the upper amphibolite grade metamorphism. With the exception of the grain interpreted as inherited older Pb, the uppermost Pb-Pb age is in agreement with the U-Pb age derived by Van Breeman *et al.*(1986) Therefore, Pb-Pb analysis of multiple grains can be used as a reconnaissance age tool for dating polymetamorphic granites, but must be supplemented by U-Pb dating if a precise intrusion age is desired.

3.3 Pine Cove Pluton

3.3.1 General Geology

The Pine Cove pluton is located 5 km south of the Cosby Batholith in the Britt Domain (a.k.a. PINE, Figure 3.2). The pluton is a foliated granitic body with a mineralogy of quartz (20%), k-feldspar (20%) and biotite (10%) (Dickin, pers. comm.).

Zircon grains (Plate 3.5) are euhedral to subhedral prismatic crystals with l:w=2:1 to 4:1. The colour is pink with few black inclusions. Fractures are uncommon in these zircons. The size of the grains used for evaporation varied from 0.3 mm to 0.5 mm in length.

3.3.2 Previous Isotopic Work

The Pine Cove Pluton has not been dated by means of U-Pb or Rb-Sr geochronology. Work by Dickin (unpublished data) has resulted in a Nd model age of 2.41 Ga. This model age may imply that this pluton formed from a melt of Archean and Penokean aged crust.

Plate 3.5   Zircon grains from PINE.

0.25 mm
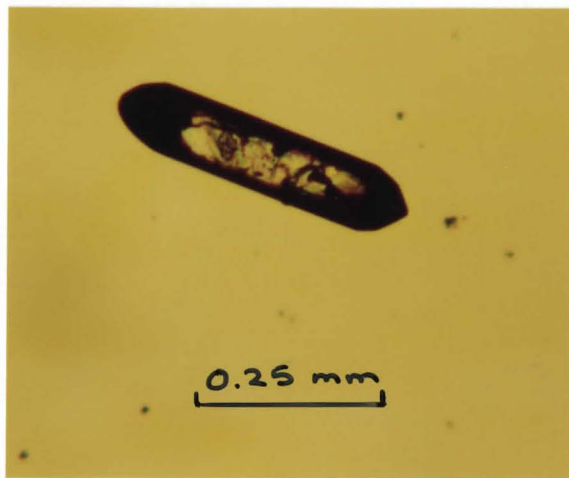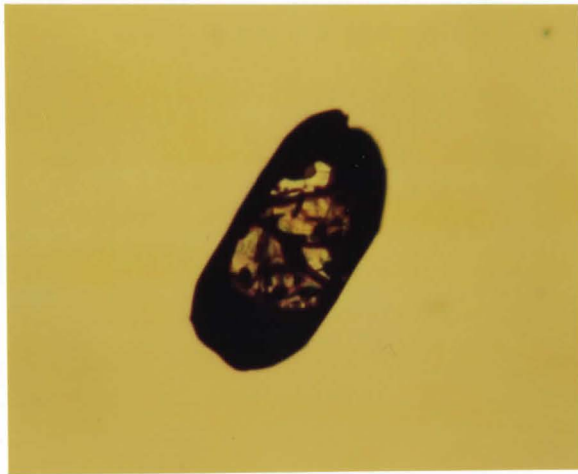
3.3.3 Results

The data from the Pine Cove Pluton (Table 3.4) contains a large amount of common Pb so that a direct average of $^{207}Pb/^{206}Pb$ could not be calculated. 12 zircons out of 16 provided data that could be used to calculate an age. The data from each zircon varied little in $^{206}Pb/^{204}Pb$ or $^{207}Pb/^{204}Pb$ so that a best fit line could not be accurately calculated. Therefore, the data from all 12 zircons were combined to define a slope (Figure 3.10) and intercept (Figure 3.11). The resultant ages are 1331±15 Ma and 1318±19 Ma (2σ), respectively. Both ages are within 2σ of each other. The MSWD of the slope is 0.85 which implies the error of ±15 is considered to be an overestimation. The MSWD of the intercept is equal to 1, thus the error of ±19 accurately describes the scatter in the data.

3.3.4 Conclusions

The Pine Cove Pluton is structurally a strategic intrusion since Dickin (pers. comm.) has shown by Sm-Nd dating of country rock screens within the body that it cross cuts and therefore postdates the juxtaposition of the two terrains (Archean and Penokean) identified by Nd model age dating (Dickin and McNutt, 1989 and Dickin *et al.*, 1990).

This means that the 1331±15 Ma minimum age of the Pine

Table 3.4 Raw data from PINE.

Name	Run	207Pb 206Pb	St. Err. (%)	207Pb 204Pb	St. Err. (%)	206Pb 204Pb	204Pb 206Pb	St. Err. (%)
PineA2P	1	0.2563263	0.353	19.947	1.091	77.709	0.012869	1.166
	2	0.2474941	0.218	21.337	1.072	86.148	0.011608	1.144
	3	0.2353376	0.208	22.033	0.188	94.174	0.010619	0.577
	4	0.2353442	0.445	22.678	1.126	96.254	0.010389	1.276
	5	0.2349841	0.284	22.345	0.470	95.157	0.010509	0.596
	6	0.2367409	0.188	23.061	0.629	97.452	0.010262	0.464
	7	0.2392079	0.306	23.023	1.006	96.423	0.010371	0.835
	8	0.2455911	0.544	23.251	1.333	94.826	0.010546	1.113
	9	0.2507737	0.69	24.691	1.760	98.724	0.010129	1.405
PineA3P	1	0.2467793	0.421	20.781	0.779	83.874	0.011923	0.840
	2	0.2281162	0.311	21.127	2.199	93.233	0.010726	2.332
	3	0.2148109	0.384	23.687	1.631	110.300	0.009066	1.346
	4	0.2060639	0.239	23.843	1.476	115.578	0.008652	1.580
	5	0.2047700	0.407	23.699	1.037	115.675	0.008645	1.283
	6	0.1968103	0.254	24.649	1.521	125.216	0.007986	1.367
	7	0.1955952	0.456	24.605	2.016	125.859	0.007945	1.815
	8	0.1865566	0.266	26.107	0.746	139.864	0.007150	0.784
	9	0.1887745	0.335	24.892	0.754	131.731	0.007591	0.860
	10	0.1873218	0.139	25.380	0.947	135.536	0.007378	0.884
	11	0.1903248	0.337	25.649	0.965	134.874	0.007414	1.018
	12	0.1917075	0.361	25.010	1.001	130.356	0.007671	0.723
	13	0.1886026	0.393	25.142	1.080	133.456	0.007493	0.908
	14	0.1859887	0.814	25.056	2.019	135.024	0.007406	1.663
PineA4P	1	0.1879663	0.384	24.666	1.228	131.163	0.007624	1.262
	2	0.1830023	0.308	24.815	1.507	135.558	0.007377	1.230
	3	0.1801861	0.515	25.165	2.724	139.604	0.007163	2.726
PineA5P	1	0.4175627	1.029	17.865	1.004	42.913	0.023303	1.820
	2	0.4289004	0.374	17.672	0.445	41.170	0.024289	0.220
	3	0.4148356	0.402	17.444	0.833	42.095	0.023756	1.054
	4	0.3979137	0.203	18.376	1.136	46.096	0.021694	1.269

Name	Run	207Pb/206Pb	St. Err. (%)	207Pb/204Pb	St. Err. (%)	206Pb/204Pb	204Pb/206Pb	St. Err. (%)
PineA6P	1	0.1368100	0.408	36.860	0.956	268.839	0.003720	1.326
	2	0.1308584	0.14	39.671	0.618	302.984	0.003301	0.687
	3	0.1290352	0.194	41.362	0.340	320.554	0.003120	0.256
	4	0.1271737	0.122	43.918	0.491	345.077	0.002898	0.531
	5	0.1251819	0.133	44.216	0.520	358.603	0.002789	0.458
	6	0.1225465	0.191	47.862	0.575	390.183	0.002563	0.685
	7	0.1166107	0.178	54.930	2.233	470.057	0.002127	2.284
	8	0.1142611	0.779	71.526	3.638	626.056	0.001597	3.384
PineA7P	2	0.2895858	0.483	20.136	1.592	69.544	0.014379	1.793
	3	0.2560890	0.554	22.273	1.597	85.854	0.011648	2.187
PineA8P	2	0.2518923	0.48	20.506	2.013	81.494	0.012271	1.784
	3	0.2543828	0.523	20.801	2.436	81.718	0.012237	2.156
	4	0.2584850	0.504	20.860	1.739	80.725	0.012388	1.404
	5	0.2596242	0.378	21.155	1.601	81.489	0.012272	1.762
	6	0.2734472	0.465	20.229	1.706	74.081	0.013499	1.774
	7	0.2719705	0.559	20.654	1.962	75.942	0.013168	1.735
PineA9P	1	0.1260937	0.693	42.285	1.530	334.180	0.002992	2.210
	2	0.1159781	0.371	52.114	0.598	448.853	0.002228	0.752
	3	0.1107896	0.261	59.401	1.501	535.504	0.001867	1.722
	4	0.1061648	0.217	69.414	1.120	653.253	0.001531	1.112
	5	0.1034095	0.257	77.303	1.712	747.943	0.001337	1.530
	6	0.1019366	0.19	83.735	3.069	820.681	0.001219	2.864
	7	0.1017967	0.297	86.581	2.354	850.702	0.001176	2.292
	8	0.1001118	0.15	102.879	1.546	1027.749	0.000973	1.255
	9	0.0982194	0.107	118.742	2.459	1209.044	0.000827	2.374
	10	0.0979685	0.274	117.392	3.193	1197.892	0.000835	2.889
	11	0.0973782	0.281	147.986	2.666	1524.158	0.000656	2.292

Name	Run	207Pb / 206Pb	St. Err. (%)	207Pb / 204Pb	St. Err. (%)	206Pb / 204Pb	204Pb / 206Pb	St. Err. (%)
PineA11P	1	0.3528765	0.154	18.252	0.211	51.716	0.019336	0.314
	2	0.3581824	0.095	18.200	0.194	50.813	0.019680	0.166
	3	0.3399982	0.394	18.449	0.183	54.179	0.018457	0.549
	4	0.3134421	0.468	19.021	0.394	60.609	0.016499	0.730
	5	0.2927337	0.307	19.654	0.490	67.088	0.014906	0.628
	6	0.2897542	0.341	19.490	0.638	67.338	0.014850	0.461
	7	0.3021032	0.445	20.241	1.379	66.981	0.014930	0.920
PineA12P	1	0.1673846	0.481	26.654	0.686	158.952	0.006291	0.937
	2	0.1571920	0.416	29.302	0.647	186.098	0.005374	0.773
	3	0.1525397	0.129	30.017	0.710	196.808	0.005081	0.663
	4	0.1494635	0.216	30.864	0.687	206.369	0.004846	0.756
	5	0.1457069	0.243	32.209	0.812	220.853	0.004528	0.699
	6	0.1458710	0.228	32.374	1.092	221.961	0.004505	0.928
	7	0.1409800	0.168	33.479	1.030	237.513	0.004210	1.030
	8	0.1404775	0.219	33.614	1.113	239.664	0.004173	1.078
	9	0.1390697	0.173	34.178	0.752	245.761	0.004069	0.578
	10	0.1396958	0.426	33.963	1.830	242.648	0.004121	1.989
PineA13P	1	0.5516485	1.013	17.717	1.025	32.015	0.031235	1.970
	2	0.4757794	0.367	17.715	0.602	37.181	0.026895	0.929
	3	0.4436371	0.225	18.021	0.386	40.593	0.024635	0.448
	4	0.4189594	0.37	18.156	0.641	43.319	0.023085	0.423
	5	0.4113231	0.21	18.021	0.311	43.796	0.022833	0.354
	6	0.3978179	0.226	18.191	0.475	45.711	0.021877	0.551
	7	0.3818506	0.535	18.935	0.537	49.507	0.020199	0.768
	8	0.3582921	0.394	18.930	0.608	53.115	0.018827	0.384
PineA15P	1	0.2402272	0.53	21.699	0.702	90.267	0.011078	0.924
	2	0.2388508	0.261	22.059	0.449	92.383	0.010825	0.553
Common Pb for 1330 Ma		0.9372761		15.436		16.469	0.060720	

mass fractionation correction=0.5%

Figure 3.10   York fit of ^{206}Pb/^{204}Pb vs. ^{207}Pb/^{204}Pb data from PINE.

Pine – 1331±15 Ma (2σ)
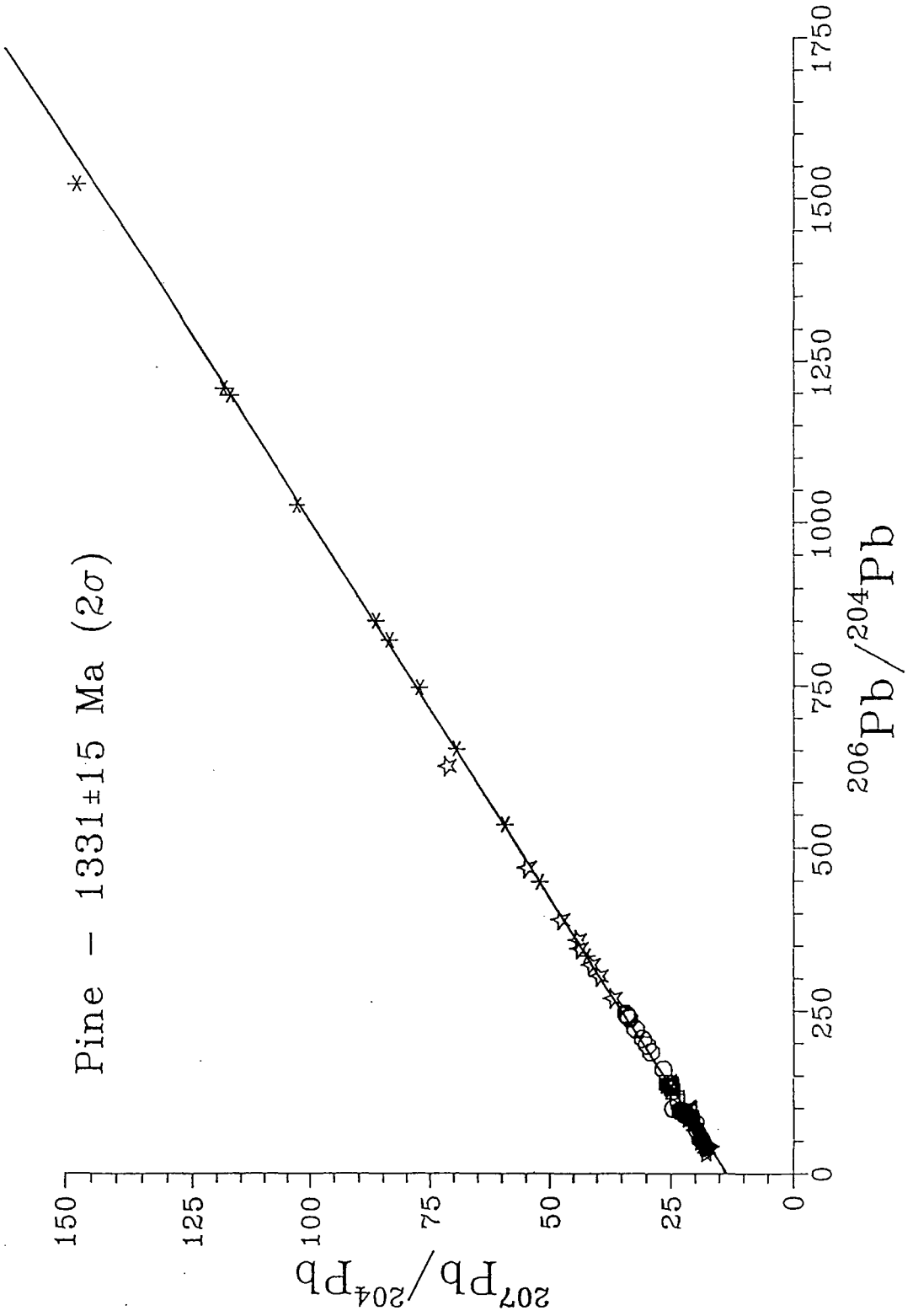
Figure 3.11   York fit of ^{204}Pb/^{206}Pb vs. ^{207}Pb/^{206}Pb data from PINE.

Pine – 1318±19 Ma (2σ)
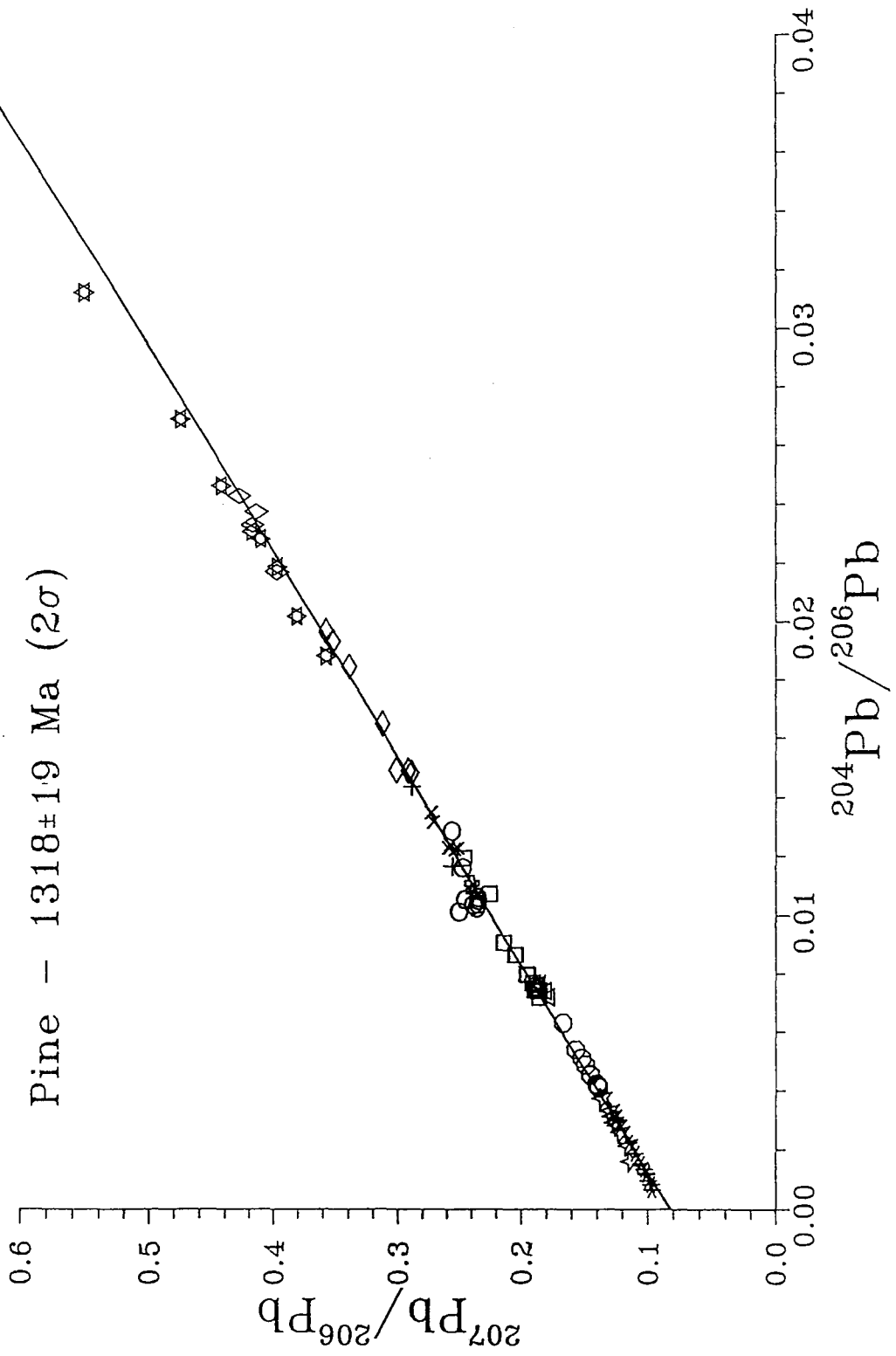
Cove pluton places a minimum age bracket on tectonic movement on the French River suture line, and constrains it to be a pre-Grenville structure. This is the first conclusive evidence for the existence of a pre-Grenville terrain boundary in the Grenville Province of Ontario.

3.4 Grenville Gneiss

3.4.1 General Geology

PE11.3 is a sample of a quartz-feldspathic gneiss common to the Central Gneiss Belt. It is located near the Britt Pluton, less than 5 km south of the proposed Penokean suture.

Its normative mineralogy of corundum=5.1% and quartz=28.5% (Dickin, unpublished data) imply that PE11.3 may be considered a paragneiss, though no sedimentary structures are seem in hand sample.

The zircon grains (Plate 3.6) in this study were all approximately 0.5 mm in length, but varied in width such that the length to width ratio ranged from 1:5 to 1:2.5. The colour of the zircons is clear, but many appear reddish due to hematite along fractures. All zircons were fractured to some degree, though less than those of PSK0.6 and PE10.2. The crystal shape varies from euhedral to rounded. The amount of roundedness ranges from only the edges and points of the zircon being rounded to an oval shaped zircon. Paragneisses are known to contain rounded zircons, since the temperature of metamorphism usually is not high enough to recrystallize them (Blatt *et al.*, 1980). Some appear subhedral due to having been broken during the rock crushing process. The zircons contain very few inclusions, most of which appeared black. The lack of zircons with fractures and inclusions may be due

Plate 3.6 Zircon grains from PE11.3: A) PE11E4P, B) PE11C3, and C) PE11E2P.

A

B

C

0.5 mm

to the fact that they are structurally weaker than clear zircons and thus, would not survive transport or crushing (Blatt *et al.*, 1980).

In thin section (Plate 3.7), the zircons are smaller in size, i.e. 0.1 mm in length. Zoning within some of the zircons is apparent (Plate 3.7B). It is unclear whether this is euhedral zoning or metamorphic rims around an older core. Euhedral zoning is usually indicative of one period of growth, i.e. crystallization, in which the rims are parallel to one another and grow outwards from the centre. An older core is not necessarily found in the centre of a metamorphic zircon and its faces can be at any angle to that of the metamorphic rims. It is unclear whether the zircon shown in Plate 3.7B has a core. It is the only zircon seen in thin section that had a core or zoning. Other zircons (Plate 3.7A) do not show any obvious zoning or cores, but do show the presence of black inclusions.

3.4.2 Previous Isotopic Work

The Nd model age of PE11.3 is 1.9 Ga (Dickin, unpublished data). Thus, it appears, as with the granitic plutons (PSK0.6 and PE10.2), this gneiss was derived from an Early Proterozoic-aged terrain.

The high degree of regional metamorphism has reset the "apparent Rb-Sr ages" to approximately 1100 Ma. This age

66

Plate 3.7A PE11.3 zircons (Z) with black inclusions in thin
section (plane polarized light).

Plate 3.7B PE11.3 zircon (Z) with zoning and/or possible
older core in thin section (plane polarized light).

A

Z

Z

0.1 mm

B

Z
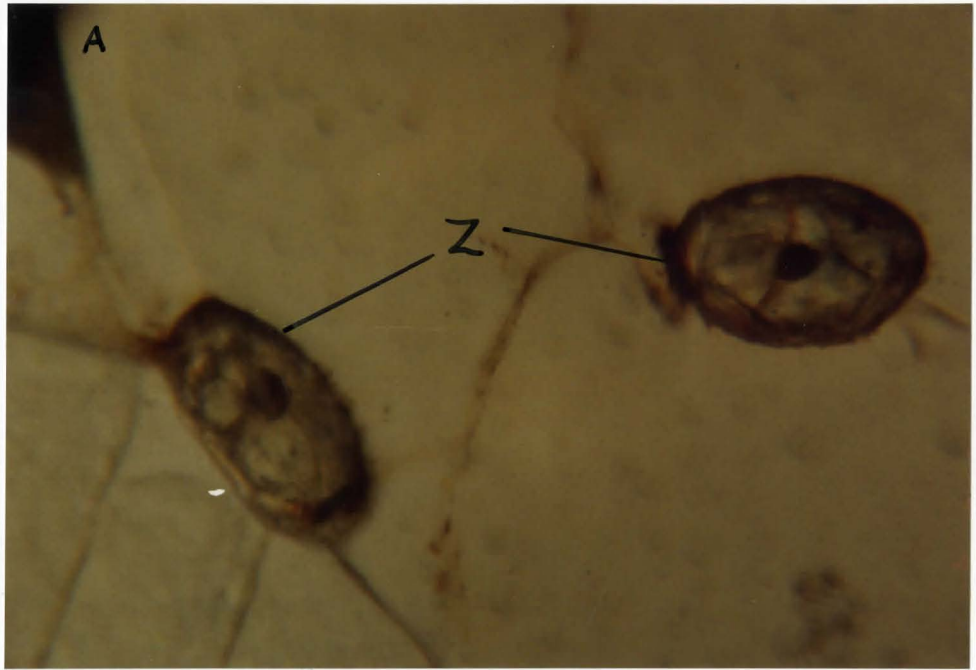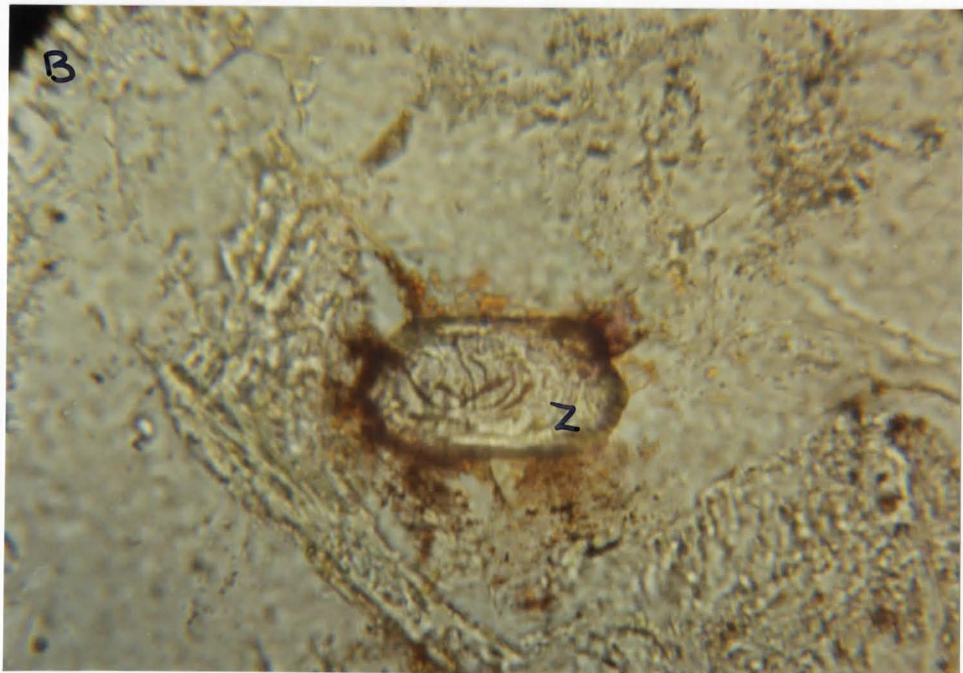
agrees with the time of shearing between the Domains in the Central Gneiss Belt (Van Breeman *et al.*, 1986).

3.4.3 Results

The apparent Pb ages of PE11.3 are shown in Table 3.5. In total, 19 zircons were studied, but only 6 resulted in usable data. The apparent ages range from 1030±2 Ma to 1101±7 Ma. The raw data used to derive these ages is given in Table 3.6. The ages of 2 zircons were derived by the slope and intercept method (Figure 3.12 and 3.13). The ages of 4 of the 6 zircons could be calculated directly from the average of the ^{207}Pb/^{206}Pb data (Figure 3.14). The lack of common Pb is probably due to the sparseness of inclusions within the zircons. These zircons provided a very stable Pb ion beam for the acquisition of more blocks of data than PSK0.6 and PE10.2. This resulted in errors in the ages, on average, that are lower than those of the previous samples. The ages of the two zircons, PE11E1P and PE11E4P, that could be calculated by the slope and intercept method, resulted in the close agreement (within 2σ) of the two methods.

Table 3.5 Ages of zircons from PE11.3 from the Britt Domain. Ages derived by a York fit of $^{206}Pb/^{204}Pb$ vs. $^{207}Pb/^{204}Pb$ data and/or $^{204}Pb/^{206}Pb$ vs. $^{207}Pb/^{206}Pb$ data or an average of $^{207}Pb/^{206}Pb$ data.

Sample	York Fit of 206/204 vs. 207/204		Age (Ma)	Error	York Fit of 204/206 vs. 207/206		Age (Ma)	Error	Average of 207/206		Age (Ma)	Error
	slope w. mfc	2 sigma		2 sigma	intercept w. mfc	2 sigma		2 sigma	average w. mfc	2 sigma /sqrt(n) n=#runs		2 sigma /sqrt(n)
BRITT DOMAIN												
PE11C1									0.073941	0.000479	1040	13
PE11C2									0.073721	0.000320	1034	9
PE11C3									0.076235	0.000265	1101	7
PE11C4									0.073568	0.000073	1030	2
PE11E1P	0.074951	0.001451	1067	39	0.075024	0.001806	1069	48				
PE11E4P	0.073829	0.000308	1037	9	0.073829	0.000346	1037	9				

mfc=mass fractionation correction of 0.5%

69

Table 3.6 Raw data from PE11.3.

Name	Run	207/206	St. Err. (%)	207/204	St. Err. (%)	206/204	204/206	St. Err. (%)
PE11C1	1	0.0738423	0.309	-772.260	99.990	-12048.193	-0.000083	99.990
	2	0.0730970	0.633	773.814	64.380	11148.272	0.000090	63.380
	3	0.0737788	0.505	279.447	99.990	4502.476	0.000222	99.990
Common Pb for 1040 Ma		0.9120918	0.000	15.501	0.000	16.995	0.058841	0.000
PE11C2	1	0.0731829	0.782	-84.903	18.435	-1169.864	-0.000855	17.098
	2	0.0732962	0.634	-9000.900	99.990	-200000.000	-0.000005	99.990
	3	0.0731189	1.163	-439.560	99.990	-5727.377	-0.000175	93.885
	4	0.0738187	0.924	441.462	99.990	6565.988	0.000152	99.990
Common Pb for 1030 Ma		0.9112443	0.000	15.503	0.000	17.013	0.058779	0.000
PE11C3	1	0.0751648	0.231	-6587.615	99.990	-57803.468	-0.000017	99.990
	2	0.0757950	0.182	6896.552	41.929	88495.575	0.000011	49.557
	3	0.0758962	0.148	2771.619	26.802	36363.636	0.000028	25.390
	4	0.0762211	0.068	4035.513	44.778	52083.333	0.000019	40.807
	5	0.0758270	0.144	3453.039	18.142	45454.545	0.000022	16.768
	6	0.0758992	0.064	2233.140	34.645	28818.444	0.000035	31.159
	7	0.0761857	0.266	1841.621	27.695	24752.475	0.000040	25.382
Common Pb for 1100 Ma		0.9171601	0.000	15.489	0.000	16.888	0.059214	0.000
PE11C4	1	0.0728835	0.135	-8561.644	99.990	-106382.979	-0.000009	99.990
	2	0.0732048	0.192	4184.100	11.368	57471.264	0.000017	10.336
	3	0.0731374	0.087	5353.319	45.539	74626.866	0.000013	44.150
	4	0.0730099	0.137	4980.080	18.852	67567.568	0.000015	17.656
	5	0.0732245	0.054	4559.964	31.277	61349.693	0.000016	28.977
	6	0.0732742	0.086	6570.302	42.599	90090.090	0.000011	39.002
	7	0.0730688	0.082	6172.840	72.779	79365.079	0.000013	65.311
	8	0.0733405	0.106	3106.555	29.591	42372.881	0.000024	28.864
	9	0.0732052	0.009	4962.779	9.547	67567.568	0.000015	8.605
	10	0.0733491	0.121	5263.158	27.646	71942.446	0.000014	26.374
	11	0.0736914	0.096	34246.575	99.990	370370.370	0.000003	99.990
Common Pb for 1020 Ma		0.9103987	0.000	15.505	0.000	17.031	0.058716	0.000

Name	Run	207 / 206	St. Err. (%)	207 / 204	St. Err. (%)	206 / 204	204 / 206	St. Err. (%)
PE11E1P	1	0.0822045	0.506	145.332	2.179	1770.538	0.000565	2.461
PE11E1PA	1	0.0812113	0.276	178.333	5.789	2186.270	0.000457	5.704
	2	0.0830869	0.891				0.000547	11.582
Common Pb for 1070 Ma				15.496		16.942	0.059025	
PE11E4P	1	0.0858308	0.136	99.859	0.513	1164.009	0.000859	0.435
	2	0.0855792	0.166	100.507	0.649	1174.536	0.000851	0.742
	3	0.0851940	0.231	99.805	0.737	1171.234	0.000854	0.613
	4	0.0858289	0.069	96.697	0.540	1126.761	0.000888	0.519
	5	0.0862971	0.147	93.565	0.557	1084.599	0.000922	0.559
	6	0.0864130	0.277	92.276	0.471	1067.464	0.000937	0.365
	7	0.0848424	0.101	105.641	1.013	1244.710	0.000803	1.008
	8	0.0844767	0.070	108.559	0.389	1285.017	0.000778	0.354
	9	0.0848807	0.094	107.989	0.485	1272.103	0.000786	0.469
	10	0.0847877	0.061	109.111	0.427	1287.001	0.000777	0.420
	11	0.0850062	0.054	110.355	0.912	1297.185	0.000771	0.878
Common Pb for 1030 Ma				15.503		17.013	0.058779	

Figure 3.12   York fit of ^{206}Pb/^{204}Pb vs. ^{207}Pb/^{204}Pb data from PE11.3.
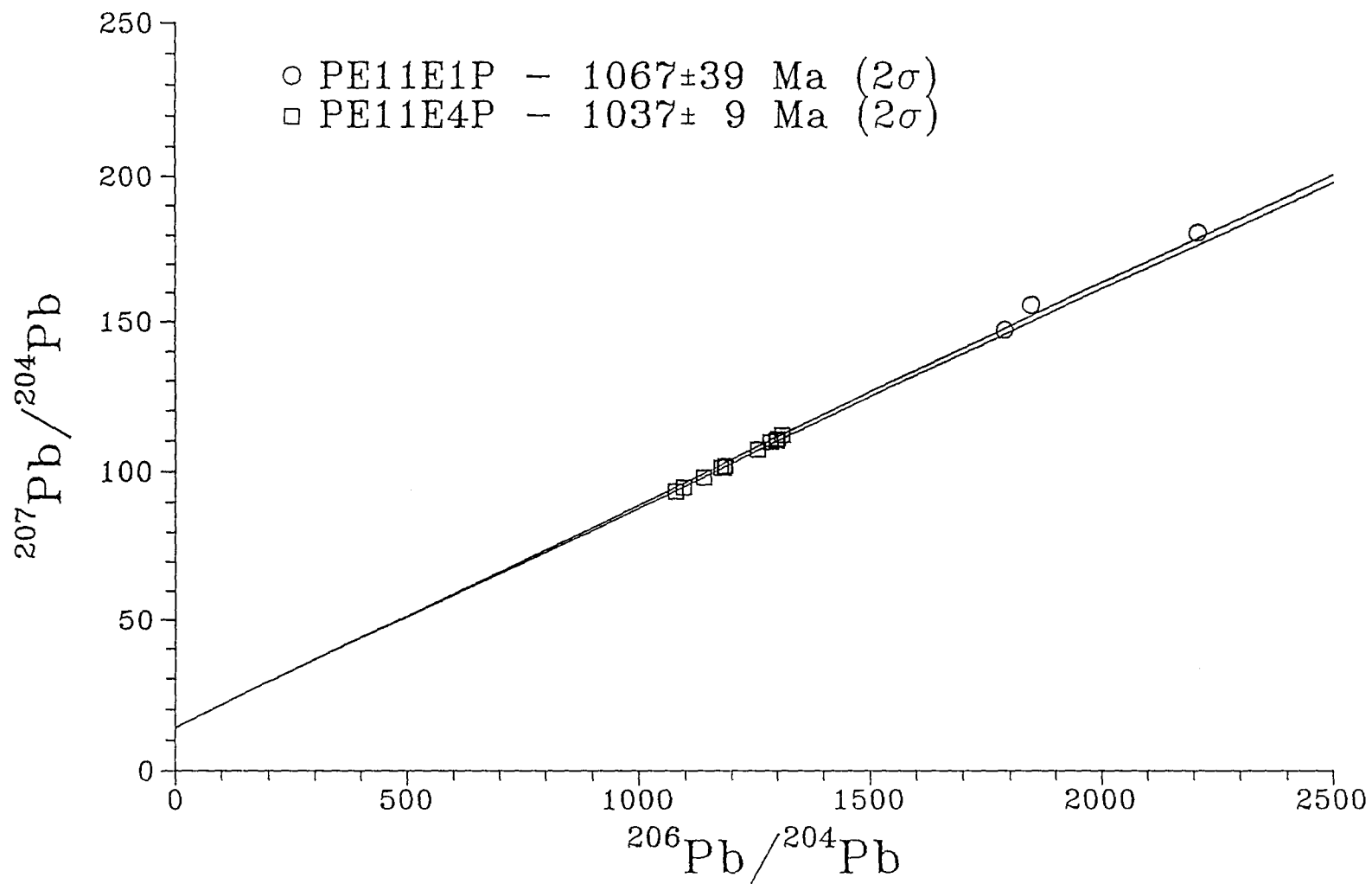
Figure 3.13   York fit of $^{204}Pb/^{206}Pb$ vs. $^{207}Pb/^{206}Pb$ data from PE11.3.
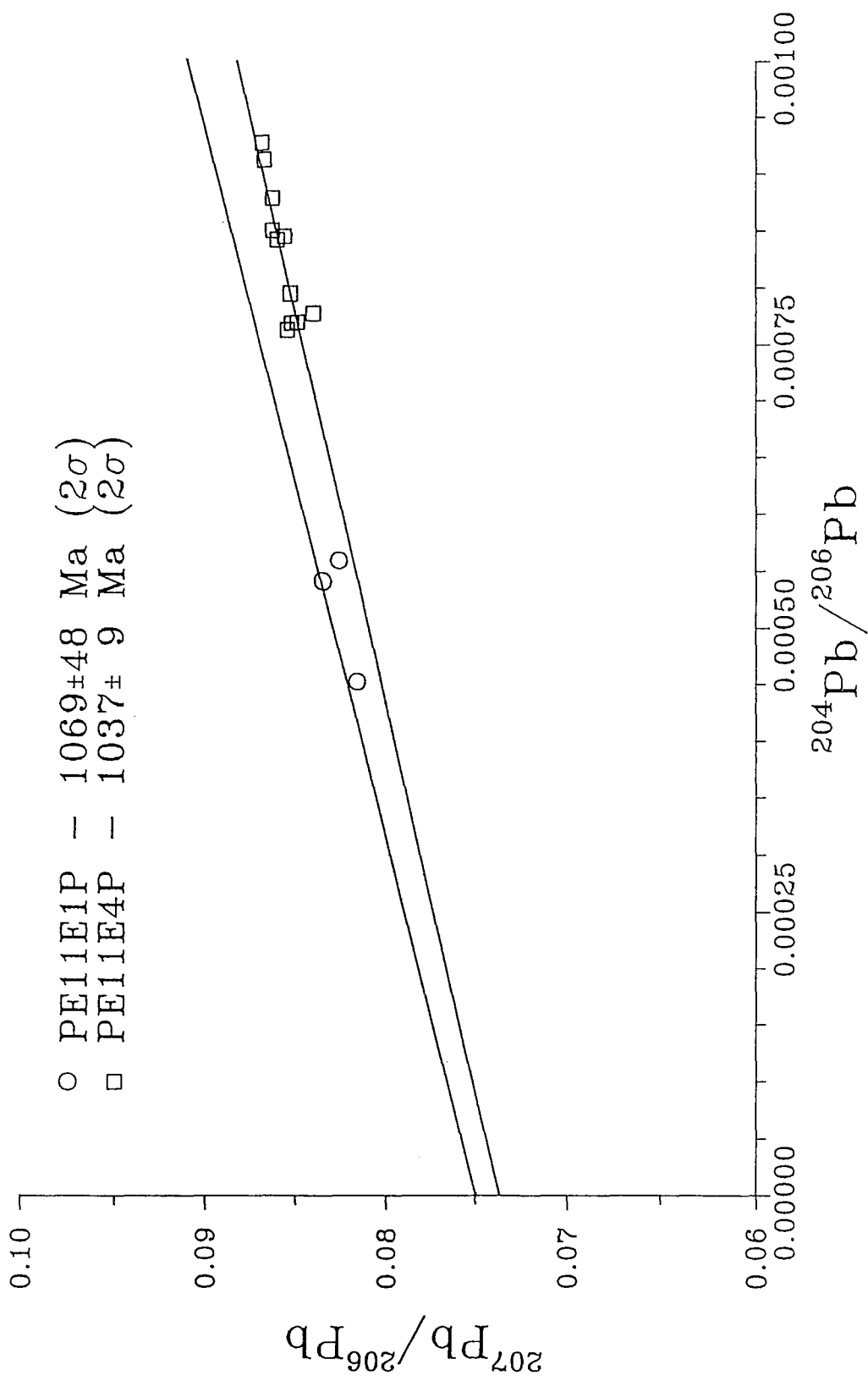
Figure 3.14 ^{207}Pb/^{206}Pb histogram of data from PE11.3.

Age (Ma)

986   1014   1041   1069   1095   1121

PE11C1 — 1040±13 Ma (2 St. Err.)
PE11C2 — 1034± 9 Ma (2 St. Err.)
PE11C3 — 1101± 7 Ma (2 St. Err.)
PE11C4 — 1030± 2 Ma (2 St. Err.)

Normalized Frequency

2 Standard Error (Ma)

$^{207}Pb/^{206}Pb$
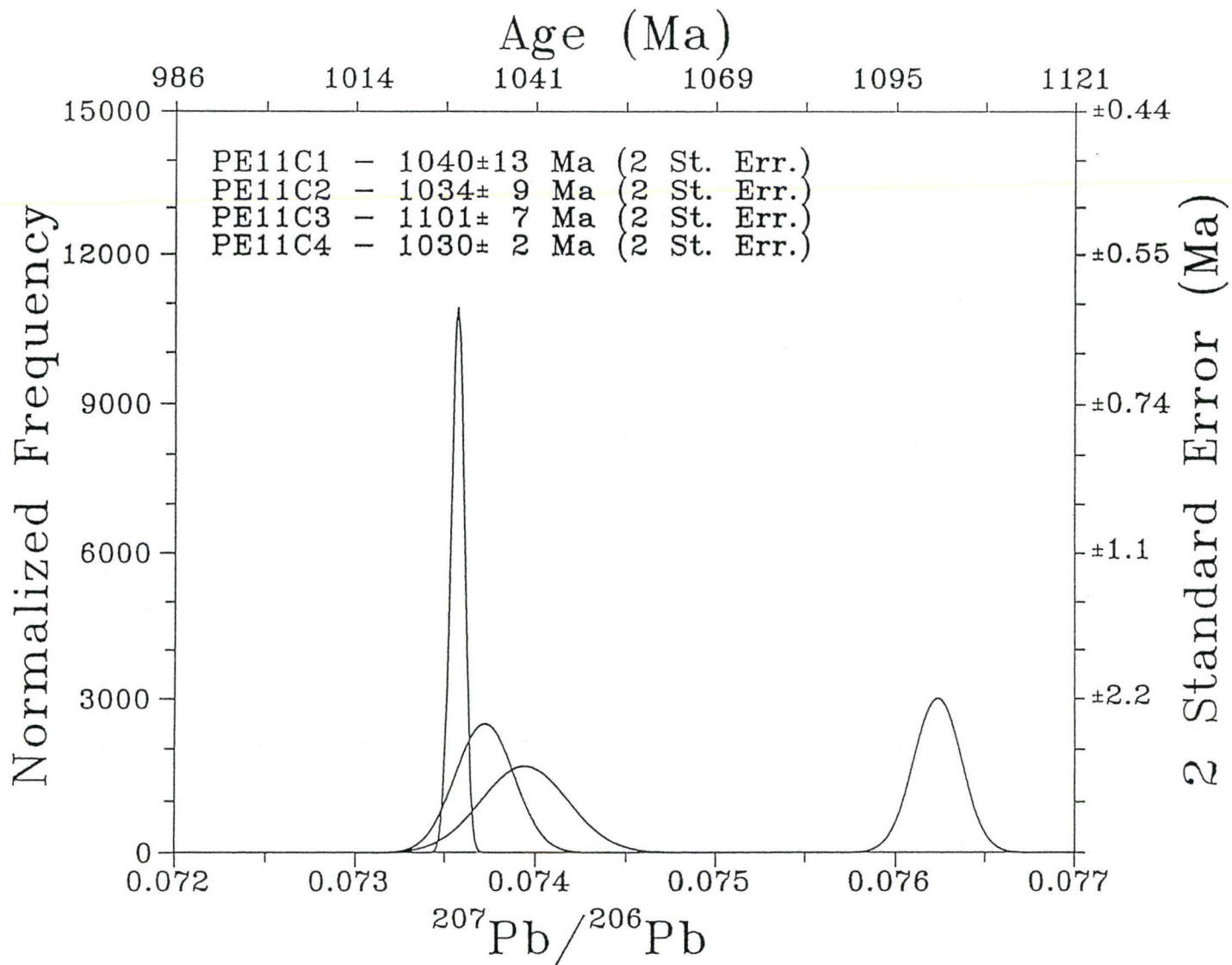
3.4.4 Conclusions

The study of a paragneiss that has undergone upper amphibolite facies metamorphism reveals that there has been a complete isotopic resetting to the time of last metamorphism. The samples of the orthogneisses and the paragneiss, PEll.3, are found within ten kilometres of each other. The response to metamorphism of different lithologies at different localities reveal different ages. The small zircons of the paragneiss were probably easier to reset than those from the orthogneisses.

3.5 French River Quartzite

3.5.1 General Geology

The French River Quartzite (CBQ) is an orthoquartzite located north of the proposed Penokean suture in the Britt Domain. The sample was collected near Highway 535 east of Highway 69.

The Ontario Geological Survey (OGS) Report 116 of the Burwash area (Lumbers, 1975) described CBQ as a quartzite gneiss. It "resembles a quartz-rich metasandstone facies of the Mississagi Formation in the adjacent Southern Province". It is inferred to be an extension of the Mississagi formation on the basis of a similar depositional environment. The OGS report describes both the French River and Mississagi formation quartzite as having been derived from "mature, well-sorted sands". The environment of deposition is thought to be a shallow water delta or littoral zone.

In thin section, CBQ is dominated by quartz (approximately 95%) with weakly aligned biotite. The average size of the quartz grains is 4mm in diameter. Apatite and zircon occur as accessory minerals.

The zircons (Plate 3.8 and 3.9) appear typical of detrital grains (Poldervaart, 1955). The average size of the zircons was smaller than previous samples due to abrasion by transport or sorting in the sedimentary environment. The

75

Plate 3.8 A) and B) CBQ zircons (Z) in thin section (plane polarized light).

Plate 3.9 Heavy mineral fraction from CBQ. Zircons (Z) are euhedral to slightly rounded colourless crystals. Apatite (yellow square crystals) are also present.

A

Z

0.15 mm

B

Z

0.15 mm

Z

1.0 mm
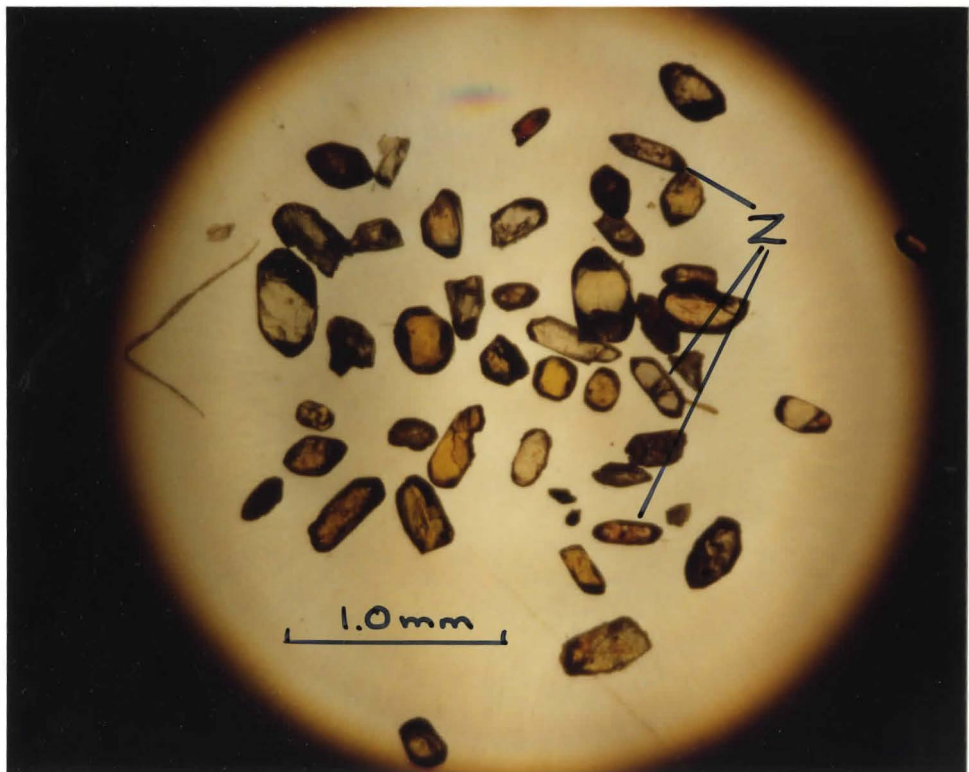
zircons studied were approximately 0.25 mm in length. The grains also showed differing amounts of fracturing and roundedness. The colour ranged from a very light pink to a darker pink. Based only upon colour, there seemed to be only one population of zircons. The colour could not be used to indicate provenance since the colour may only be due to varying amounts of reddish hematite along fractures formed during weathering. Under ultraviolet light different detrital populations may sometimes be distinguished by the amount of fluorescence (Blatt *et al.*, 1980). The zircons from CBQ, however, showed no discernable difference in fluorescence. Most zircons are fractured, but show no obvious zoning or older cores. Thus, the provenance is believed to be igneous, rather than metamorphic, in origin.

3.5.2 Previous Isotopic Work

The French River Quartzite has not been previously dated by the U-Pb method. Dickin and McNutt (1989) have derived a Sm-Nd age for the sample CBQ. It resulted in a model age of 2.42 Ga. Since CBQ is a metasedimentary rock, this model age is believed to be the result of the mixing of sediment of two differently aged terrains. One contributing terrain is believed to the Archean-aged (2.7 Ga) Superior Province to the north. The age of the younger source of sediment is not obvious since it could be a Penokean (1.85-1.9) Ga or

Hudsonian (1.7 Ga) terrain to the south. Zircon dating of the detrital grains would help resolve this question of provenance.

3.5.3 Results

Only 4 zircons of 52 studied resulted in usable data to derive ages. The small size and presumably low concentrations of Pb made these samples difficult to analyze. The ages of the four zircons is given in Table 3.7 and the raw data in Table 3.8.

The ages were determined for one zircon, CBQA1 by both the slope and intercept method (Figure 3.15 and 3.16) of the data since common Pb was present. Both ages, 1883 ± 3 and 1885 ± 4 Ma, agree within error. The age of CBQK6P could not be calculated using the intercept method due to large errors in its $^{207}Pb/^{206}Pb$ data. The remaining two zircons, CBQB8 and CBQG2, were determined by the average of their $^{207}Pb/^{206}Pb$ data (Figure 3.17 and 3.18). Two of the three zircons from the 1.9 Ga terrain, have ages that agree within 2σ. The third has a large error, 1930±40 Ma, so this age could be ignored. The agreement of the ages indicates that their has been no large degree of Pb loss from these zircons.

Table 3.7 Ages of zircons from CBQ from the Britt Domain. Ages derived by a York fit of $^{206}Pb/^{204}Pb$ vs. $^{207}Pb/^{204}Pb$ data and/or $^{204}Pb/^{206}Pb$ vs. $^{207}Pb/^{206}Pb$ data or an average of $^{207}Pb/^{206}Pb$ data.

Sample	York Fit of 206/204 vs. 207/204		Age (Ma)	Error	York Fit of 204/206 vs. 207/206		Age (Ma)	Error	Average of 207/206		Age (Ma)	Error
	slope w. mfc	2 sigma		2 sigma	intercept w. mfc	2 sigma		2 sigma	average w. mfc	2 sigma /sqrt(n) n=#runs		2 sigma /sqrt(n)
BRITT DOMAIN												
CBQA1	0.115194	0.000211	1883	3	0.115351	0.000232	1885	4				
CBQB8									0.186754	0.001640	2714	14
CBQG2									0.116080	0.000780	1897	12
CBQK6P	0.118279	0.002608	1930	40								

mfc=mass fractionation correction of 0.5%

Table 3.8   Raw data from CBQ.

Name	Run	207/206	St. Err. (%)	207/204	St. Err. (%)	206/204	204/206	St. Err. (%)
CBQA1	1	0.1156313	0.077	1763.047	8.069	15243.902	0.000066	7.502
	2	0.1159217	0.041	1228.803	3.167	10615.711	0.000094	2.903
	3	0.1158887	0.102	1237.777	3.774	10695.187	0.000094	3.608
	4	0.1159040	0.065	1395.673	6.321	11990.408	0.000083	5.596
	5	0.1158473	0.047	1416.832	5.811	12269.939	0.000082	5.790
	6	0.1156591	0.045	1662.510	7.633	14388.489	0.000070	7.269
	7	0.1161526	0.042	1544.163	5.888	13262.599	0.000075	5.655
Common Pb for 1890 Ma		0.9909641		15.244		15.383	0.065007	
CBQB8	1	0.1866438	0.475	-337.701	99.990	-2115.059	-0.000473	99.990
	2	0.1850063	0.706	122.675	30.792	671.682	0.001489	28.869
Common Pb for 2700 Ma		1.0773744		14.690		13.635	0.073341	
CBQG2	1	0.1155026	0.336	-122.742	91.460	-1142.857	-0.000875	89.722
Common Pb for 1890 Ma		0.9909641		15.244		15.383	0.065007	
CBQK6P	2	0.2049221	1.405	32.357	0.987	160.847	0.006217	0.903
Common Pb for 1920 Ma		0.9939956		15.230		15.322	0.065266	

Figure 3.15 York fit of ^{206}Pb/^{204}Pb vs. ^{207}Pb/^{204}Pb data from CBQ.
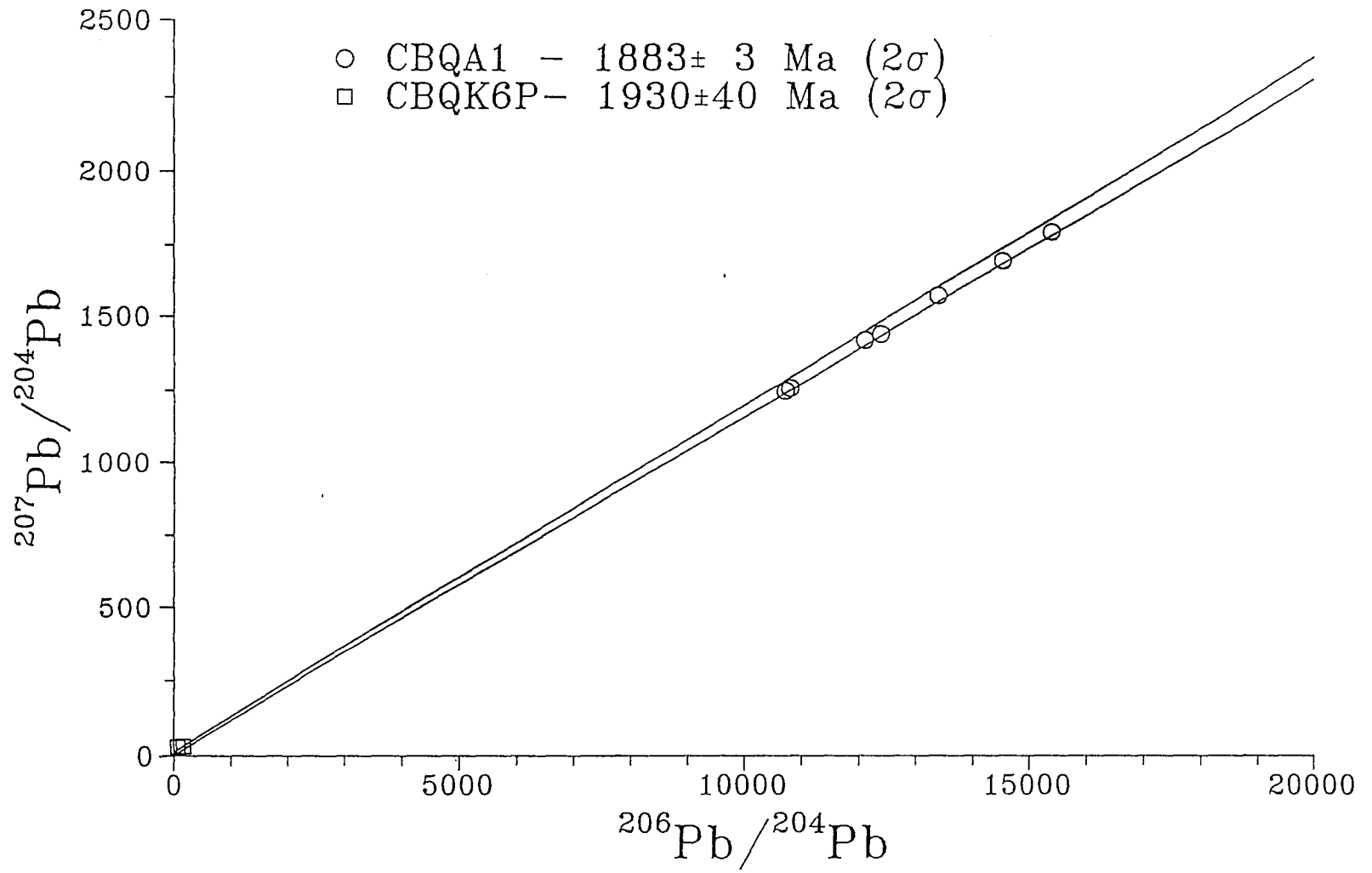
Figure 3.16 York fit of ^{204}Pb/^{206}Pb vs. ^{207}Pb/^{206}Pb data from CBQ.

CBQA1 — 1185±4 Ma(2σ)
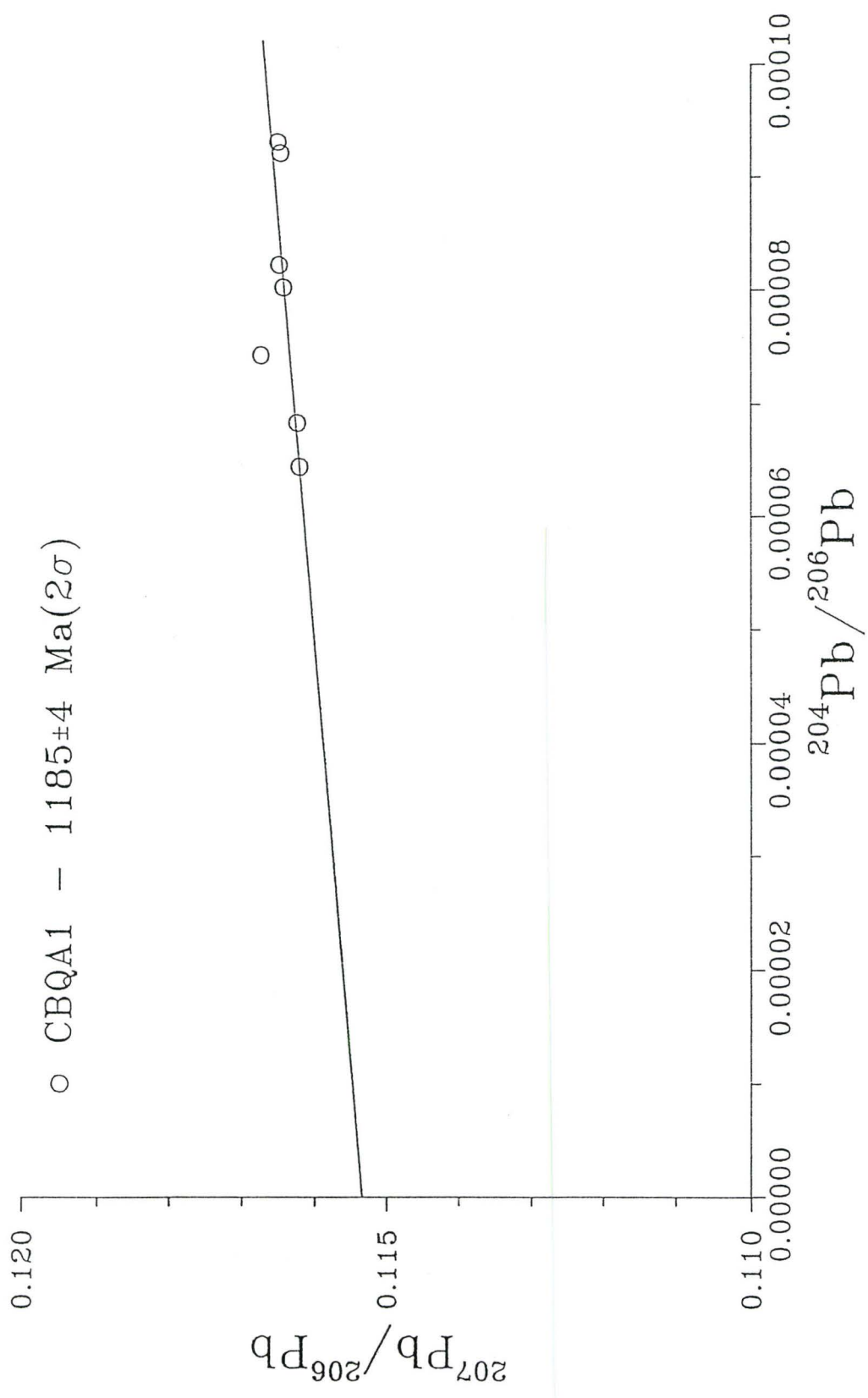
Figure 3.17 ^{207}Pb/^{206}Pb histogram of data from CBQ.
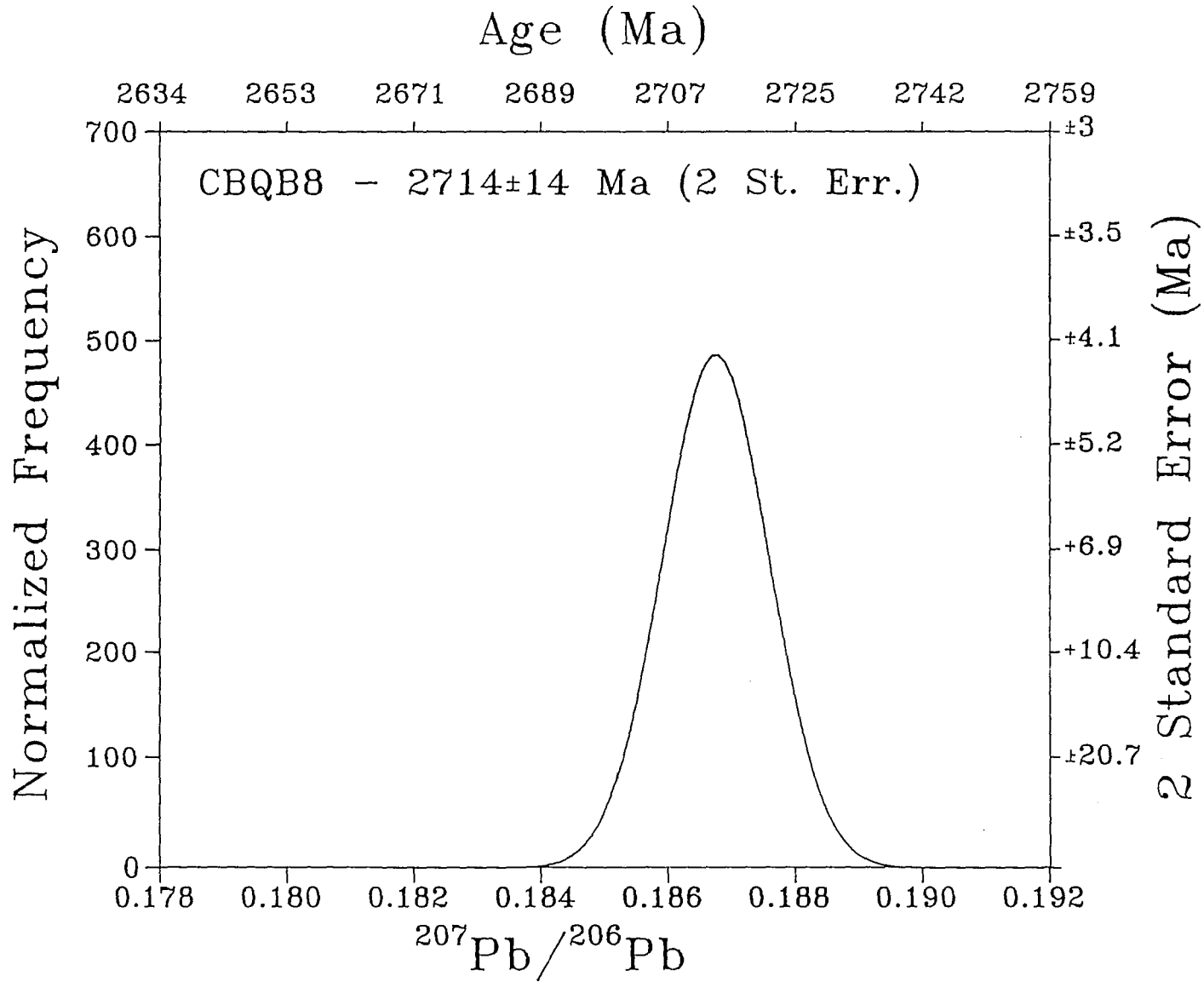
Figure 3.18 ^{207}Pb/^{206}Pb histogram of data from CBQ.
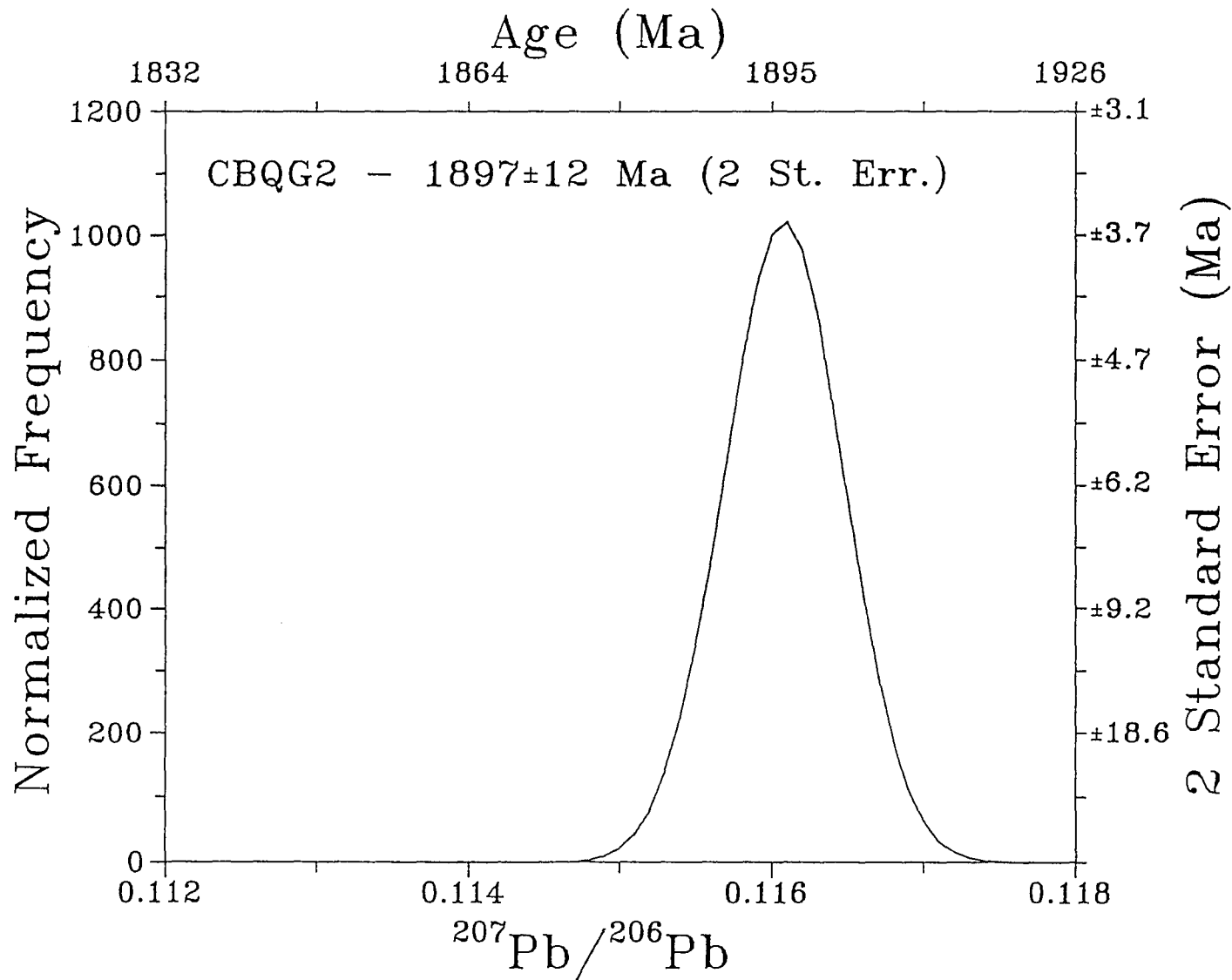
3.5.4 Conclusions

CBQ, an orthoquartzite, is a metasediment which originated from material from two different terrains (Figure 3.19). They are an Archean terrain reflecting the Kenorean orogeny (2.7 Ga) and an Early Proterozoic terrain from the Penokean orogeny (1.9 Ga). The age of deposition of the Mississagi Formation is thought to be between 2.45 and 2.25 Ga (Roscoe, 1973). The lower limit is defined by the presence of cross-cutting Nippising diabase dykes that are 2.2 Ga old (Fairbairn *et al.*, 1969). The presence of 1.9 Ga old zircons in CBQ imply that the quartzite could not be an extension of the Mississagi Formation, but may have been deposited in a similar environment. The Cosby batholith is an anorogenic pluton of approximately the same age (1400 Ma) as the Britt Pluton (Lumbers, 1975). Surveys of the area imply that it intrudes into the quartzite. Metasedimentary inclusions near the contact of the batholith imply contamination of the pluton by the metasediments (Lumbers, 1975). Therefore, this constrains the minimum age at which the quartzite may have been deposited, sometime between 1900 and 1400 Ma ago.

It is more likely that the quartzite is an equivalent of the Michigami Formation of the Marquette Range Supergroup in Michigan and Wisconsin. The Marquette Range Supergroup is predominantly a passive continental-margin sequence deposited between 2.1 and 1.85 Ga (Barovich *et al.*, 1989). This

Figure 3.19 Age histogram for CBQ. Three zircons are shown
to be from a Penokean aged terrain and one from an Archean
aged terrain. The age and error of each zircon is represented
by a distribution with width 1σ. The distribution is
normalized so that the area under each curve is equal.
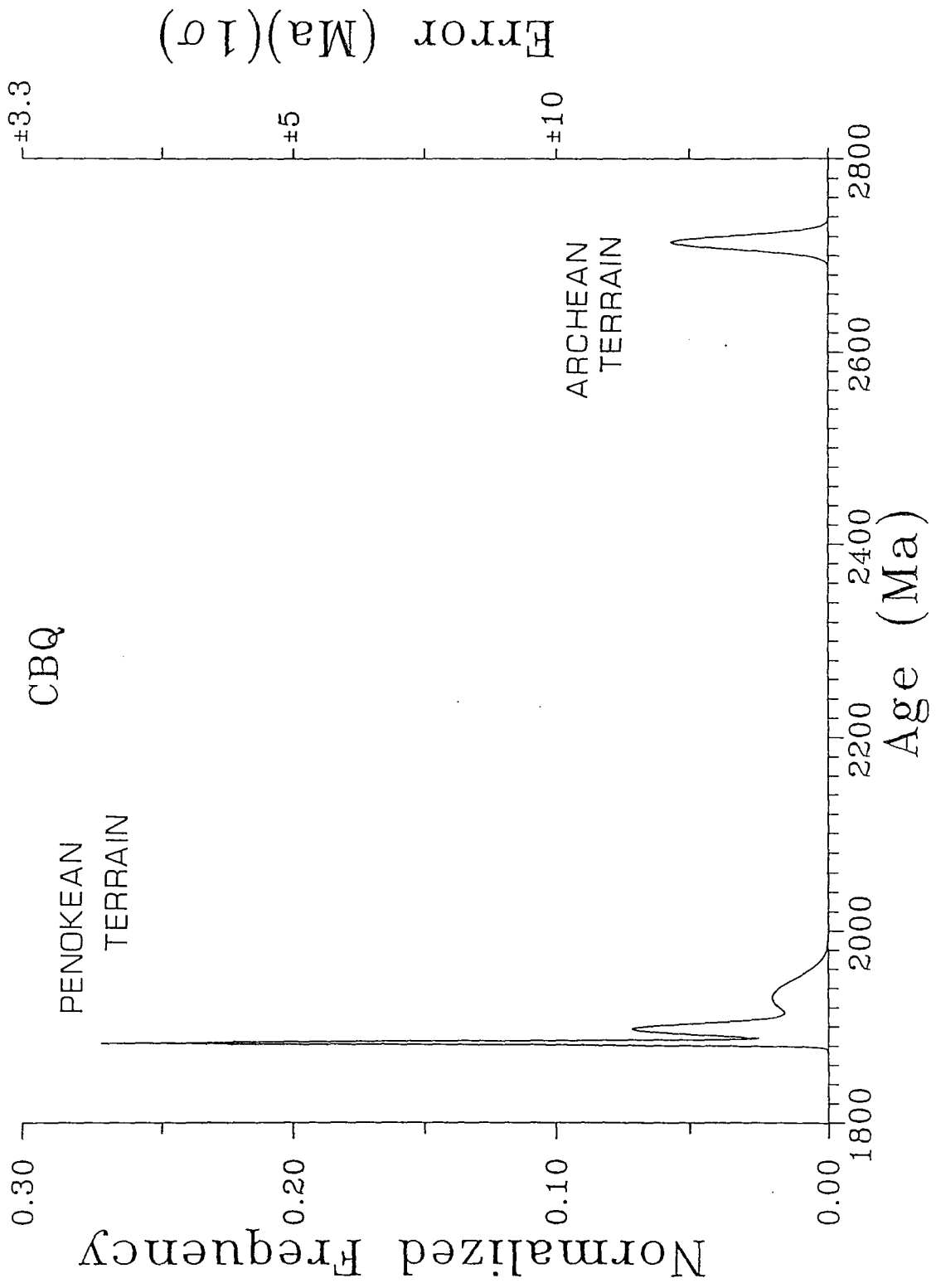
supergroup is divided into a northern and southern terrain which is believed to represent miogeosynclinal sediments and an accreted oceanic island-arc, respectively.

Nd model ages and ϵ_{Nd} values of the northern terrain fall within two age groups. One group with Archean ages that range from 2.68 to 3.07 Ga is located in the lower part of the Marquette Range Supergroup. Samples from the upper part of the sequence range in age between 2.0 and 2.3 Ga. The origin of these sediments appears to be from an Archean crust (Superior Province) and an Early Proterozoic terrain accreted during the Penokean orogeny. The abrupt change of the provenance of an Archean to an Early Proterozic terrain is proposed to be due to a juxtaposition of sediments caused by tectonic faulting.

The sample CBQ could represent an area of sedimentation between these two terrains (Figure 3.20), Archean and Early Proterozic. This is supported by its mixed Nd model age of 2.42 Ga and the presence of zircons from both sources.

87

Figure 3.20   Accretion of a Penokean island arc onto the
Superior Province (after Dickin and McNutt, 1989).

Superior | Southern | Passive
Margin

2.2

1.9 Ga

EROSION Island arc

1.9

MIXED AREA

Proterozoic
Mobile
Belt

Archean Foreland

Collision

Penokean
Suture ▼

1.85

▲
Ga
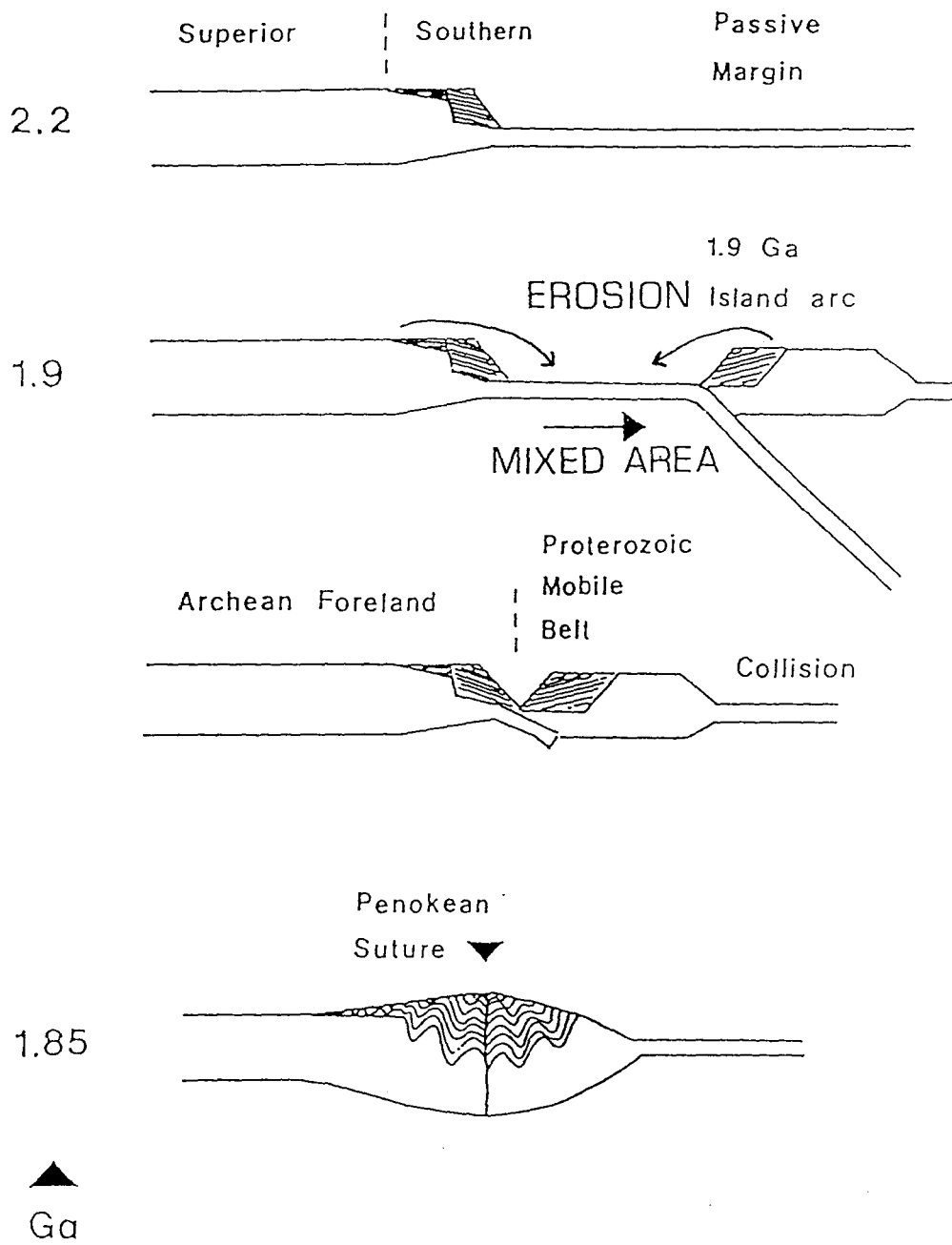
CHAPTER 4

4.1   The Winnipeg River Belt

4.1.1   General Geology

The Superior Province is the largest subdivision of the Canadian Shield (Figure 4.1). It is a remnant of an Archean aged craton (Goodwin *et al.*, 1972) with reported ages of volcanic and plutonic rocks between 3.1 and 2.6 Ga. It has undergone several episodes of metamorphism at about 3.0 and 2.7 Ga ago (Card, 1990).

The Superior Province is composed many linear east-west trending subprovinces. The division is based upon characteristic tectonic features (Goodwin *et al.*, 1972) i.e., lithology, structure and metamorphic grade. It is thought that the Superior Province is an accreted arc terrain which becomes younger in a southerly direction. The linear subprovinces are composed of greenstone belts (metamorphosed oceanic crust), metasedimentary belts (metamorphosed accreted sediments), metavolcanic belts (metamorphosed volcanic arcs), and batholithic-orthogneisses (metamorphosed plutonic rocks and basement crust). These rock assemblages are analogous to those accumulated by modern oceanic island arc and continental arc collisions (Card, 1990).

The English River Subprovince (Figure 4.2 A and B) is

89

Figure 4.1 Subdivisions of the western Superior Province of
the Canadian Shield (after Douglas and Price, 1972).

Figure 4.2

NAIN

CHURCHILL

HUDSON PLATFORM

GRENVILLE

SUPERIOR

APPALACHIAN OROGEN

Sachigo Belt

Berens Belt

Uchi Belt

English River Belt

Wabigoon Belt

Quetico Belt

Wawa

0   400   800
km
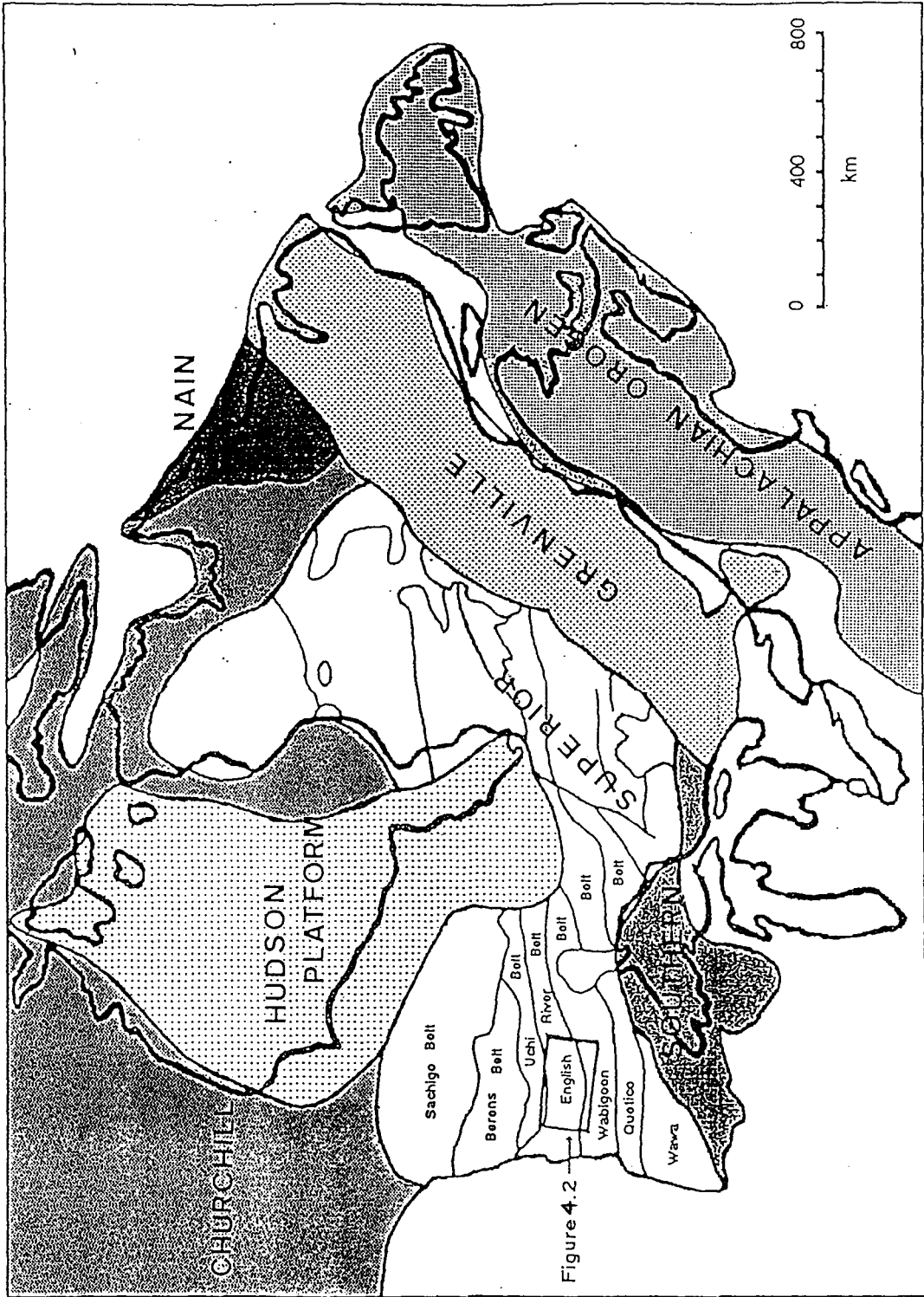
Figure 4.2A   Location map of the English River Subprovince.
Samples 605, CED1, CED6, and CED7 were collected from site
CEDAR and sample 703 from 703.

Map showing the region from Kenora to Sioux Lookout, Ontario, including Lake of the Woods, Eagle L., Wabigoon L., Clay L., English River, Lac Seul, and CEDAR. Towns marked include Kenora, Vermilion Bay, Dryden, Ear Falls, Sioux Lookout, and locations 703 and 72. Highways 17 and 105 are indicated. Coordinates shown: 95°, 94°, 93°, 92° longitude and 50° latitude. Scale bar shows 0–40 Km.
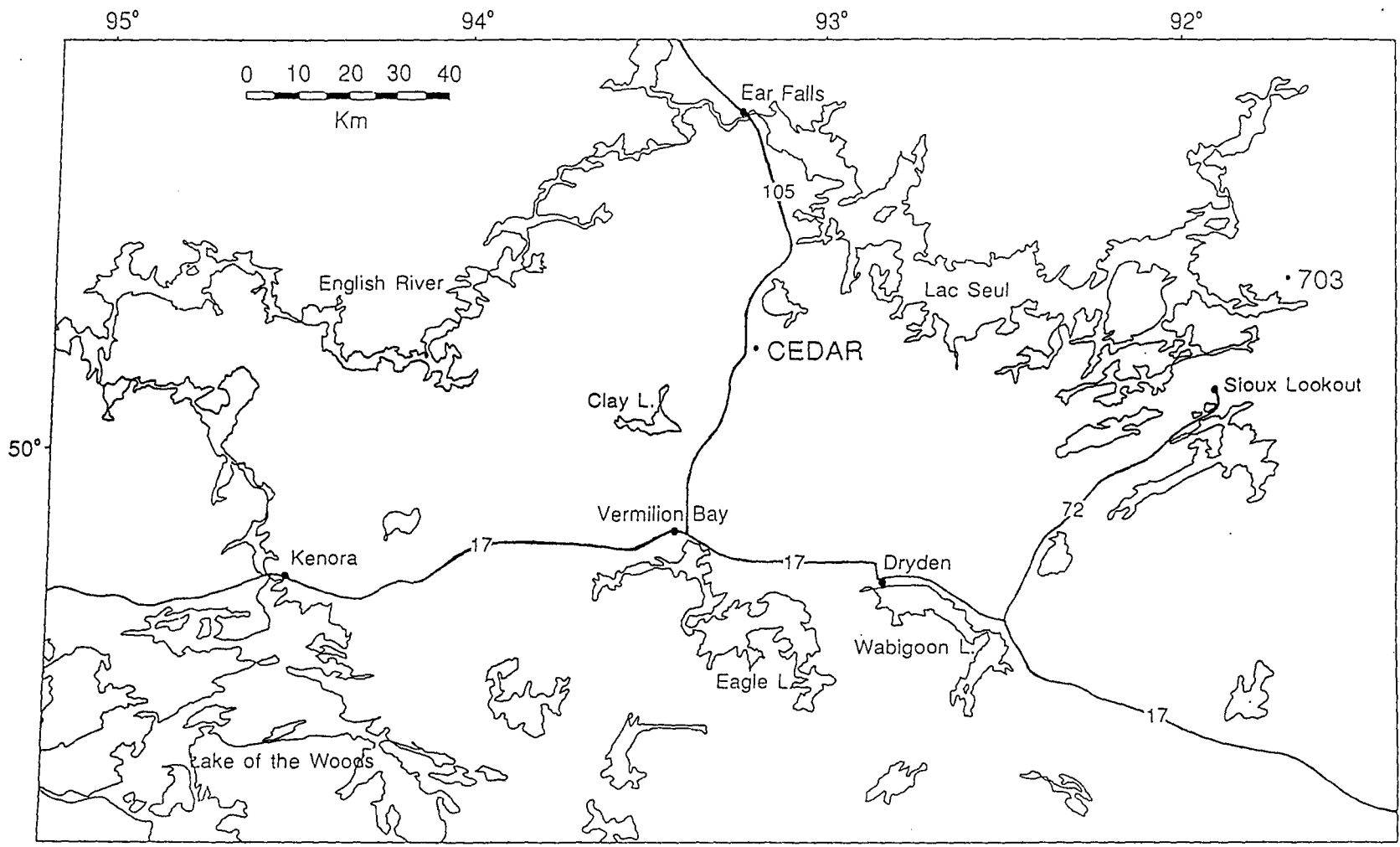
Figure 4.2B   Sample location and general geology map of the English River Subprovince.   Samples 605, CED1, CED6, and CED7 were collected from site **CEDAR** and sample 703 from **703.**   The English River Subprovince is further divided (Beakhouse, 1977) into the Ear Falls-Manigotagan Belt (paragneisses) and the Winnipeg   River   Belt   (batholithic-orthogneisses)   (after Beakhouse, 1983 and Beakhouse, 1985).

Uchi Subprovince

Ear Falls Manigotagan Belt

Winnipeg River Belt

Wabigoon Subprovince

Cedar

95°
94°
93°
92°
50°

Potassic suite
Sodic suite
Mafic suite
Metavolcanic rock
Metasedimentary rock
Orthogneiss

km
0 10 20 30 40
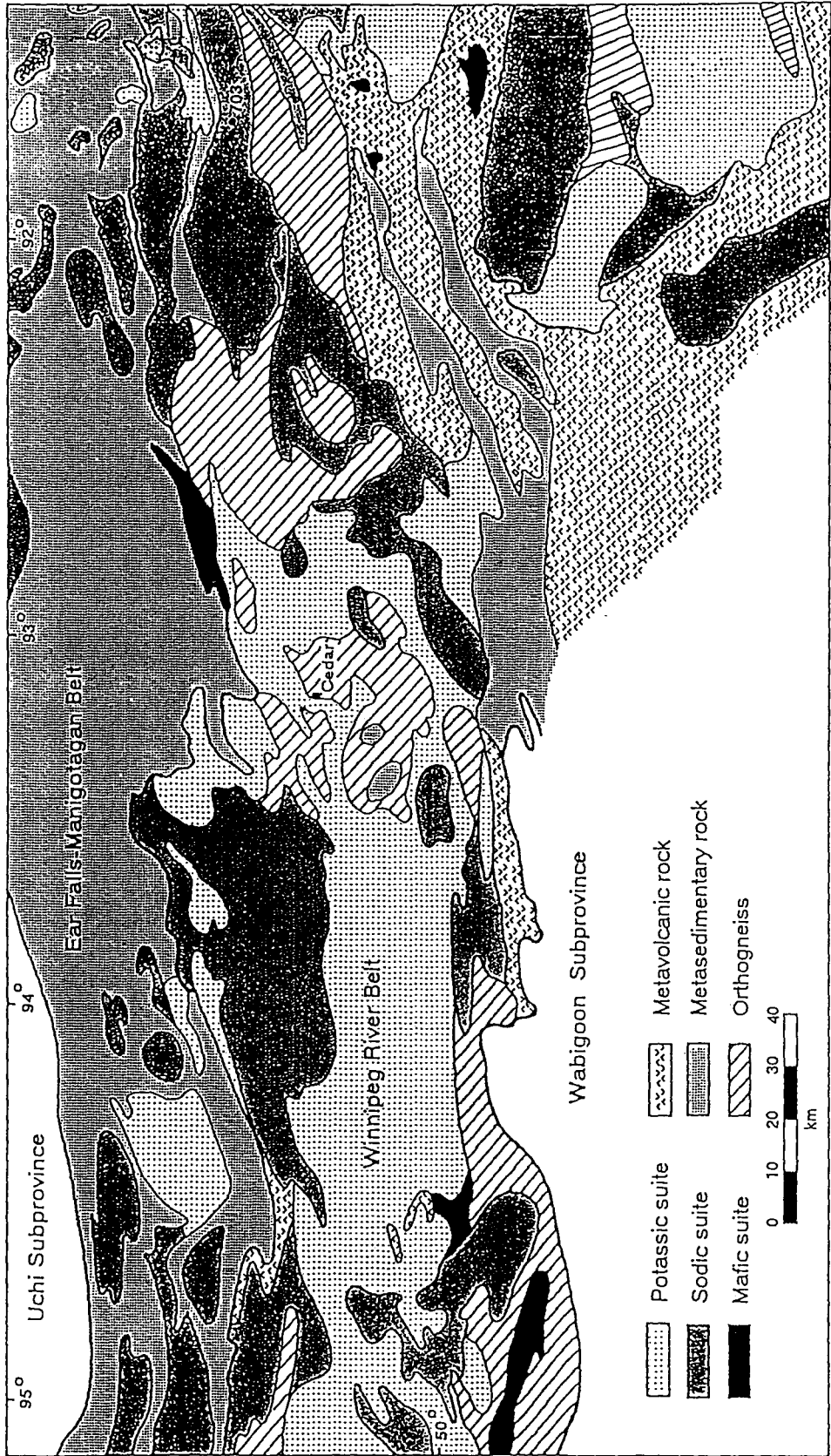
composed of metasediments and batholithic-orthogneisses. It is bounded to the north and south by the Uchi and Wabigoon Subprovinces (greenstone tonalite terrains). The English River Subprovince can be further subdivided into two belts, the Ear Falls-Manigotagan Belt in the north and the Winnipeg River Belt in the south (Beakhouse, 1977).

The Ear Falls-Manigotagan Belt is dominantly composed of metasediments (paragneisses) and minor amounts of metavolcanics (Beakhouse, 1985). It is in the upper amphibolite facies. Its origin is thought to be a linear sedimentary basin (Beakhouse, 1983).

The Winnipeg River Belt is a batholithic-orthogneiss terrain (Beakhouse, 1983) of predominantly (>90%) felsic plutonic rocks. Plutons tend to be tonalitic to granitic and the orthogneisses are composed of an "assemblage of variably deformed, polygenetic quartz dioritic to granitic rocks" (Beakhouse, 1983). The orthogneisses are thought to predate the Kenoran orogeny. It also contains the remnants of a dominantly volcanic supracrustal sequence (Beakhouse, 1985). Its origin is poorly understood. The orthogneisses may be basement crust onto which the sediments and volcanic arc were accreted (Goodwin *et al.*, 1972).

Samples studied in this work come from two localities in the Winnipeg River Belt. Samples 605, CED1, CED6, and CED7, were collected from a tonalitic orthogneiss from the Cedar Lake dome near the position CEDAR (Figure 4.2 A and B).

Sample 703 is located east of CEDAR at 703 in the Lac Seul sodic batholith.

The orthogneiss occurs as a heterogeneous biotite to hornblende-biotite banded gneiss (Westerman, 1977). The orthogneiss is thought to be the oldest plutonic component of the Belt due to the presence of older supracrustal remnants. These occur as discontinuous volcanic and sedimentary inclusions less than 20 m across (Beakhouse, 1983).

The sodic plutonic suite includes diorites, tonalites, and granodiorities metamorphosed to gneisses. The sodic plutons are thought to have been emplaced after the volcanism (metavolcanics) and sedimentation (paragneisses) of the Ear Falls-Manigotagan Belt (Beakhouse, 1983).

Chronologically, the sequence of rock types found in the English River Subprovince are thought to occur in the following order: 1) supracrustal remnants, 2) orthogneisses, 3) metavolocanics and paragneisses, and 4) sodic, potassic, and mafic plutons. The time span that this sequence covers is thought be about 1 Ga. The early history of the basement rock is unclear. The Winnipeg River Belt was thought to have recrystallized at about 3000 Ma (Beakhouse, 1983). The supracrustal remnants are believed to be older than this. The latest major metamorphism occurred during the Kenoran orogeny (approx. 2700 Ma).

4.2   Cedar Lake and Lac Seul Tonalitic Gneisses

4.2.1   General Geology

The Cedar Lake gneiss is a domal structure deformed by upper amphibolite metamorphism into a banded gneiss. It is a fine to medium grained biotite to hornblende-biotite gneiss (Beakhouse, 1983).

Westerman (1977) noted that the earliest deformation found in the Cedar Lake orthogneiss is not found in the paragneiss. Thus, he concludes that the tonalitic gneiss may have been emplaced before the progenitor of the paragneiss was formed. The presence of supracrustal remnants as inclusions in the Cedar Lake dome also lead one to believe that this is a very old structure.

In thin section and as grains, the zircons from the Cedar Lake gneiss vary from site to site, but are usually consistent within the same hand specimen. The variation in the Cedar Lake gneiss is surprising due to the fact that they were collected within 1 km on one another. This variation is probably due to the heterogeneous nature of this gneiss.

Colour varies from light brown to dark chocolate brown. Size and length to width ratios vary from long (0.7 mm in length) prismatic (l:w=4:1) crystals to small (0.1 mm in length) blocky (l:w=1:1) crystals. The shape of the crystals ranged from euhedral to subhedral. A very small number were

anhedral.

The zircons from 605 in thin section (Plate 4.1 A and B) show evidence of magmatic zoning. The presence of older cores is unclear. Plate 4.1 C shows a pleochroic halo around the zircon grain in biotite. This feature is very common in all thin sections. The halo is indicative of a zircon that is very old and/or contains a high concentration of U and Th. The halo is due to radiation damage in the surrounding mineral.

The zircons grains used in this study vary from long chocolate brown prismatic crystals (Plate 4.2 A, B, and C). Zircons that were handpicked early in this study were this type of crystal. Eventually, these crystals were exhausted and the smaller, lighter coloured grains (Plate 4.2 D, E, and F) were used. The change in colour may solely be due to the difference in thickness of the crystals. The grains vary from euhedral to subhedral. All are fractured to some extent and contain inclusions. No obvious cores are seen in the grains.

Zircons in CED1 (Plate 4.3 A and B) are a very common mineral. Magmatic zoning is easily seen in most zircons in thin section. There are no obvious cores. Pleochroic halos around the zircons are also present.

The zircon grains from CED1 (Plate 4.4) were the smallest grains used in this study. Sizes ranged from 0.1 to 0.4 mm in length. The crystals tended to be more stubby (l:w=3:1) than other zircons. Crystal shape tended to be more subhedral than

Plate 4.1 605 zircons (z) in thin section. A and B: note
zoning and possible core (plane polarized light). C: note
pleochroic halo around zircon (cross polarized light).

A

0.15mm

B

0.15mm

C

0.25mm

Z
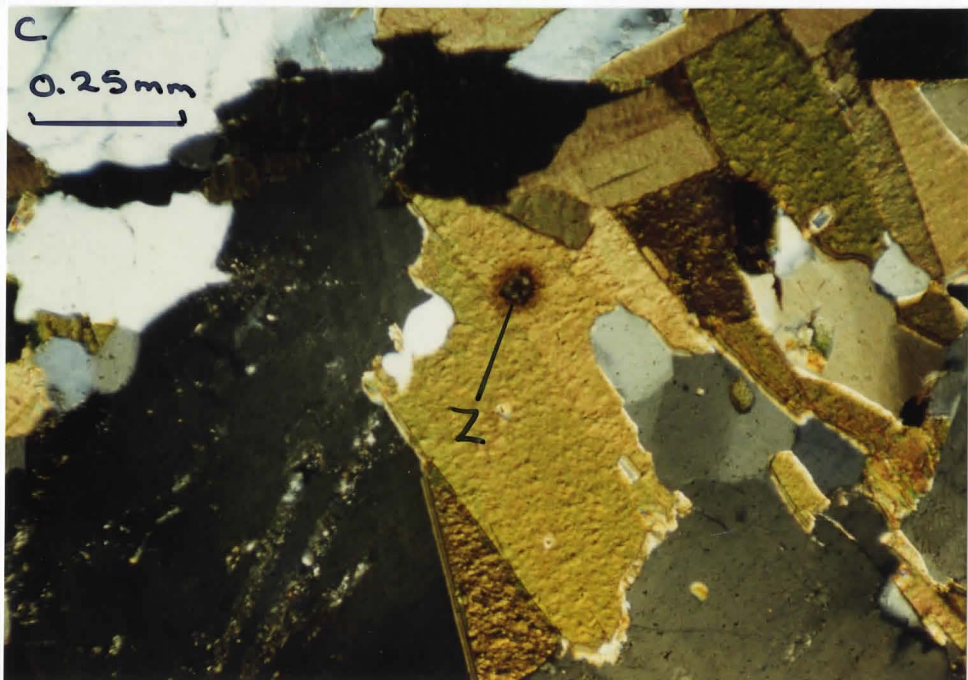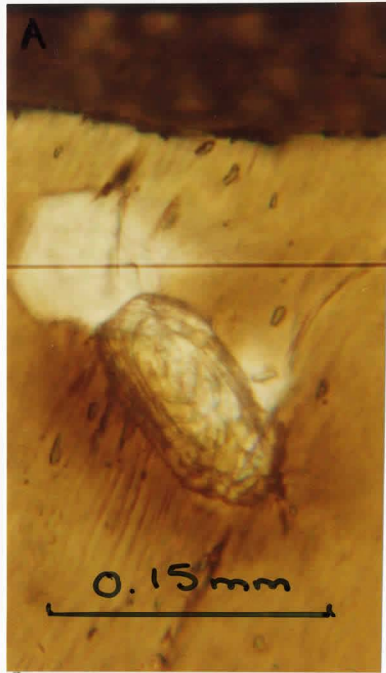
Plate 4.2 Zircon grains from 605: A) 605E3P, B) 605E6P, C) 605E7P, D) 605F2P, E) 605F5P, and F) 605F6P.

A

B

0.5 mm

C

D

E

F

Plate 4.3 Zircons (z) from CED1 in thin section. Faint zoning and halos are visible in A) and B), respectively (crossed polarized light).

A   0.15 mm

B   0.25 mm
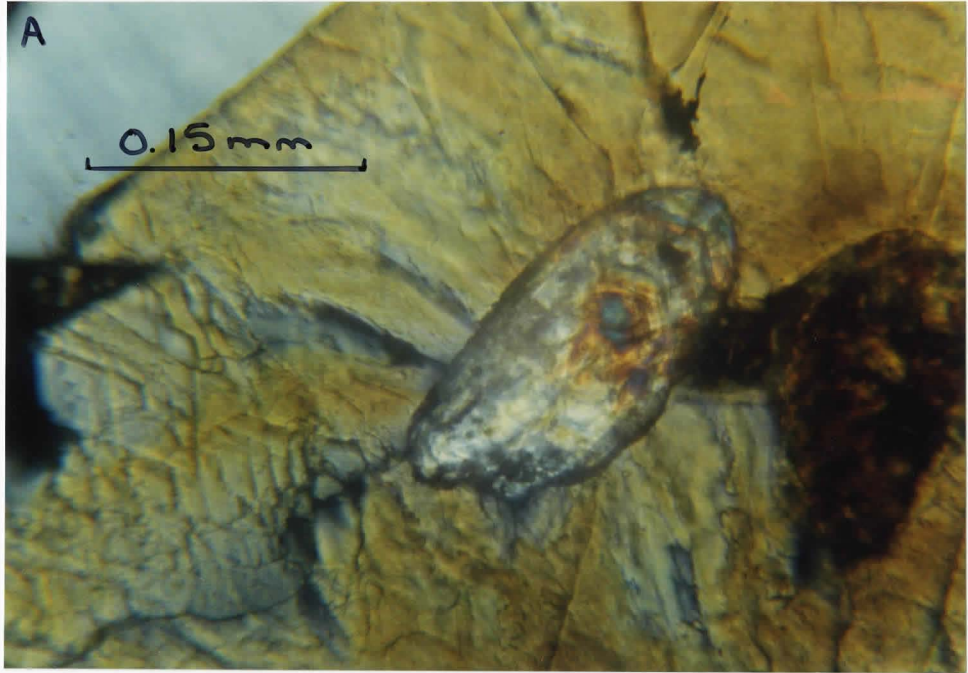
Plate 4.4 Zircon grains from CED1: A) CED1A3, B) CED1A4, C) CED1F2P, D) CED1J4P, E) CED1J5P, and F) CED1B3 (3391±2 Ma).

A

B

0.5 mm

C

D

E

F

euhedral. The edges of the faces are slightly rounded rather than sharp. Also, the surface of the faces tends to be mottled or rough rather than flat. The points of all the zircons are well preserved, in most cases. Thus, the roundedness is probably not due to an erosional process, but a high degree of metamorphism.

Zircons from CED6 (Plate 4.5) show fine magmatic zoning. There is no obvious evidence for cores. Pleochroic halos around the zircons are present. The zircons grains (Plate 4.6) vary from euhedral to anhedral.

CED7 zircons in thin section (Plate 4.7) appear magmatic in origin. No obvious cores are present. The zircons grains (Plate 4.8) are highly fractured. Unfractured pieces appear almost colourless rather than brown. Crystals appear subhedral due to their slightly rounded appearance.

Zircons from 703 (Plate 4.9) in thin section may shown the existence of older cores. The internal zoning does not always coincide with the orientation of the faces of the probable core.

The zircons grains (Plate 4.10) are euhedral to subhedral and tend to be fractured.

Plate 4.5 CED6 zircons (z) in thin section. Zoning and halos are visible in A) and B), respectively (plane polarized light).

A

0.15 mm

B

0.25 mm

Z
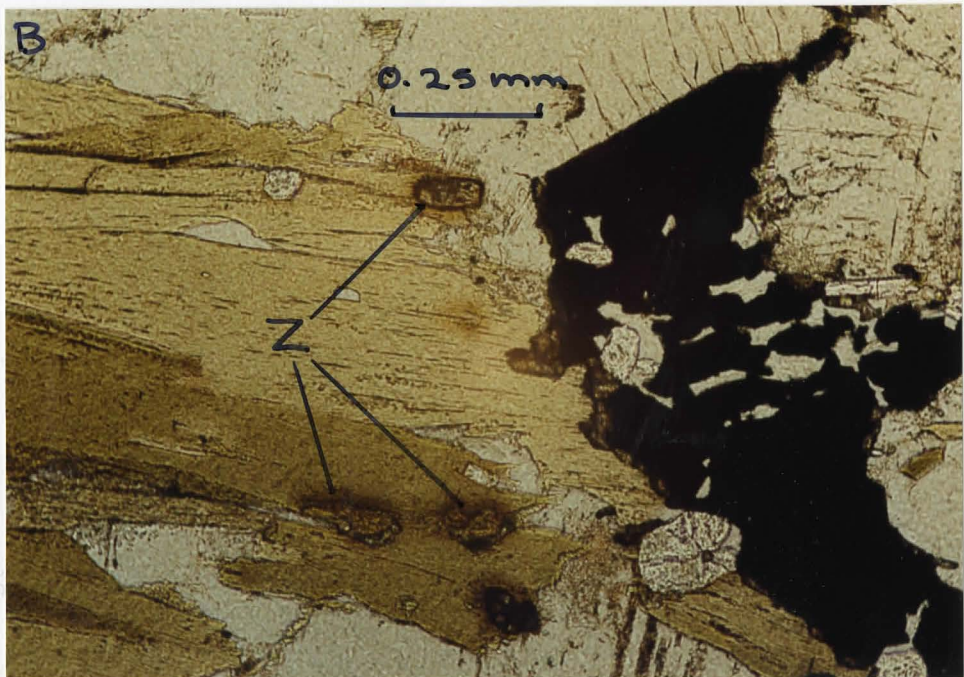
Plate 4.6 Zircon grains from CED6: A) CED6A1, B) CED6B2, C) CED6B3, and D) CED6E1.

A

B

0.5mm

C

D

Plate 4.7 Zircon from CED7 in thin section. Zoning is very clear (plane polarized light).

Plate 4.8 Zircon grains from CED7: A) CED7A1P, B) CED7A2P, and C) CED7A4P.

0.15 mm

A

B

C

0.5 mm

104
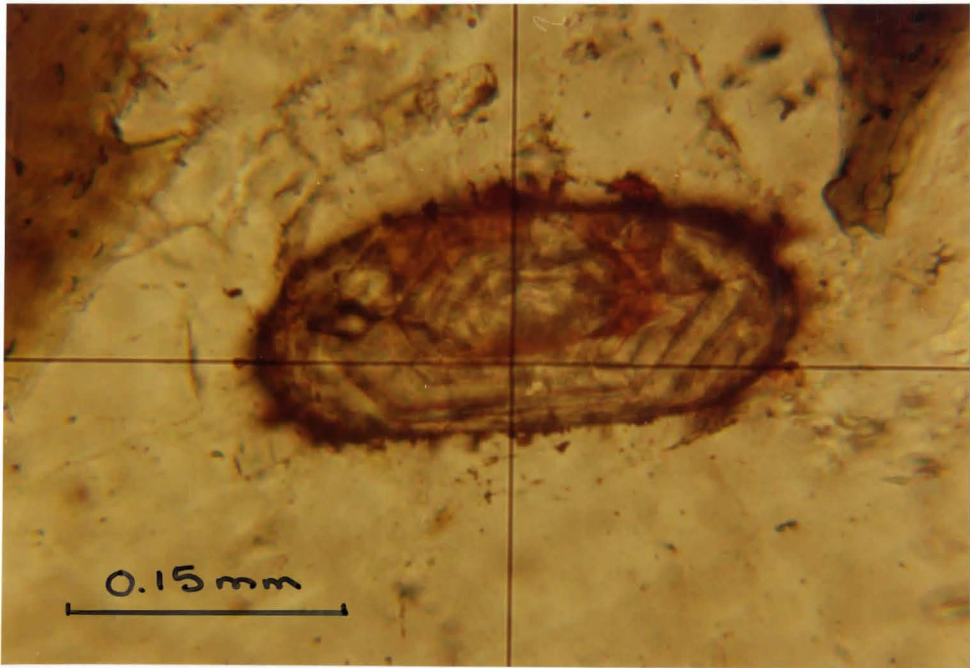
Plate 4.9 Zircons from 703 in thin section. A) and B) show possible cores (plane polarized light).

A

0.15 mm

B
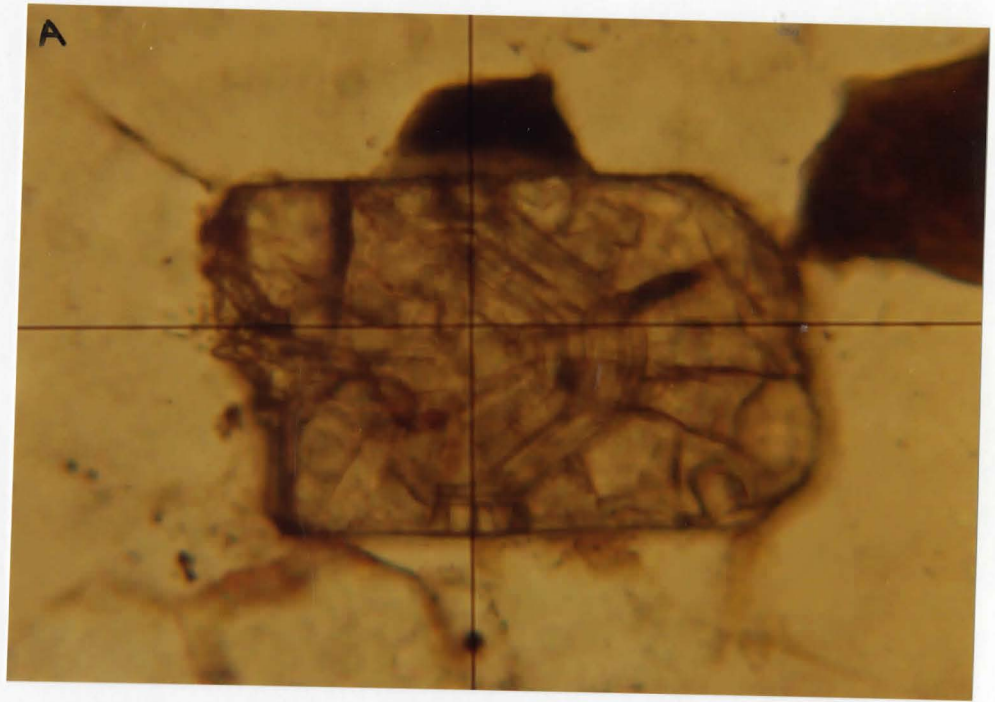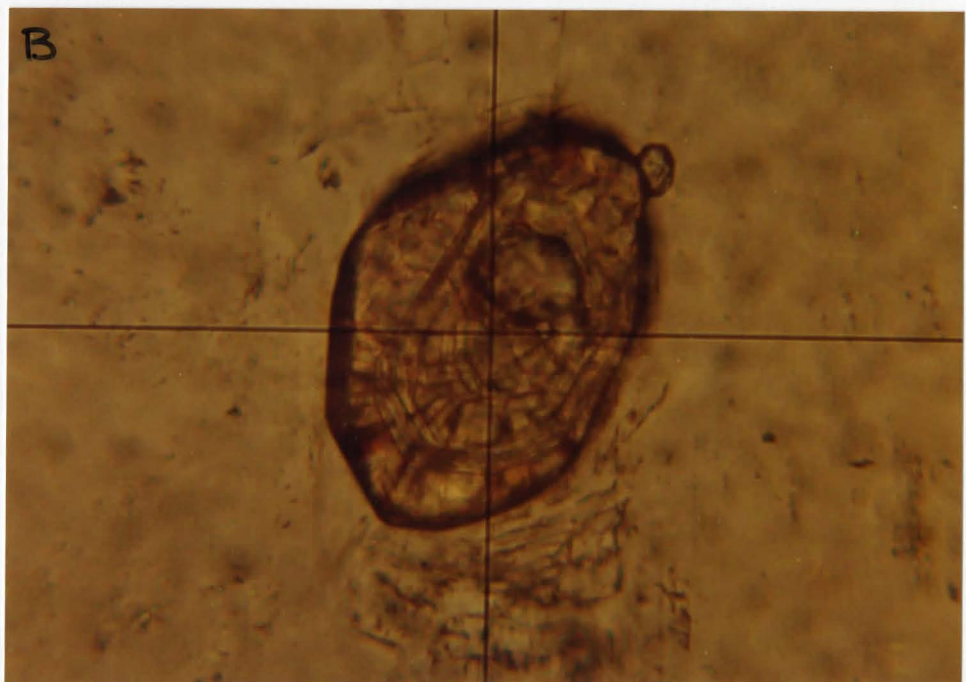
Plate 4.10 Zircon grains from 703: A) 703A2P, B) 703A4P,
C) 703A6P, and D) 703A6P.

A   B

0.5mm

C   D

4.2.2 Previous Isotopic Work

U-Pb zircon geochronology has been conducted upon various gneisses in the English River Subprovince including the Cedar Lake and Lac Seul gneisses. Beakhouse (1983) found ages of 2830+15/-9 Ma (age of crystallization) and 2790±10 Ma (age of metamorphism) for other tonalitic gneisses in the Winnipeg River Belt. The Cedar Lake gneiss has been dated (Beakhouse, 1983) to reveal minimum ages of about 2720 and 2750 Ma. The emplacement of the surrounding Lount Lake Batholith (2700±2 Ma) is related to the Kenoran orogeny. Thus, the Cedar Lake gneiss may have been heavily reset by the metamorphism.

Corfu (1988) has also studied zircons from the Cedar Lake gneiss. $^{207}Pb/^{206}Pb$ ages of abraded zircons vary from 3143 to 3168 Ma. The U-Pb upper intercept has been calculated to be 3170+20/-5 Ma. This is believed to be the oldest reliable age known for the Superior Province (Corfu, 1988). The lower intercept is about 2680 Ma. A scatter in ages from titanite and apatite minerals imply a period of low grade metamorphism between 2640 and 2520 Ma.

The Lac Seul tonalitic gneiss has been dated by Krogh et $al.$ (1976) to be 3040±40 Ma. A second stage of zircon growth occurred at 2681±20 Ma.

Hinton and Long (1979) have used a high resolution ion-microprobe to study the Pb from zircons from the Lac Seul tonalitic gneiss. Two zircons resulted in a minimum age of

3300±100 Ma. This age has been treated with scepticism by some authours (Beakhouse, 1983) due to the newness of the ion microprobe technique. Other zircons were found with cores of 2930±50 Ma and rims of 2700 Ma.

Nd model ages (Dickin, unpublished data) have been derived from the sites in the Cedar Lake gneiss from which zircons were collected. 79-2 is the sample that Beakhouse (1983) examined in his thesis. Samples used in this study (605, CED1, CED6 and CED7) were collected within 1 km of 79-2. They are as follows:

Sample	Nd Model Age (Ga)
605	3.58
CED1	3.72
CED6	3.90
CED7	3.49
79-2	3.22

Thus, the tonalites must have been formed, in part, from a crust which is older than any zircons (3.17 or 3.3 Ga) yet found in the Superior Province.

4.2.3 Results

4.2.3.1 605

31 zircons were tested from 605, but only 15 resulted in data suitable to derive ages (Table 4.1). Most ages were calculated from the slope or intercept of a York fit (York,

1969) of the data (Table 4.6). Figure 4.3A displays data with $^{206}Pb/^{204}Pb<10,000$ whilst Figure 4.3B consists of data with $^{206}Pb/^{204}Pb>10,000$. Likewise, for the intercept plots the data set has been divided into $^{204}Pb/^{206}Pb<0.0001$ (Figure 4.4A) and $^{204}Pb/^{206}Pb>0.0001$ (Figure 4.4B).

Only 3 of the 15 zircons could be derived by the average of the $^{207}Pb/^{206}Pb$ alone (Figure 4.5). The presence of common Pb in the remaining zircons required a correction to be made.

In all cases the ages derived by both the slope and intercept method were within 2σ of each other.

All the ages from 605 can be combined into an age histogram (Figure 4.6). The upper and lower extremes are 3183±2 Ma and 2698±17 Ma, respectively. Most of the zircon ages tend to cluster around 2900 Ma.

4.2.3.2 CED1

A large number of zircons, 54, were tested from CED1, but only 10 were suitable to derive ages (Table 4.2). Half of the zircons were derived by the slope (Figure 4.7) and/or intercept (Figure 4.8) method. Ages that were derived by both methods are within 2σ of each other. The remaining zircons were derived from the average of $^{207}Pb/^{206}Pb$ (Figure 4.9) due to the lack of common Pb found in these zircons (Table 4.7). The lack of common Pb may be due to the lesser amounts of fracturing or inclusions found in these zircons.

Ages range from 2561±137 Ma to 3391±2 Ma (Figure 4.10). The younger age has a high error. If this age is discarded then the youngest age would be 2889±70 Ma. Most ages are found to be between 3000 and 3200 Ma.

The oldest age, 3391±2 Ma, is unusual due to the very good quality and quantity of data obtained from this zircon. Common Pb was nonexistent so that the age was determined by the average of ^{207}Pb/^{206}Pb data. The Pb beam is also very stable. The standard error of the blocks of ^{207}Pb/^{206}Pb is low (i.e. <0.5%) as compared to other zircons from CED1 with standard errors between 1 and 6%. The quantity of data represents approximately 4.5 hours of data collection and 23 blocks of data. This is more data than derived from any other zircon in this study.

4.2.3.3 CED6

6 zircons from a total of 18 from CED6 resulted in age determinations (Table 4.3). The data from which these ages are derived is given in Table 4.8. Only 2 ages were determined by the slope of the data (Figure 4.11). The intercept method resulted in ages with errors too large to be considered reasonable. Large errors in the ^{204}Pb/^{206}Pb data may have been part of the problem. Most ages were derived from the average of ^{207}Pb/^{206}Pb (Figure 4.12) due to the lack of common Pb in the zircons. Ages range from 2408±9 Ma to

2975±18 Ma (Figure 4.13). Inbetween ages tend to cluster around 2700 Ma.

4.2.3.4 CED7

15 zircons from CED7 were studied, but only 7 were used to derive ages (Table 4.4). Measurable amounts of common Pb were found in all zircons (Table 4.9), thus the ages could only be determined from the slope (Figure 4.14) and intercept (Figure 4.15) methods. Both methods were within 2σ of each other in cases when both could be determined. Ages range over a narrow time span from 3060±8 Ma and 3186±4 Ma (Figure 4.16).

4.2.3.5 703

5 zircons from a total of 10 from 703 gave ages (Table 4.5). The presence of common Pb in these zircons (Table 4.10) require that the ages be determined by the slope (Figure 4.17) and intercept (Figure 4.18) methods. The ages by both methods is within 2σ of each other. The ages range over an narrow time span from 2801±5 Ma to 2911±24 Ma (Figure 4.19).

111

Table 4.1 Ages of zircons from 605 from the Cedar Lake tonalite. Ages derived by a York fit of $^{206}Pb/^{204}Pb$ vs. $^{207}Pb/^{204}Pb$ data and/or $^{204}Pb/^{206}Pb$ vs. $^{207}Pb/^{206}Pb$ data or an average of $^{207}Pb/^{206}Pb$ data.

Sample	York Fit of 206/204 vs. 207/204		Age (Ma)	Error (2 sigma)	York Fit of 204/206 vs. 207/206		Age 06 (Ma	Error (2 sigma)	Average of 207/206		Age (Ma)	Error (2 sigma)
	slope w. mfc	2 sigma			intercept w. mfc	2 sigma			average w. mfc	2 sigma /sqrt(n)		
CEDAR LAKE TONALITE - 605												
605A1	0.215997	0.001536	2951	11								
605A2	0.208098	0.000396	2891	3	0.207791	0.000240	2888	2				
605A4					0.212060	0.000272	2921	2	0.212152	0.000237	2922	2
605A6	0.228995	0.001345	3045	9	0.221665	0.031214	2993	218				
605B3	0.204681	0.005200	2864	41	0.201312	0.054950	2837	413				
605C1	0.249667	0.000294	3183	2								
605E3PC	0.206605	0.000597	2879	5								
605E4PB									0.209751	0.000455	2904	4
605E6P	0.232255	0.000486	3068	3	0.212722	0.045580	2926	327				
605E7P	0.200078	0.000350	2827	3	0.200299	0.001388	2829	11				
605E8P	0.221039	0.000060	2988	1	0.220618	0.009740	2985	7				
605F2P	0.184952	0.001888	2698	17	0.185909	0.003086	2706	27				
605F4P	0.218593	0.002016	2970	15	0.216582	0.009476	2955	70				
605F5P									0.210308	0.000796	2908	6
605F6P	0.235042	0.001080	3087	7	0.235042	0.001334	3087	18				

mfc=mass fractionation correction of 0.5%

112

Table 4.2 Ages of zircons from CED1 from the Cedar Lake tonalite. Ages derived by a York fit of $^{206}Pb/^{204}Pb$ vs. $^{207}Pb/^{204}Pb$ data and/or $^{204}Pb/^{206}Pb$ vs. $^{207}Pb/^{206}Pb$ data or an average of $^{207}Pb/^{206}Pb$ data.

Sample	York Fit of 206/204 vs. 207/204		Age (Ma)	Error (2 sigma)	York Fit of 204/206 vs. 207/206		Age 06 (Ma)	Error (2 sigma)	Average of 207/206		Age (Ma)	Error (2 sigma)
	slope w. mfc	2 sigma			intercept w. mfc	2 sigma			average w. mfc	2 sigma /sqrt(n)		
CEDAR LAKE TONALITE - CED1												
CED1A3									0.246485	0.004978	3162	32
CED1A4									0.255705	0.005624	3220	+34/-35
CED1B3									0.285079	0.000363	3391	2
CED1F2									0.243260	0.002914	3141	19
CED1G3	0.170315	0.014335	2561	137								
CED1H3P									0.219599	0.002213	2978	16
CED1H4P	0.234728	0.001053	3085	7	0.236211	0.001948	3095	13				
CED1I12P	0.246920	0.004978	3165	32	0.246364	0.006986	3162	45				
CED1J4P	0.204994	0.011025	2866	86	0.207872	0.009136	2889	70				
CED1J5P	0.223708	0.002149	3008	15	0.225272	0.002300	3019	16				

mfc=mass fractionation correction of 0.5%

113

Table 4.3   Ages of zircons from CED6 from the Cedar Lake tonalite.   Ages derived by a York fit of ^{206}Pb/^{204}Pb vs. ^{207}Pb/^{204}Pb data and/or ^{204}Pb/^{206}Pb vs. ^{207}Pb/^{206}Pb data or an average of ^{207}Pb/^{206}Pb data.

Sample	York Fit of 206/204 vs. 207/204		Age (Ma)	Error (2 sigma)	York Fit of 204/206 vs. 207/206		Age 06 (Ma)	Error (2 sigma)	Average of 207/206		Age (Ma)	Error (2 sigma)
	slope	2 sigma			intercept w. mfc	2 sigma			average w. mfc	2 sigma /sqrt(n)		
CEDAR LAKE TONALITE - CED6												
CED6A1	0.184667	0.000754	2695	7								
CED6B1									0.185473	0.000126	2702	1
CED6B2	0.219272	0.002239	2975	16								
CED6B3									0.219211	0.002384	2975	18
CED6C3									0.176239	0.001087	2618	10
CED6E1									0.155601	0.000810	2408	9

mfc=mass fractionation correction of 0.5%

114

Table 4.4 Ages of zircons from CED7 from the Cedar Lake tonalite. Ages derived by a York fit of ^{206}Pb/^{204}Pb vs. ^{207}Pb/^{204}Pb data and/or ^{204}Pb/^{206}Pb vs. ^{207}Pb/^{206}Pb data or an average of ^{207}Pb/^{206}Pb data.

Sample	York Fit of 206/204 vs. 207/204		Age (Ma)	Error (2 sigma)	York Fit of 204/206 vs. 207/206		Age 06 (Ma)	Error (2 sigma)	Average of 207/206		Age (Ma)	Error (2 sigma)
	slope	2 sigma			intercept w. mfc	2 sigma			average w. mfc	2 sigma /sqrt(n)		

CEDAR LAKE TONALITE - CED7

Sample	slope	2 sigma	Age (Ma)	Error (2 sigma)	intercept w. mfc	2 sigma	Age 06 (Ma)	Error (2 sigma)	average w. mfc	2 sigma /sqrt(n)	Age (Ma)	Error (2 sigma)
CED7A1P	0.231328	0.001564	3061	11	0.231118	0.001124	3060	8				
CED7A2P	0.234675	0.002145	3084	15	0.235152	0.000754	3087	5				
CED7A4P	0.250404	0.001839	3187	12	0.250207	0.000708	3186	4				
CED7A7P	0.246538	0.001534	3163	10								
CED7B1P	0.233806	0.006738	3078	+58/-61	0.235743	0.003199	3091	+21/-22				
CED7B4P	0.233813	0.005069	3078	34	0.232152	0.006936	3067	61				
CED7C4P	0.245785	0.003825	3158	+24/-25								

mfc=mass fractionation correction of 0.5%

Table 4.5   Ages of zircons from 703 from the Lac Seul tonalite.   Ages derived by a York fit of $^{206}Pb/^{204}Pb$ vs. $^{207}Pb/^{204}Pb$ data and/or $^{204}Pb/^{206}Pb$ vs.$^{207}Pb/^{206}Pb$ data or an average of $^{207}Pb/^{206}Pb$ data.

Sample	York Fit of 206/204 vs. 207/204		Age (Ma)	Error (2 sigma)	York Fit of 204/206 vs. 207/206		Age 06 (Ma)	Error (2 sigma)	Average of 207/206		Age (Ma)	Error (2 sigma)
	slope	2 sigma			intercept w. mfc	2 sigma			average w. mfc	2 sigma /sqrt(n)		

LAC SEUL TONALITE - 703

Sample	slope	2 sigma	Age	Error	intercept	2 sigma	Age	Error				
703A2P	0.196979	0.000621	2801	5	0.196942	0.007220	2801	6				
703A4P	0.208128	0.002384	2891	19	0.210695	0.003450	2911	26				
703A6P	0.207936	0.004490	2890	35	0.209394	0.006024	2901	46				
703A7P	0.204930	0.001290	2866	10	0.205067	0.002418	2867	19				
703B2P	0.210685	0.004068	2911	31	0.210649	0.003144	2911	24				

mfc=mass fractionation correction of 0.5%

116

Table 4.6 Raw data from 605

Name	Run	207Pb / 206Pb	St. Err. (%)	207Pb / 204Pb	St. Err. (%)	206Pb / 204Pb	204Pb / 206Pb	St. Err. (%)
605A1	1	0.2123809	0.081	7830.854	11.518	36900.369	0.000027	11.660
	2	0.2123997	0.045	5319.149	4.299	24937.656	0.000040	4.201
	3	0.2125659	0.098	4618.938	10.891	21551.724	0.000046	10.440
	5	0.2182307	0.069	9066.183	7.752	41493.776	0.000024	7.165
	6	0.2165662	0.075	10660.981	9.995	49261.084	0.000020	9.719
	7	0.2163061	0.047	7987.220	19.443	36764.706	0.000027	18.269
	8	0.2144568	0.048	11299.435	4.532	52631.579	0.000019	4.313
	9	0.2158042	0.015	10309.278	2.218	47846.890	0.000021	2.029
Common Pb for 2950 Ma		1.1040613		14.408		13.050	0.076628	
605A2	1	0.2067778	0.041	7604.563	3.557	36900.369	0.000027	3.314
	2	0.2071309	0.033	6447.453	3.027	30395.137	0.000033	1.615
	3	0.2070175	0.007	7225.434	2.118	34843.206	0.000029	1.984
	4	0.2073966	0.032	6724.950	3.380	32467.532	0.000031	3.219
	5	0.2069803	0.021	6553.080	3.320	31645.570	0.000032	3.137
	6	0.2069328	0.049	6688.963	6.087	32258.065	0.000031	5.835
	7	0.2067349	0.037	6835.270	4.486	33112.583	0.000030	3.810
	8	0.2071523	0.022	6131.208	5.966	29585.799	0.000034	5.506
	9	0.2074034	0.024	5963.029	3.488	28735.632	0.000035	3.198
	10	0.2073121	0.032	5844.535	3.570	28089.888	0.000036	3.461
	14	0.2075570	0.035				0.000028	15.231
Common Pb for 2880 Ma		1.0967010		14.494		13.216	0.075666	

Name	Run	207Pb 206Pb	St. Err. (%)	207Pb 204Pb	St. Err. (%)	206Pb 204Pb	204Pb 206Pb	St. Err. (%)
605A4	3	0.2114207	0.046	41152.263	32.333	200000.000	0.000005	31.598
	4	0.2104344	0.035	42735.043	63.908	208333.333	0.000005	63.545
	5	0.2114719	0.016	75757.576	31.345	322580.645	0.000003	27.319
	6	0.2111404	0.051	23419.204	35.798	109890.110	0.000009	31.678
	7	0.2112465	0.058	44843.049	55.539	185185.185	0.000005	17.665
	8	0.2113387	0.038	43290.043	28.097	217391.304	0.000005	28.250
	9	0.2110695	0.016	45454.545	28.402	212765.957	0.000005	26.126
	10	0.2108037	0.043	35460.993	24.338	169491.525	0.000006	22.962
	11	0.2106999	0.067	43478.261	15.858	204081.633	0.000005	15.074
Common Pb for 2910 Ma		1.0998859		14.458		13.145	0.076075	
605A6	1	0.2295520	0.113	3984.064	3.284	17391.304	0.000058	3.114
	2	0.2262718	0.092	4372.540	10.684	19305.019	0.000052	10.169
	3	0.2279735	0.060	3203.075	28.378	13888.889	0.000072	25.854
Common Pb for 3050 Ma		1.1143638		14.275		12.810	0.078064	
605B3	2	0.2080628	0.080	7518.797	32.336	36363.636	0.000028	30.984
	3	0.2101073	0.111	4601.933	19.986	22831.050	0.000044	21.475
	4	0.2110322	0.231				0.000029	82.620
Common Pb for 2910 Ma		1.0998859		14.458		13.145	0.076075	
605C1	2	0.2486131	0.021	5991.612	1.575	24096.386	0.000042	1.454
	3	0.2488907	0.022	6150.062	1.382	24691.358	0.000041	1.306
	4	0.2487288	0.032	6131.208	4.541	24630.542	0.000041	4.385
Common Pb for 3180 Ma		1.1272116		14.080		12.491	0.080058	

Name	Run	207Pb 206Pb	St. Err. (%)	207Pb 204Pb	St. Err. (%)	206Pb 204Pb	204Pb 206Pb	St. Err. (%)
605E3PC	3	0.2092310	0.192	1233.654	15.440	5910.165	0.000169	14.494
	4	0.2117436	0.263	618.812	9.388	2955.956	0.000338	8.928
	5	0.2107452	0.136	745.101	21.303	3513.703	0.000285	20.257
	6	0.2087320	0.122	1179.245	6.227	5640.158	0.000177	5.113
	7	0.2088728	0.179	1277.139	10.624	6172.840	0.000162	9.570
Common Pb for 2900 Ma		1.0987926		14.470		13.169	0.075936	
605E4PB	3	0.2092439	0.262	2962.963	63.645	14245.014	0.000070	61.430
	4	0.2078328	0.124	4714.757	33.046	22321.429	0.000045	29.883
	5	0.2093344	0.251	1026.799	30.955	5005.005	0.000200	29.493
	6	0.2084119	0.178	709.572	16.922	3408.316	0.000293	16.818
Common Pb for 2900 Ma		1.0987926		14.470		13.169	0.075936	
605E6P	1	0.2383908	0.090	731.208	1.278	3069.368	0.000326	1.183
	2	0.2366695	0.051	617.436	1.357	2611.648	0.000383	1.248
	3	0.2467420	0.119	513.716	0.509	2188.184	0.000457	0.507
	4	0.2349780	0.058	527.788	0.718	2246.181	0.000445	0.674
	5	0.2343803	0.076	536.740	0.926	2290.426	0.000437	0.837
	6	0.2344545	0.064	574.614	2.350	2449.780	0.000408	2.159
	7	0.2348646	0.046	565.004	1.419	2405.581	0.000416	1.327
	8	0.2348997	0.037	577.267	3.061	2458.210	0.000407	2.806
	9	0.2355440	0.072	557.165	2.194	2319.647	0.000431	1.153
Common Pb for 3090 Ma		1.1183921		14.217		12.712	0.078666	

Name	Run	207Pb / 206Pb	St. Err. (%)	207Pb / 204Pb	St. Err. (%)	206Pb / 204Pb	204Pb / 206Pb	St. Err. (%)
605E7P	3	0.2107141	0.057	250.019	0.299	1192.464	0.000839	0.510
	4	0.2101192	0.071	234.170	1.128	1114.827	0.000897	1.129
	5	0.2104388	0.071	222.559	0.848	1057.418	0.000946	0.770
	6	0.2099457	0.050	221.391	0.692	1054.519	0.000948	0.651
	7	0.2101777	0.097	221.082	0.422	1052.521	0.000950	0.367
	8	0.2104819	0.040	214.179	0.801	1017.708	0.000983	0.753
	9	0.2103823	0.070	214.744	0.620	1020.512	0.000980	0.627
	10	0.2110028	0.009	209.820	0.771	994.135	0.001006	0.742
Common Pb for 2910 Ma		1.0998859		14.458		13.145	0.076075	
605E8P	1	0.2252788	0.053	559.065	0.142	2475.860	0.000404	0.298
	2	0.2244283	0.084				0.000579	15.797
	3	0.2240387	0.030	586.648	0.555	2618.487	0.000382	0.509
	4	0.2239793	0.031	599.305	0.152	2675.943	0.000374	0.143
	5	0.2239750	0.025	619.540	0.428	2766.252	0.000362	0.408
Common Pb for 3000 Ma		1.1092807		14.343		12.930	0.077340	
605F2P	1	0.1941834	0.290	288.976	8.944	1490.313	0.000671	8.740
	2	0.1925074	0.326	278.489	5.316	1451.379	0.000689	4.986
Common Pb for 2700 Ma		1.0773744		14.690		13.635	0.073341	
605F4P	1	0.2215415	0.607	340.611	3.330	1532.332	0.000653	3.717
	2	0.2296148	0.519	221.122	4.266	961.631	0.001040	4.235
	3	0.2373844	1.010	185.099	17.593	779.970	0.001282	17.529
Common Pb for 2950 Ma		1.1040613		14.408		13.050	0.076628	

Name	Run	207Pb 206Pb	St. Err. (%)	207Pb 204Pb	St. Err. (%)	206Pb 204Pb	204Pb 206Pb	St. Err. (%)
605F5P	1	0.2145439	0.230	1510.118	9.144	7097.232	0.000141	8.702
	2	0.2097524	0.171	4885.198	62.263	23310.023	0.000043	58.715
	3	0.2095315	0.130	32679.739	99.990	175438.596	0.000006	99.990
	4	0.2086934	0.108	16393.443	66.182	78125.000	0.000013	63.838
	5	0.2092343	0.098	13586.957	46.200	63694.268	0.000016	41.807
	6	0.2088547	0.074	20000.000	73.264	95238.095	0.000011	70.428
	7	0.2092278	0.116	14619.883	23.211	70921.986	0.000014	21.201
	8	0.2091079	0.129	15290.520	18.976	72992.701	0.000014	18.710
	9	0.2091048	0.053	15015.015	26.520	72463.768	0.000014	24.357
	10	0.2088808	0.062	17391.304	26.170	84033.613	0.000012	24.868
	11	0.2095205	0.096	13477.089	11.951	64516.129	0.000016	11.530
	12	0.2099711	0.078	10741.139	13.290	51020.408	0.000020	12.056
	13	0.2106971	0.124	13054.830	22.789	62111.801	0.000016	21.877
Common Pb for 2910 Ma		1.0998859		14.458		13.145	0.076075	
605F6P	1	0.2465577	0.126	243.167	1.304	985.319	0.001015	1.352
	2	0.2426875	0.129	258.365	0.695	1065.530	0.000939	0.685
	3	0.2473445	0.345	233.852	3.215	946.790	0.001056	3.300
Common Pb for 3090 Ma		1.1183921		14.217		12.712	0.078666	

Figure 4.3A York fit of ^{206}Pb/^{204}Pb vs. ^{207}Pb/^{204}Pb data from 605 with ^{206}Pb/^{204}Pb<10,000.

Legend:

◇	605E3PC	–	2879± 5	Ma	(2σ)	
☆	605E6P	–	3068± 3	Ma	(2σ)	
△	605E7P	–	2827± 3	Ma	(2σ)	
+	605E8P	–	2988± 1	Ma	(2σ)	
○	605F2P	–	2698±17	Ma	(2σ)	
✪	605F4P	–	2970±15	Ma	(2σ)	
◇	605F6P	–	3087± 7	Ma	(2σ)	

X-axis: $^{206}Pb/^{204}Pb$

Y-axis: $^{207}Pb/^{204}Pb$

118
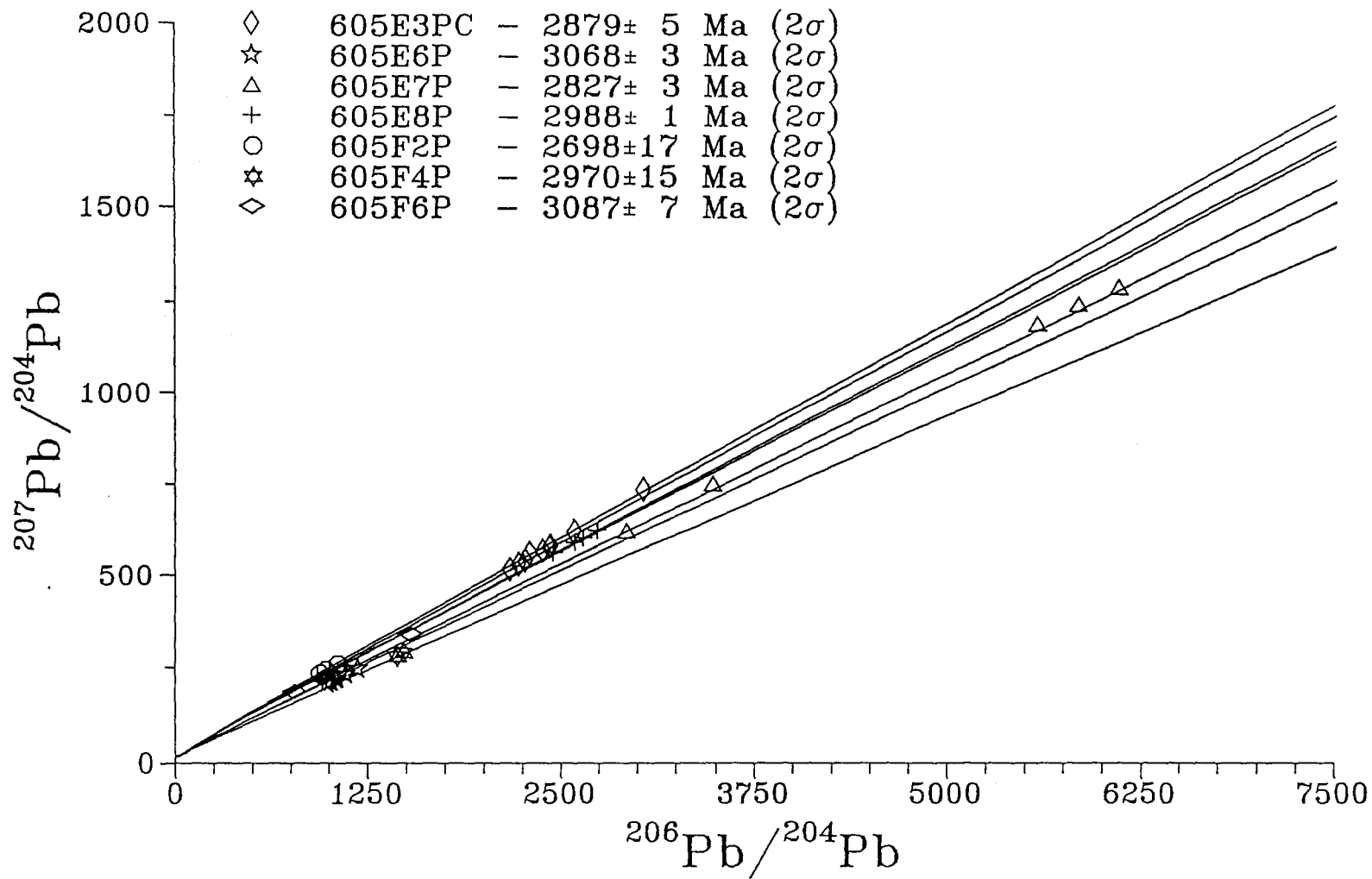
Figure 4.3B York fit of $^{206}Pb/^{204}Pb$ vs. $^{207}Pb/^{204}Pb$ data from 605 with $^{206}Pb/^{204}Pb>10,000$.
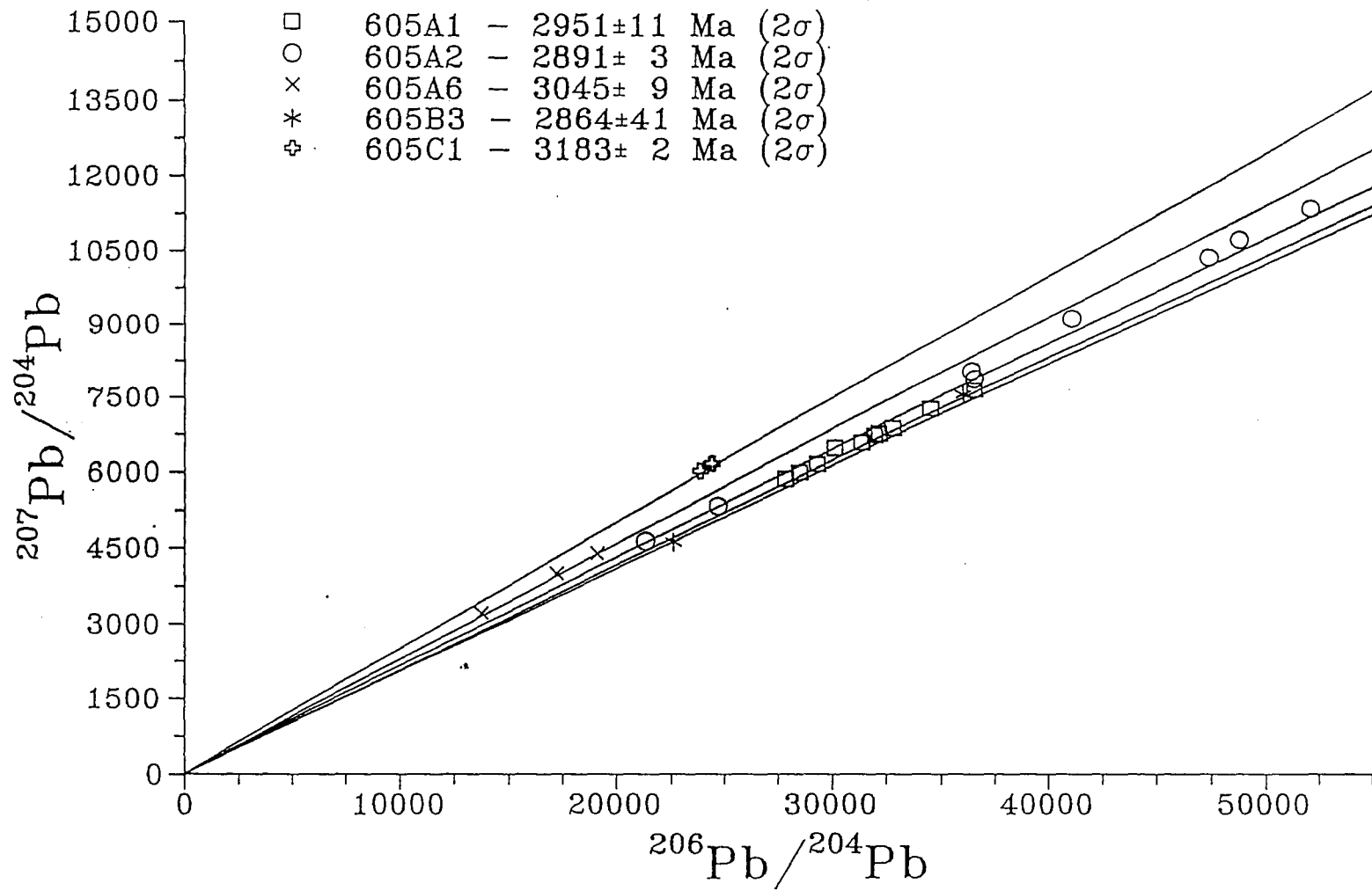
Figure 4.4A York fit of ^{204}Pb/^{206}Pb vs. ^{207}Pb/^{206}Pb data from 605 with ^{204}Pb/^{206}Pb<0.0001.

Legend:
- □ 605A2P — 2888± 2 Ma (2σ)
- + 605A4P — 2921± 2 Ma (2σ)
- × 605A6 — 2993±218 Ma (2σ)
- ∗ 605B3 — 2837±413 Ma (2σ)

Y-axis: $^{207}Pb/^{206}Pb$

X-axis: $^{204}Pb/^{206}Pb$

120
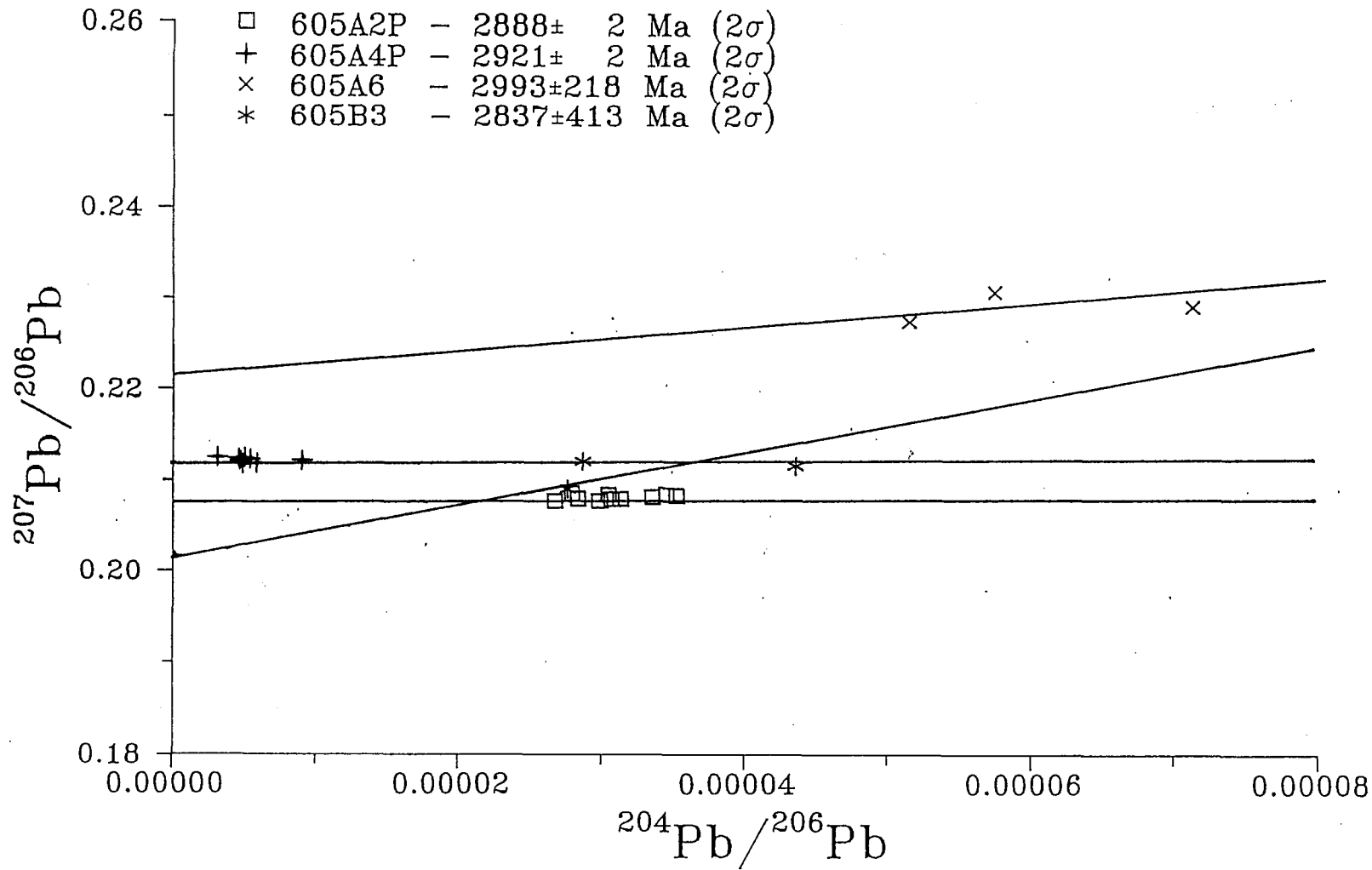
Figure 4.4B York fit of ^{204}Pb/^{206}Pb vs. ^{207}Pb/^{206}Pb data from 605 with ^{204}Pb/^{206}Pb>0.0001.
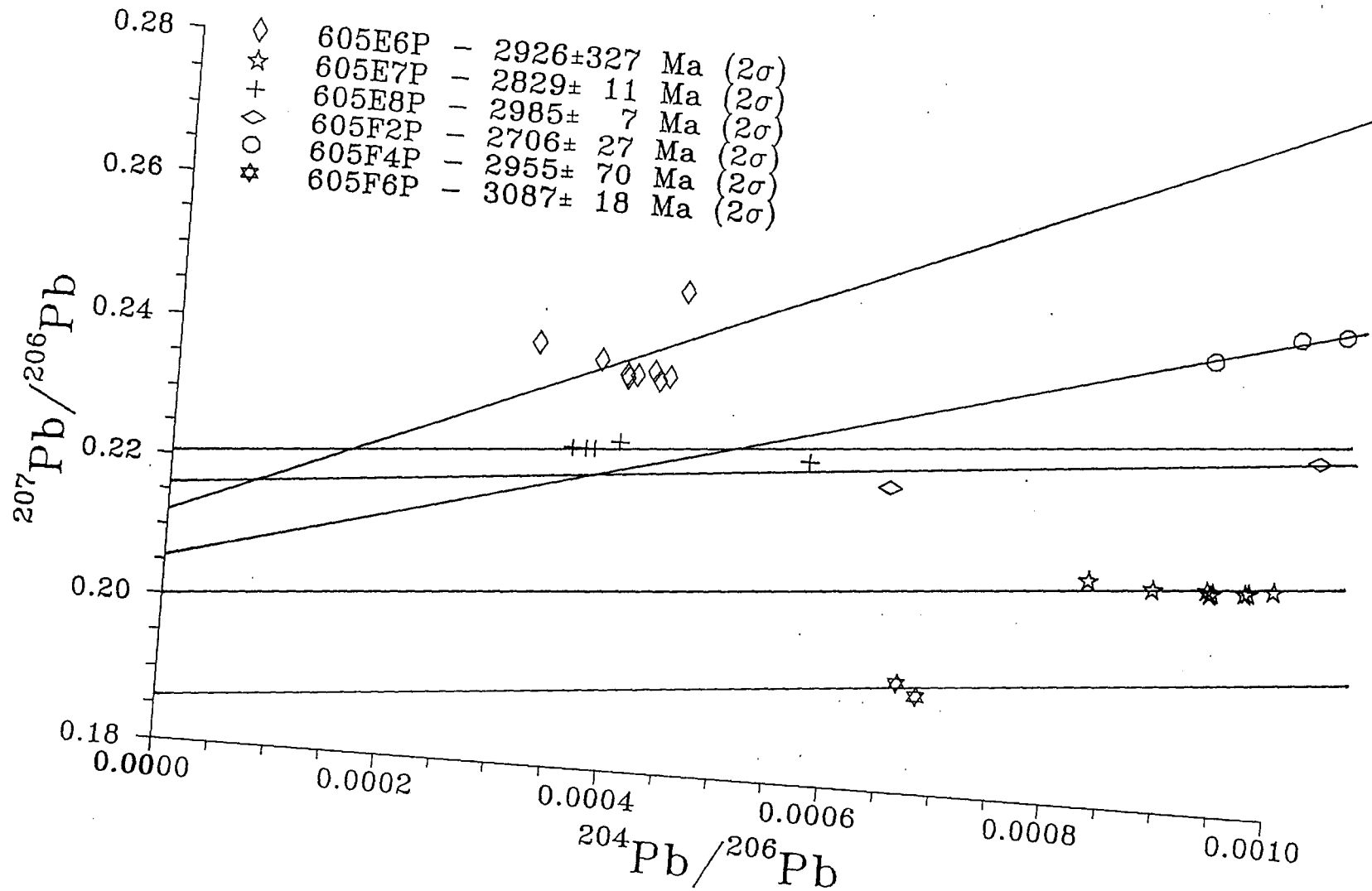
121

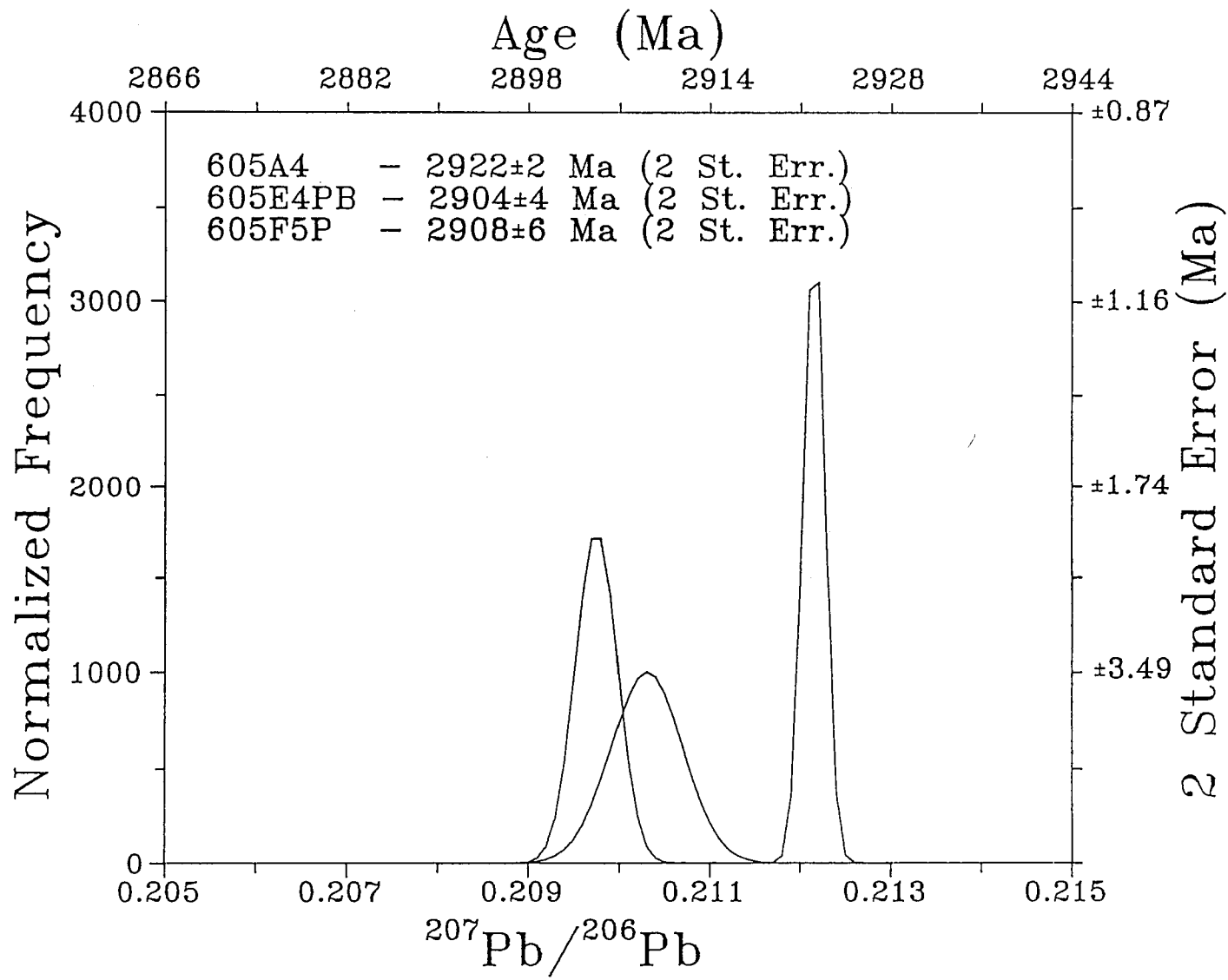Figure 4.5 $^{207}Pb/^{206}Pb$ histogram of data from 605.

Figure 4.6 Age histogram of 605.

Table 4.7   Raw data from CED1
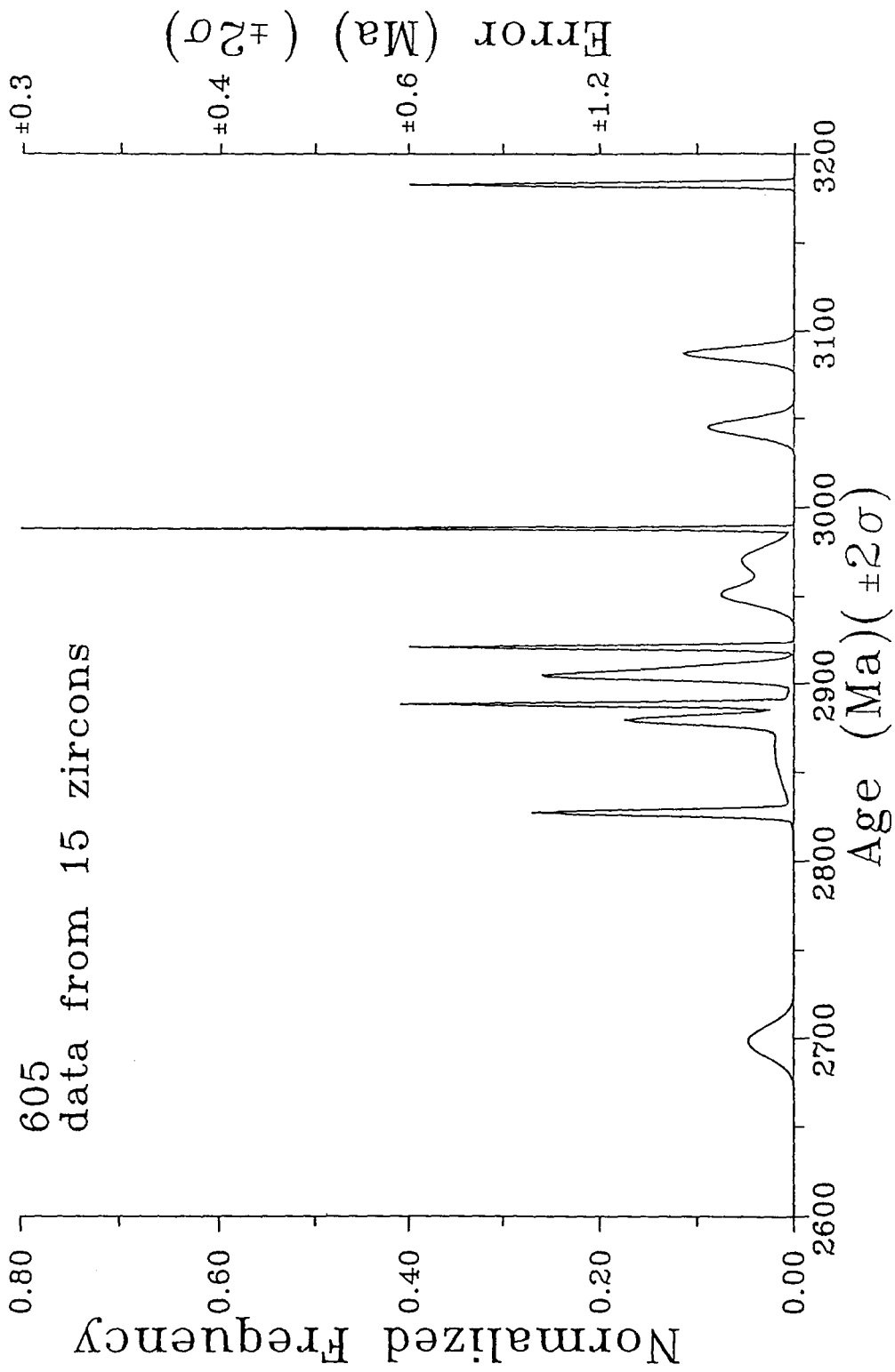
Name	Run	207Pb 206Pb	St. Err. (%)	207Pb 204Pb	St. Err. (%)	206Pb 204Pb	204Pb 206Pb	St. Err. (%)
CED1A3	1	0.2455060	2.585	23584.906	99.990	95238.095	0.000011	99.501
	2	0.2350651	0.985	7473.842	93.601	29850.746	0.000034	87.678
	3	0.2389282	1.503	10917.031	60.258	45871.560	0.000022	56.317
	4	0.2467677	2.487	-8375.209	63.808	-36101.083	-0.000028	56.958
	5	0.2366222	3.188	15948.963	99.990	74626.866	0.000013	97.844
	6	0.2372686	1.628	35087.719	99.990	169491.525	0.000006	99.990
	7	0.2540733	2.576	-59171.598	99.990	-200000.000	-0.000005	99.990
	8	0.2165917	5.799	144927.536	99.990	555555.556	0.000002	99.990
	9	0.2233879	6.624	9398.496	29.539	40160.643	0.000025	32.231
	10	0.2547066	3.060	5497.526	33.606	17985.612	0.000056	16.533
	11	0.2544776	1.474	10266.940	99.990	30674.847	0.000033	99.990
	13	0.2491760	0.070	1326.612	60.916	5408.329	0.000185	60.230
Common Pb for 3120 Ma		1.1213704		14.173		12.639	0.079120	
CED1A4	1	0.2566387	1.179	1224.290	12.281	8557.248	0.000117	26.647
	2	0.2577831	11.314	1987.281	21.187	7272.727	0.000138	20.384
	3	0.2488759	1.176	54644.809	99.990	43668.122	0.000023	99.990
Common Pb for 3190 Ma		1.1280982		14.064		12.467	0.080212	
CED1B3	1	0.2825789	0.090	2639.916	24.579	9354.537	0.000107	23.001
	2	0.2832449	0.060	72463.768	99.990	294117.647	0.000003	99.990
	3	0.2830475	0.103	27100.271	59.873	97087.379	0.000010	55.306
	4	0.2820097	0.152	18416.206	89.869	63694.268	0.000016	83.141
	5	0.2830203	0.077	-29325.513	99.990	-101010.101	-0.000010	98.588
	6	0.2832610	0.053	-25125.628	61.326	-107526.882	-0.000009	75.811
	7	0.2832306	0.116	44444.444	99.990	142857.143	0.000007	99.990
	8	0.2834378	0.047	-116279.070	99.990	-500000.000	-0.000002	99.990
	9	0.2834642	0.045	27027.027	99.990	97087.379	0.000010	99.990
	10	0.2834768	0.089	28490.028	99.990	107526.882	0.000009	99.990
	11	0.2828476	0.081	23474.178	95.693	86956.522	0.000012	99.990

Name	Run	207Pb / 206Pb	St. Err. (%)	207Pb / 204Pb	St. Err. (%)	206Pb / 204Pb	204Pb / 206Pb	St. Err. (%)
CED1B3	12	0.2830148	0.091	34722.222	99.990	114942.529	0.000009	99.990
	13	0.2836360	0.144	-17482.517	92.628	-59523.810	-0.000017	86.695
	14	0.2843440	0.161	-10256.410	50.394	-36231.884	-0.000028	48.114
	15	0.2834609	0.165	-147058.824	99.990	-476190.476	-0.000002	99.990
	16	0.2836197	0.098	30769.231	99.990	99009.901	0.000010	99.990
	17	0.2850842	0.088	17391.304	99.990	63291.139	0.000016	99.990
	18	0.2847604	0.076	22421.525	44.218	75187.970	0.000013	39.304
	19	0.2847418	0.060	-94339.623	99.990	-277777.778	-0.000004	99.990
	20	0.2844766	0.038	7861.635	41.681	27624.309	0.000036	39.408
	21	0.2850497	0.078	6891.799	40.204	24570.025	0.000041	39.437
	22	0.2847311	0.197	1800.180	47.897	6540.222	0.000153	46.831
	23	0.2858325	0.422	-11037.528	99.990	-40000.000	-0.000025	99.990
Common Pb for 3380 Ma		1.1450496		13.728		11.989	0.083410	
CED1F2	1	0.2397988	0.264	1228.954	32.315	5241.090	0.000191	30.493
	2	0.2415917	0.495	-28735.632	99.990	-49261.084	-0.000020	99.990
	3	0.2447581	0.442	-293.720	84.108	-1261.830	-0.000793	82.541
Common Pb for 3130 Ma		1.1223147		14.158		12.615	0.079271	
CED1G3	1	0.1860913	0.902	114.879	36.223	629.525	0.001589	34.692
	2	0.1814935	0.499	131.522	18.245	722.857	0.001383	17.616
	3	0.1824143	0.693	177.800	29.119	967.680	0.001033	26.441
	5	0.1831941	0.323	326.563	31.388	1777.778	0.000563	30.047
Common Pb for 2680 Ma		1.0751407		14.709		13.681	0.073094	

Name	Run	207Pb/206Pb	St. Err. (%)	207Pb/204Pb	St. Err. (%)	208Pb/204Pb	204Pb/206Pb	St. Err. (%)
CED1H3P	3	0.2191164	0.449	53.376	18.219	241.045	0.004149	17.234
	4	0.2205690	0.689	137.935	47.727	630.438	0.001586	44.089
	5	0.2210036	0.618	-426.967	52.174	-1891.432	-0.000529	49.354
	6	0.2158111	0.318	-799.488	37.073	-3656.307	-0.000274	34.727
	7	0.2160346	0.611	1630.789	41.145	7547.170	0.000133	40.114
Common Pb for 2970 Ma		1.1061375		14.382		13.002	0.076911	
CED1H4PB	2	0.2475310	0.258	247.506	1.897	1000.901	0.000999	1.851
	3	0.2487252	0.210	253.608	5.300	1018.019	0.000982	5.157
	4	0.2464207	0.237	281.001	5.638	1137.398	0.000879	5.088
	5	0.2460891	0.180	296.200	5.224	1201.201	0.000833	5.108
	6	0.2452883	0.117	299.356	4.494	1218.621	0.000821	4.316
	7	0.2442261	0.106	309.684	3.369	1265.022	0.000791	3.133
	8	0.2437957	0.152	322.321	2.968	1323.276	0.000756	2.991
	9	0.2430749	0.081	320.266	1.848	1316.136	0.000760	1.656
	10	0.2436813	0.128	340.623	2.420	1400.756	0.000714	2.243
	11	0.2436829	0.131	334.526	3.410	1372.684	0.000729	3.336
	12	0.2436450	0.097	356.875	2.604	1464.129	0.000683	2.502
	13	0.2440022	0.087	349.895	2.805	1433.692	0.000696	2.584
	14	0.2435956	0.071	337.998	2.895	1390.047	0.000719	2.558
	15	0.2436472	0.176	345.662	2.330	1418.037	0.000705	2.242
	16	0.2442097	0.122	317.702	1.994	1325.205	0.000755	1.097
	17	0.2433941	0.124	367.336	1.950	1511.031	0.000662	1.329
	18	0.2437657	0.147	336.010	3.247	1378.170	0.000726	2.972
	19	0.2444619	0.116	337.838	1.844	1382.361	0.000723	1.650
Common Pb for 3160 Ma		1.1252691		14.112		12.541	0.079738	

Name	Run	207Pb 206Pb	St. Err. (%)	207Pb 204Pb	St. Err. (%)	206Pb 204Pb	204Pb 206Pb	St. Err. (%)
CED1I12P	2	0.2983165	1.486	30.335	6.309	102.089	0.009795	7.123
	4	0.2666457	1.137	75.956	18.642	276.648	0.003615	19.114
	5	0.2566927	0.265	220.473	19.592	849.257	0.001178	18.181
	6	0.2563473	0.592				0.001000	30.024
	7	0.2576236	0.785	152.711	21.966	596.019	0.001678	20.405
Common Pb for 3030 Ma		1.1123036		14.302		12.858	0.077773	
CED1J4P	1	0.2382940	0.372	78.610	6.284	328.774	0.003042	6.226
	2	0.2256926	0.205	138.808	21.294	622.549	0.001606	19.599
Common Pb for 2860 Ma		1.0946241		14.518		13.263	0.075398	
CED1J5P	1	0.2624316	0.158	73.782	1.812	281.096	0.003558	1.857
	2	0.2594932	0.060	80.122	1.550	308.842	0.003238	1.475
	3	0.2583316	0.151	83.437	0.855	322.737	0.003099	0.815
	4	0.2592722	0.200	84.990	1.539	327.579	0.003053	1.404
	5	0.2731205	1.176				0.004216	6.014
	6	0.2758136	0.525	56.828	1.396	206.156	0.004851	1.317
	7	0.2751878	0.168	58.797	0.779	213.479	0.004684	0.752
	8	0.2765435	0.254	61.286	1.323	225.887	0.004427	2.107
Common Pb for 3010 Ma		1.1103363		14.330		12.906	0.077483	

Figure 4.7 York fit of ^{206}Pb/^{204}Pb vs. ^{207}Pb/^{204}Pb data from CED1.

Legend:

☆ CED1G3 — 2561±137 Ma (2σ)
◇ CED1H4P — 3085± 7 Ma (2σ)
△ CED1I12P — 3187± 12 Ma (2σ)
□ CED1J4P — 2866± 86 Ma (2σ)
○ CED1J5P — 3008± 15 Ma (2σ)

$^{207}Pb/^{204}Pb$ (y-axis)

$^{206}Pb/^{204}Pb$ (x-axis)
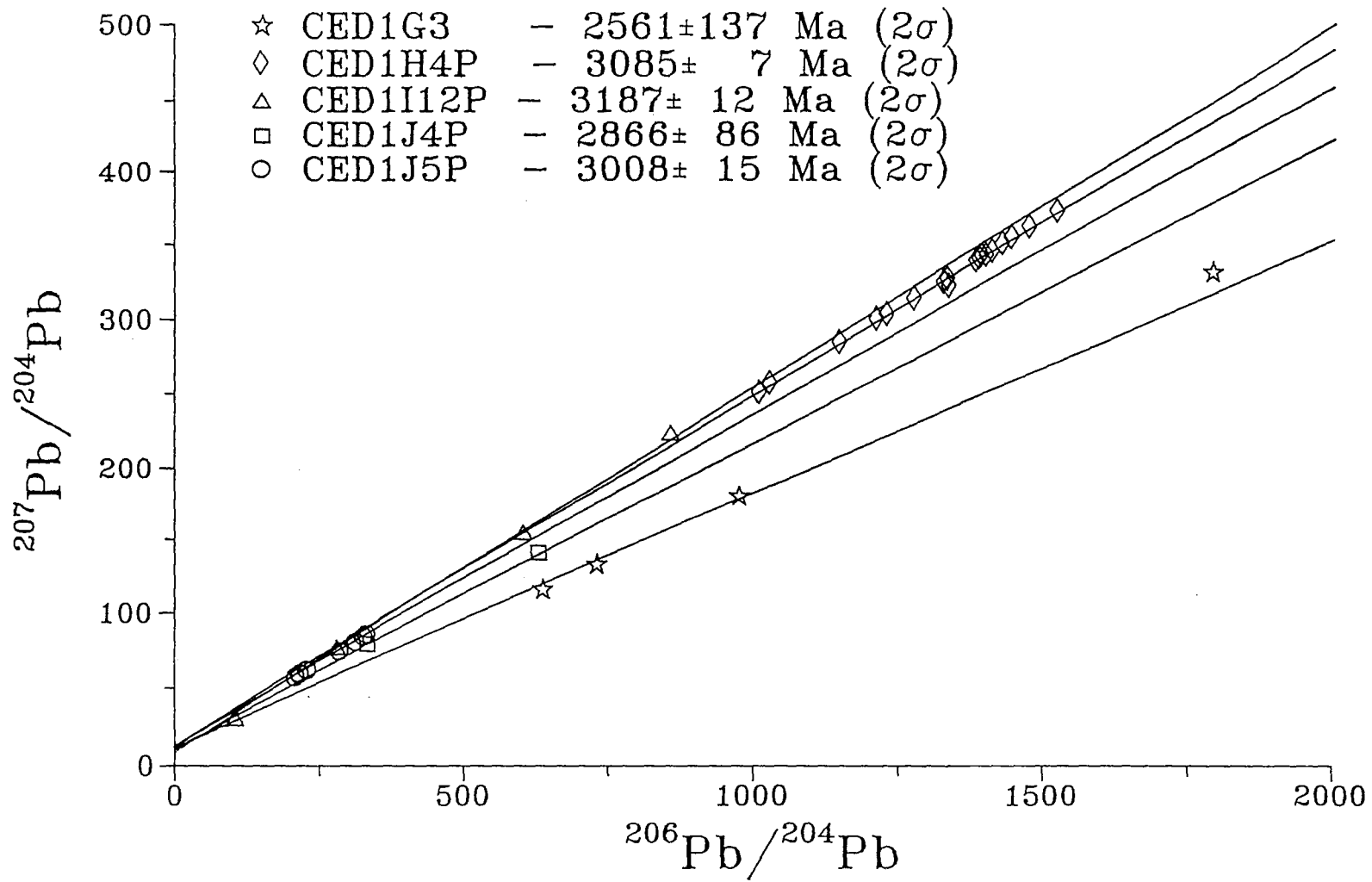
Figure 4.8 York fit of ^{204}Pb/^{206}Pb vs. ^{207}Pb/^{206}Pb data from CED1.

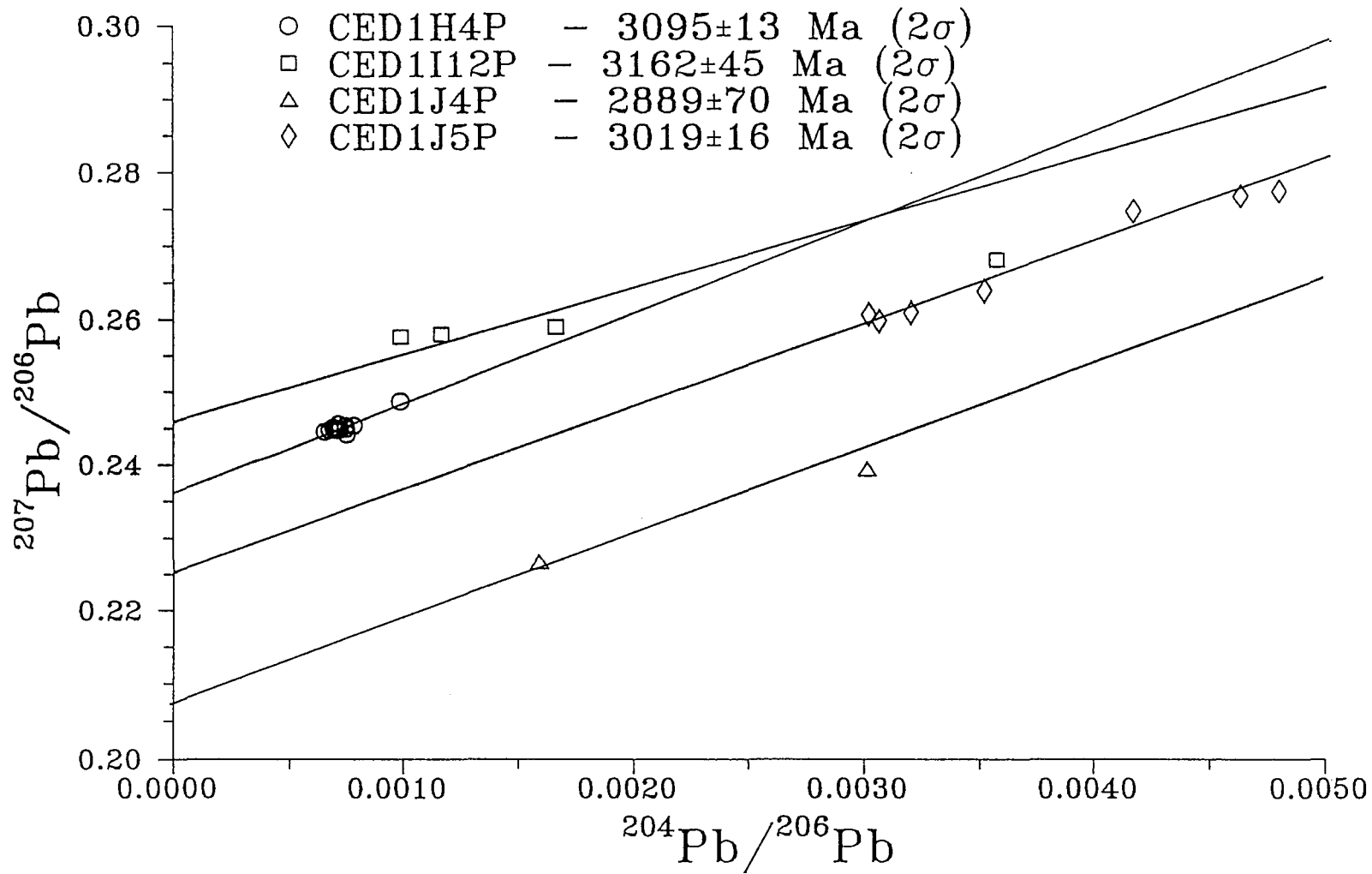Figure 4.9 $^{207}Pb/^{206}Pb$ histogram of data from CED1.
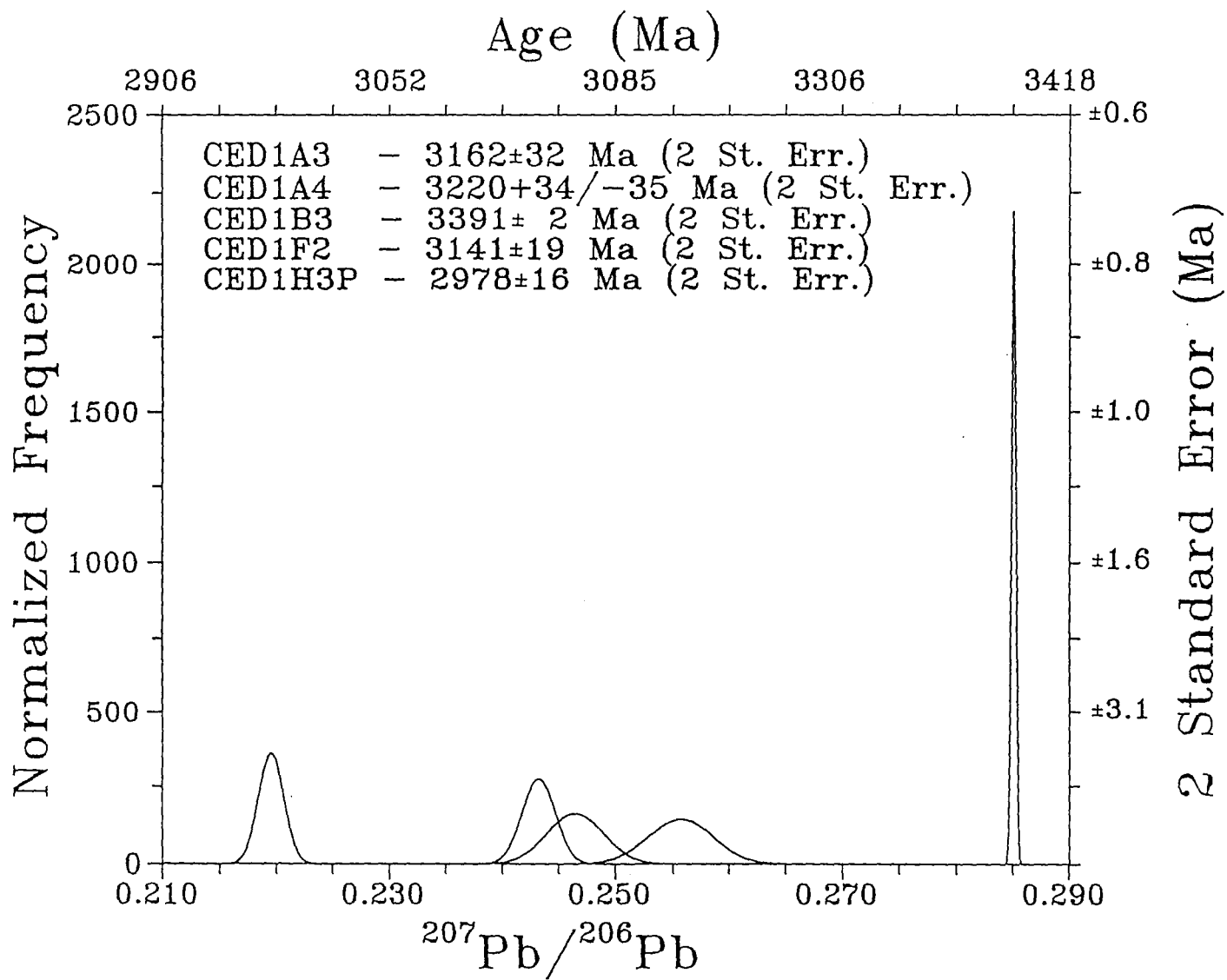
Figure 4.10 Age histogram of CED1.

Table 4.8 Raw data from CED6
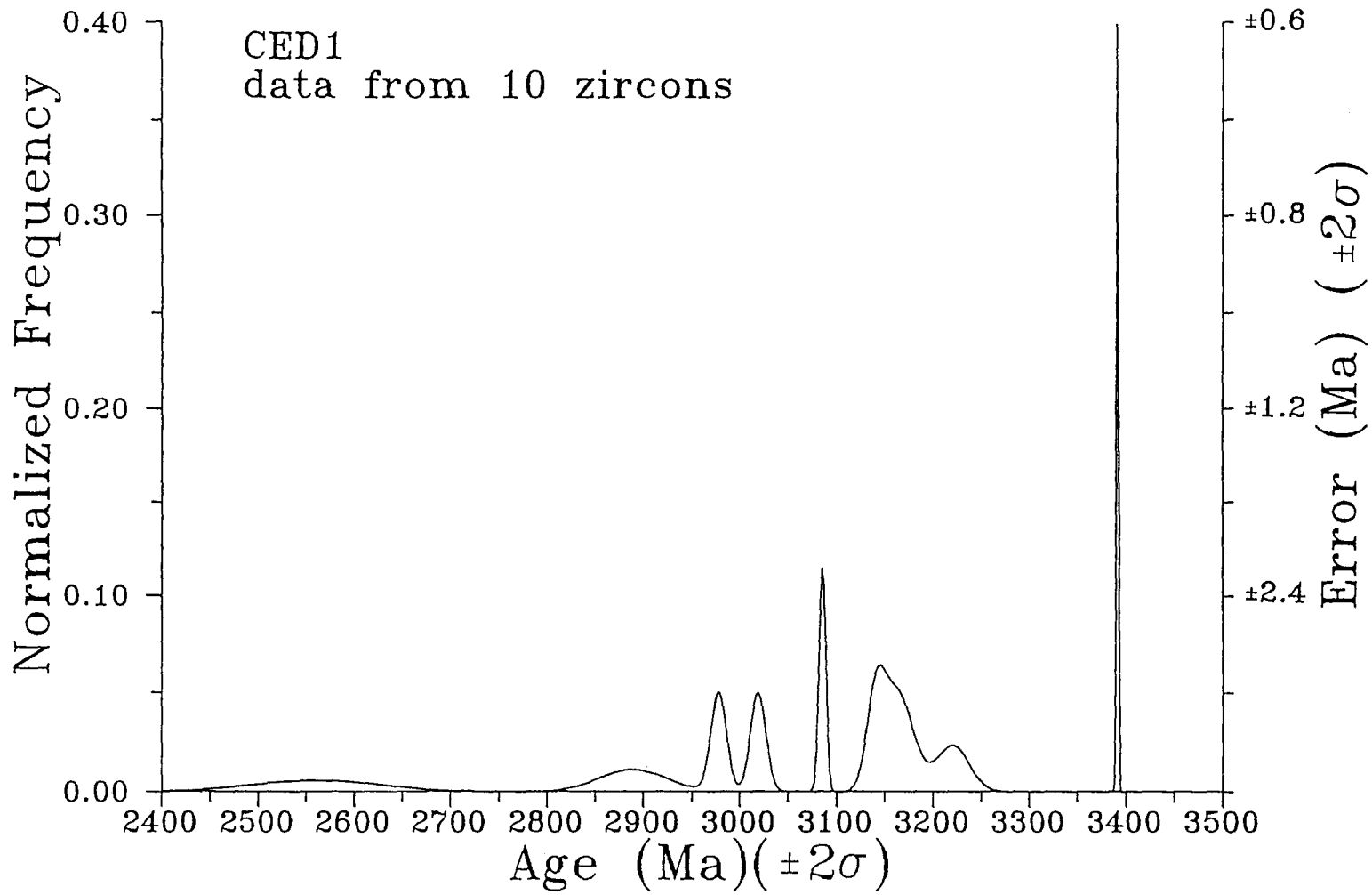
Name	Run	207Pb / 206Pb	St. Err. (%)	207Pb / 204Pb	St. Err. (%)	206Pb / 204Pb	204Pb / 206Pb	St. Err. (%)
CED6A1	1	0.1844952	0.051	3057.169	2.219	16528.926	0.000061	2.033
	2	0.1850822	0.065	2832.059	3.848	15360.983	0.000065	3.636
	3	0.1856850	0.098	2460.025	6.213	13280.212	0.000075	5.838
	4	0.1855144	0.090	1030.822	5.244	5571.031	0.000180	4.764
Common Pb for 2700 Ma		1.0770925		14.670		13.620	0.073421	
CED6B1	1	0.1845390	0.179	-1400.756	82.997	-7867.821	-0.000127	81.791
	3	0.1844761	0.179	8250.825	99.990	39062.500	0.000026	99.990
	4	0.1851919	0.262	6006.006	99.990	35587.189	0.000028	99.990
	5	0.1843830	0.099	3992.016	21.728	20833.333	0.000048	21.163
	6	0.1844534	0.229	2379.253	38.027	13123.360	0.000076	36.720
	8	0.1846547	0.181	-1390.821	57.575	-7651.109	-0.000131	52.582
	9	0.1848728	0.223	-1906.214	51.147	-11507.480	-0.000087	48.163
	10	0.1844696	0.269	-4703.669	99.990	-23364.486	-0.000043	99.990
	11	0.1857085	0.334	-1362.027	99.990	-6811.969	-0.000147	99.990
Common Pb for 2690 Ma		1.0762923		14.700		13.658	0.073217	
CED6B2	1	0.2204552	0.283	1410.636	46.764	6410.256	0.000156	44.921
	2	0.2213968	0.221	593.859	39.184	2697.599	0.000371	38.423
Common Pb for 2980 Ma		1.1071814		14.369		12.978	0.077053	

Name	Run	207Pb 206Pb	St. Err. (%)	207Pb 204Pb	St. Err. (%)	206Pb 204Pb	204Pb 206Pb	St. Err. (%)
CED6B3	1	0.2180627	0.340	-1347.164	99.990	-7558.579	-0.000132	99.990
	2	0.2167159	0.617	-9910.803	99.990	-140645.070	-0.000007	99.990
	3	0.2163031	0.302	-4340.278	99.990	-19960.060	-0.000050	99.990
	4	0.2167879	0.617	-1309.929	99.990	-6514.656	-0.000154	99.990
	5	0.2227119	0.713	-932.140	99.990	-4725.898	-0.000212	99.990
Common Pb for 2960 Ma		1.1050974		14.395		13.026	0.076770	
CED6C3	1	0.1743173	0.233	611.471	47.206	3679.176	0.000272	41.392
	2	0.1763484	0.272	1378.170	99.990	7942.812	0.000126	99.990
	3	0.1762416	0.230	-2601.457	27.581	-14814.815	-0.000068	24.121
	4	0.1745408	0.849	-209.996	32.363	-1238.237	-0.000808	30.471
Common Pb for 2620 Ma		1.0686062		14.766		13.818	0.072369	
CEDE1	1	0.1542801	0.098	1376.462	20.394	8810.573	0.000114	19.447
	2	0.1549157	0.171	1517.22	12.022	12091.898	0.000083	23.034
	3	0.1553525	0.163	5030.181	99.990	35335.689	0.000028	99.990
	4	0.1552571	0.261	1610.825	54.967	7418.398	0.000135	19.766
	5	0.1579554	0.432	-887.075	54.125	-5668.934	-0.000176	49.153
Common Pb for 2410 Ma		1.0457791		14.940		14.286	0.069999	

Figure 4.11   York fit of ^{206}Pb/^{204}Pb vs. ^{207}Pb/^{204}Pb data from CED6.
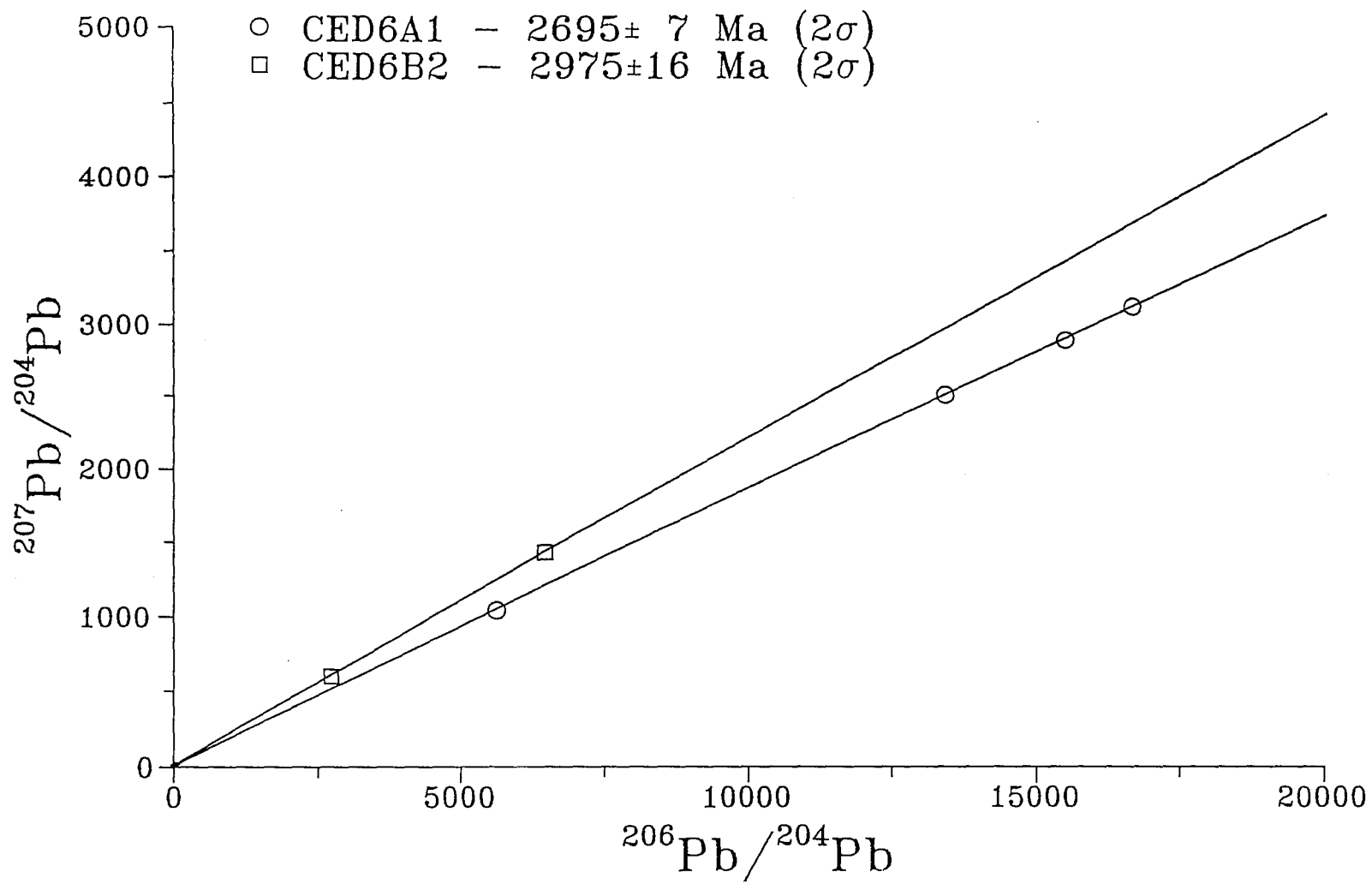
Figure 4.12 ^{207}Pb/^{206}Pb histogram of data from CED6.

Age (Ma)

2346   2558   2742   2906   3052

CED6B1 — 2702± 1 Ma (2 St. Err.)
CED6B3 — 2975±18 Ma (2 St. Err.)
CED6C3 — 2618±10 Ma (2 St. Err.)
CED6E1 — 2408± 9 Ma (2 St. Err.)

Normalized Frequency

7500
6000
4500
3000
1500
0

±0.24
±0.30
±0.41
±0.61
±1.2

2 Standard Error (Ma)

0.150   0.170   0.190   0.210   0.230
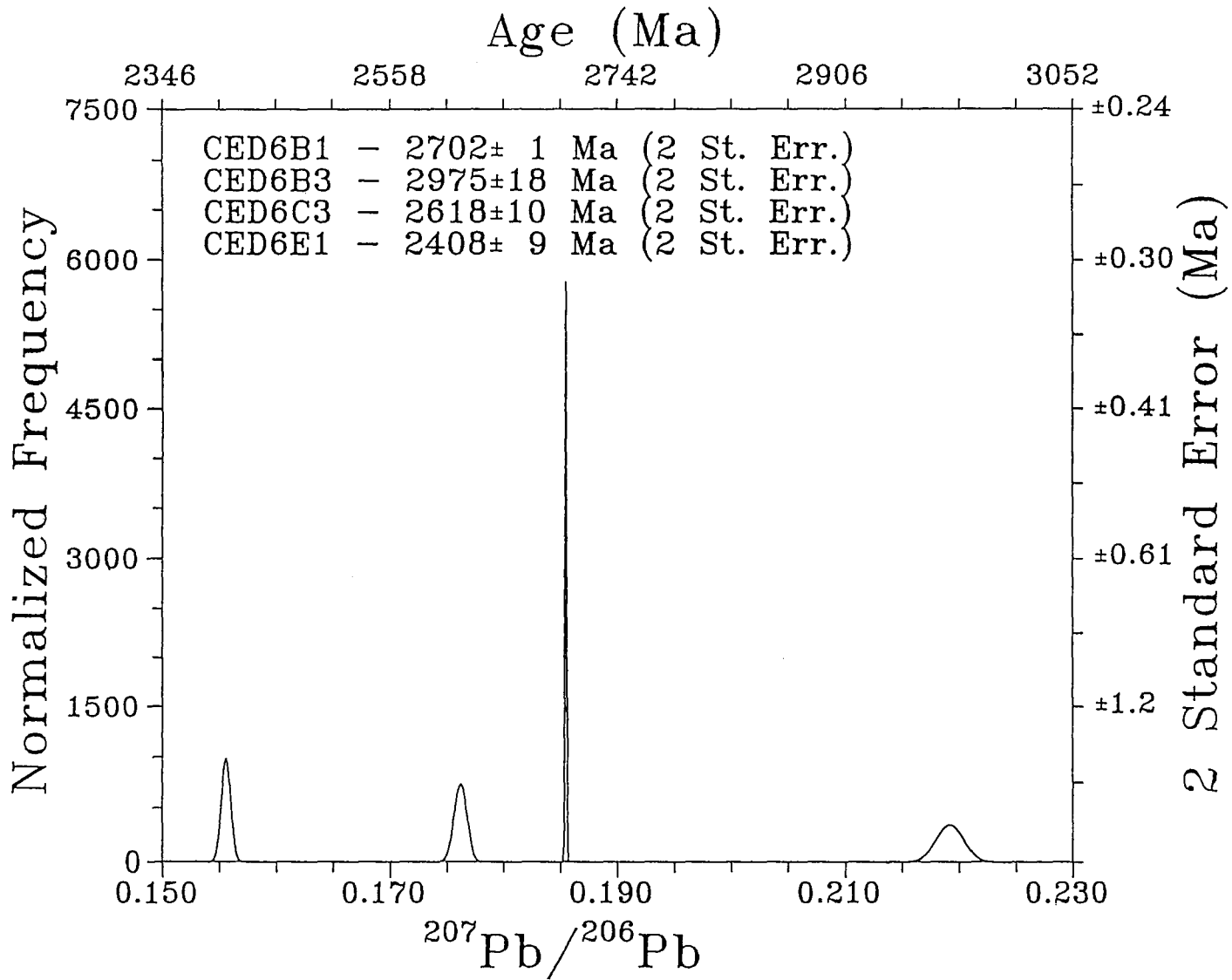
$^{207}Pb/^{206}Pb$

Figure 4.13 Age histogram of CED6.
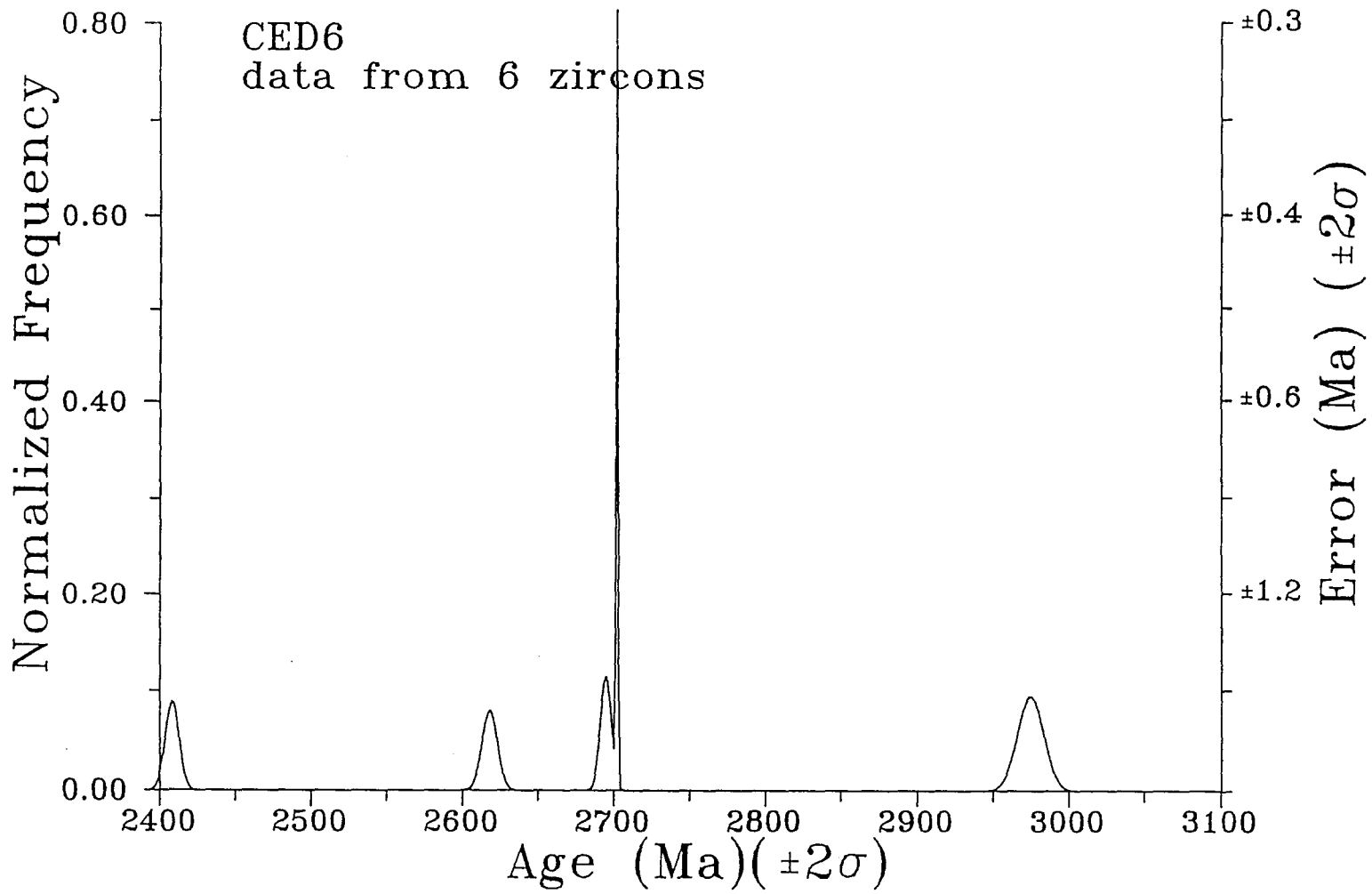
Table 4.9 Raw data from CED7

Name	Runs	207Pb/206Pb	St. Err. (%)	207Pb/204Pb	St. Err. (%)	206Pb/204Pb	204Pb/206Pb	St. Err. (%)
CED7A1P	1			101.363	3.820	389.226		4.200
	2	0.2492708	0.117	139.593	1.578	559.065	0.001789	1.625
	3	0.2475025	0.170	148.580	1.218	600.348	0.001666	1.037
	4	0.2467765	0.081	162.027	1.154	656.875	0.001522	1.150
	5	0.2469265	0.072	166.337	1.277	674.445	0.001483	1.135
	6	0.2446931	0.122	193.125	1.123	789.702	0.001266	1.072
	7	0.2452893	0.164	191.652	0.667	780.640	0.001281	0.577
	8			229.489	3.667	943.218		3.570
Common Pb for 3070 Ma		1.1163702		14.246		12.761	0.078364	
CED7A2P	2	0.2346423	0.074	1130.327	10.769	4791.567	0.000209	10.440
	3	0.2342924	0.062	2512.563	7.709	10695.187	0.000094	7.228
	4	0.2342653	0.091	2882.675	13.269	12422.360	0.000081	12.945
	5	0.2344235	0.063	2374.733	4.563	9451.796	0.000106	6.519
	6	0.2340392	0.139	2172.968	12.138	9345.794	0.000107	11.791
Common Pb for 3080 Ma		1.1173746		14.232		12.737	0.078511	
CED7A4P	1	0.2494657	0.039	2259.376	2.457	9049.774	0.000111	2.418
	2	0.2491869	0.031	2754.062	1.681	11037.528	0.000091	1.687
	3	0.2499213	0.023	2930.832	1.594	11737.089	0.000085	1.446
	4	0.2501375	0.041	3370.408	3.360	13477.089	0.000074	3.204
	5	0.2507265	0.042	3617.945	5.023	14367.816	0.000070	4.235
Common Pb for 3190 Ma		1.1280982		14.064		12.467	0.080212	
CED7A7P	2	0.2460211	0.289	633.112	5.383	2547.771	0.000393	5.686
	3	0.2421505	0.606	665.868	19.795	2717.391	0.000368	17.946
Common Pb for 3150 Ma		1.1243136		14.127		12.565	0.079586	

133

Figure 4.14   York fit of ^{206}Pb/^{204}Pb vs. ^{207}Pb/^{204}Pb data from CED7.

CED7A1P — 3061±11 Ma (2σ)
CED7A2P — 3084±15 Ma (2σ)
CED7A4P — 3187±12 Ma (2σ)
CED7A7P — 3163±10 Ma (2σ)
CED7B1P — 3078+58/−61 Ma (2σ)
CED7B4P — 3078±34 Ma (2σ)
CED7C4P — 3158+24/−25 Ma (2σ)

134
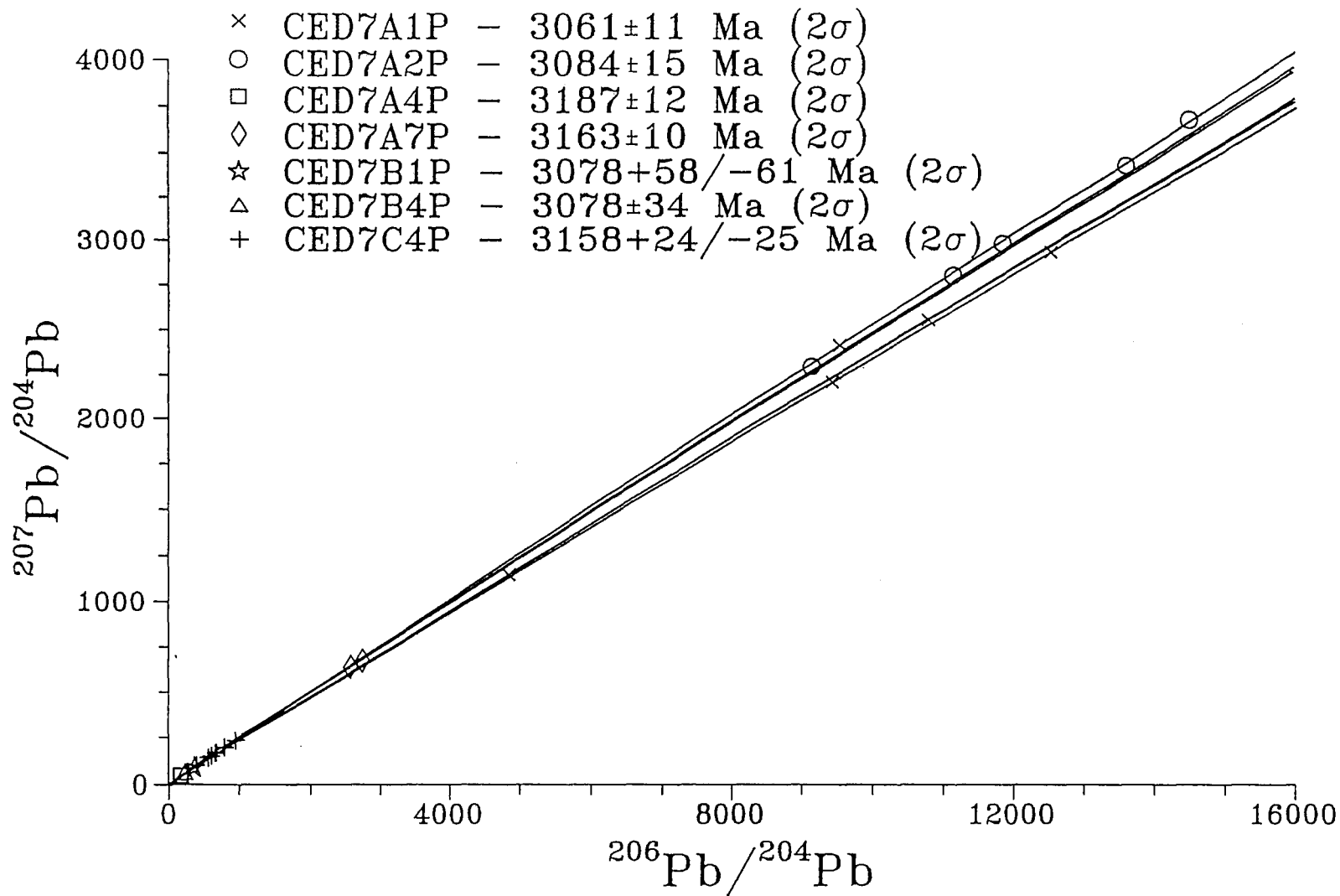
Figure 4.15 York fit of ^{204}Pb/^{206}Pb vs. ^{207}Pb/^{206}Pb data from CED7.

Legend:
- ○ CED7A1P − 3060± 8 Ma (2σ)
- □ CED7A2P − 3087± 5 Ma (2σ)
- △ CED7A4P − 3186± 4 Ma (2σ)
- ◇ CED7B1P − 3091+21/−22 Ma (2σ)
- ☆ CED7B4P − 3067±61 Ma (2σ)

x-axis: $^{204}\text{Pb}/^{206}\text{Pb}$

y-axis: $^{207}\text{Pb}/^{206}\text{Pb}$
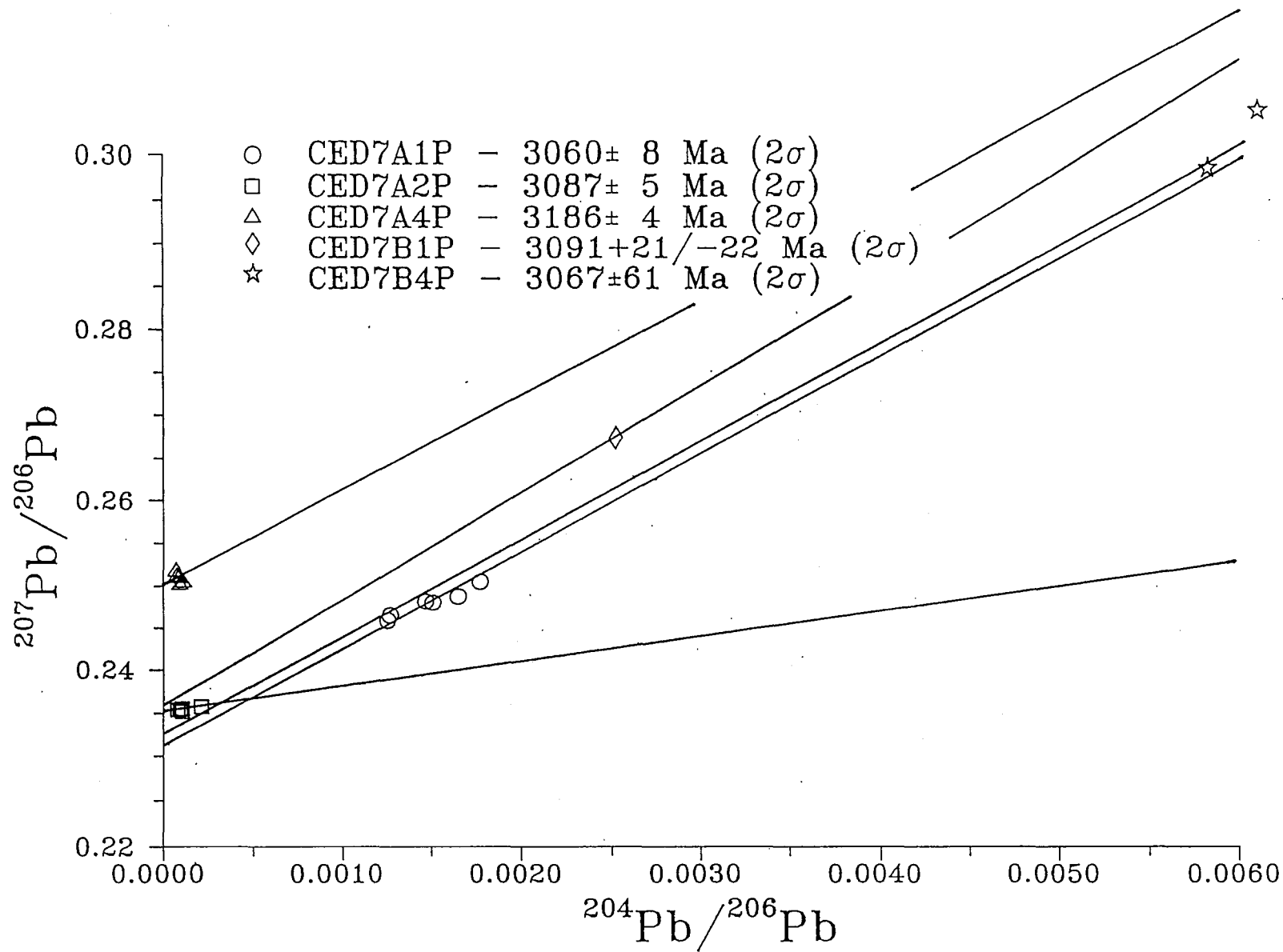
Figure 4.16 Age histogram of CED7.
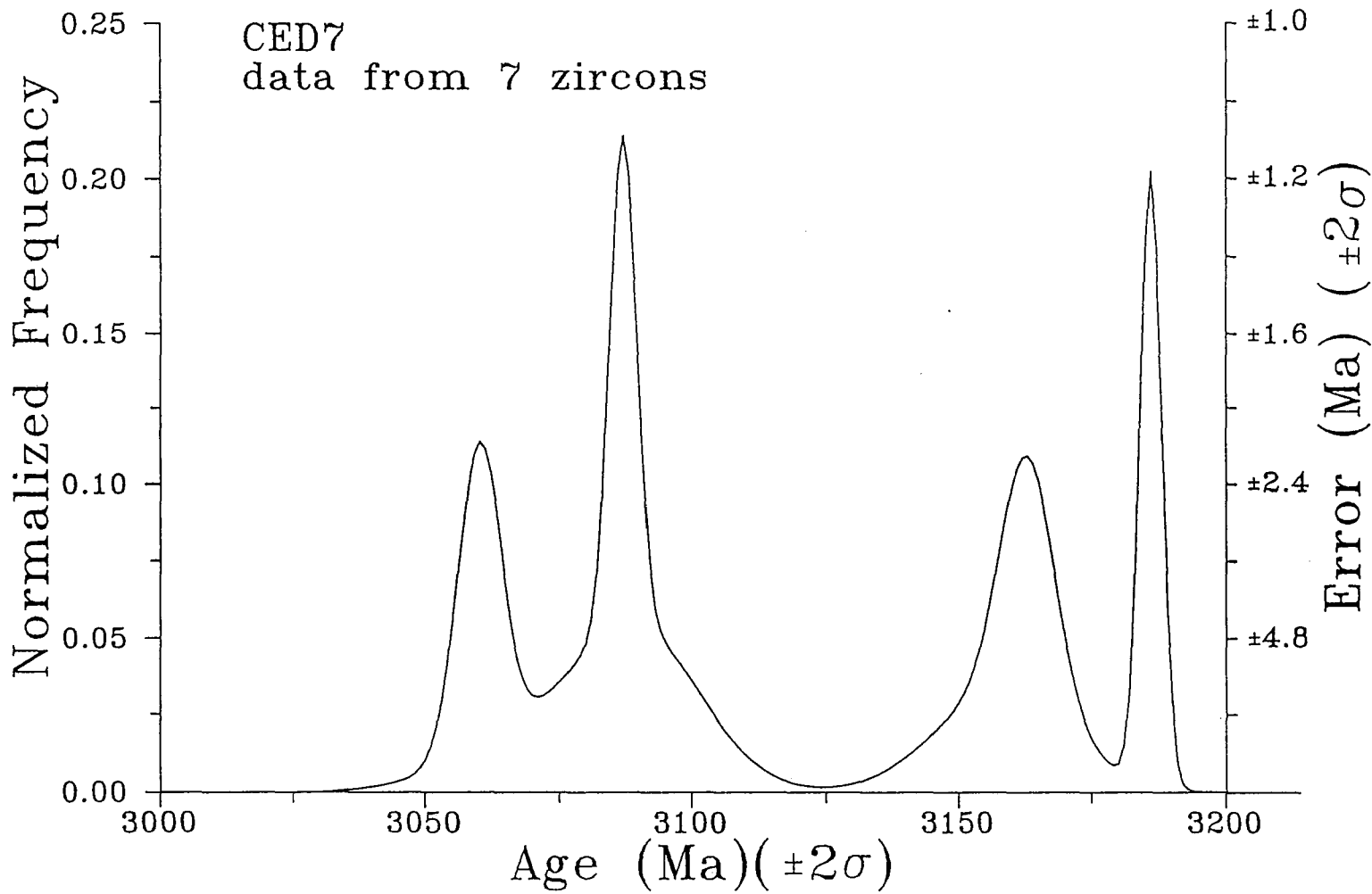
Table 4.10   Raw data from 703.

Name	Runs	207Pb/206Pb	St. Err. (%)	207Pb/204Pb	St. Err. (%)	206Pb/204Pb	204Pb/206Pb	St. Err. (%)
703A2P	2	0.2145285	0.027	136.099	0.495	634.236	0.001577	0.485
	3	0.2136609	0.075	146.460	0.769	685.354	0.001459	0.680
Common Pb for 2800 Ma		1.08810603		14.585		13.404	0.074605	
703A4P	1	0.2331621	0.649	100.619	5.816	427.936	0.002337	6.526
	2	0.2232052	0.081	161.041	0.741	720.721	0.001388	0.763
	3	0.2226754	0.028	169.877	0.439	763.475	0.001310	0.405
	4	0.2237702	0.174				0.001294	1.017
	6	0.2217185	0.098				0.000749	1.171
Common Pb for 2890 Ma		1.09770333		14.482		13.193	0.075796	
703A6P	1	0.2290786	0.090	117.448	0.722	512.479	0.001951	0.706
	2	0.2289379	0.249	139.299	6.559	614.893	0.001626	5.783
Common Pb for 2890 Ma		1.09770333		14.482		13.193	0.075796	
703A7P	1			138.141	0.935	628.141		1.394
	2	0.2195196	0.032	157.488	0.852	716.897	0.001395	0.877
	3	0.2189229	0.024	167.572	0.283	765.462	0.001306	0.262
	4	0.2188509	0.027	169.515	0.451	774.413	0.001291	0.415
	5	0.2192918	0.025	169.880	0.350	774.833	0.001291	0.327
	6	0.2198287	0.016	169.190	0.232	770.119	0.001299	0.141
	7	0.2200145	0.073	168.064	0.340	764.175	0.001309	0.336
	8	0.2214118	0.088	175.790	1.982	793.147	0.001261	1.952
Common Pb for 2870 Ma		1.09561934		14.506		13.240	0.075529	
703B2P	1	0.2375865	0.182	93.327	0.252	392.696	0.002547	0.219
	2	0.2360779	0.141	107.578	2.980	453.556	0.002205	2.949
	3	0.2383819	0.392				0.002391	4.593
Common Pb for 2900 Ma		1.09879262		14.470		13.169	0.075936	

Figure 4.17 York fit of ^{206}Pb/^{204}Pb vs. ^{207}Pb/^{204}Pb data from 703.

Legend:
- ○ 703A2P — 2801± 5 Ma (2σ)
- □ 703A4P — 2891±19 Ma (2σ)
- △ 703A6P — 2890±35 Ma (2σ)
- ◇ 703A7P — 2866±10 Ma (2σ)
- ☆ 703B2P — 2911±31 Ma (2σ)
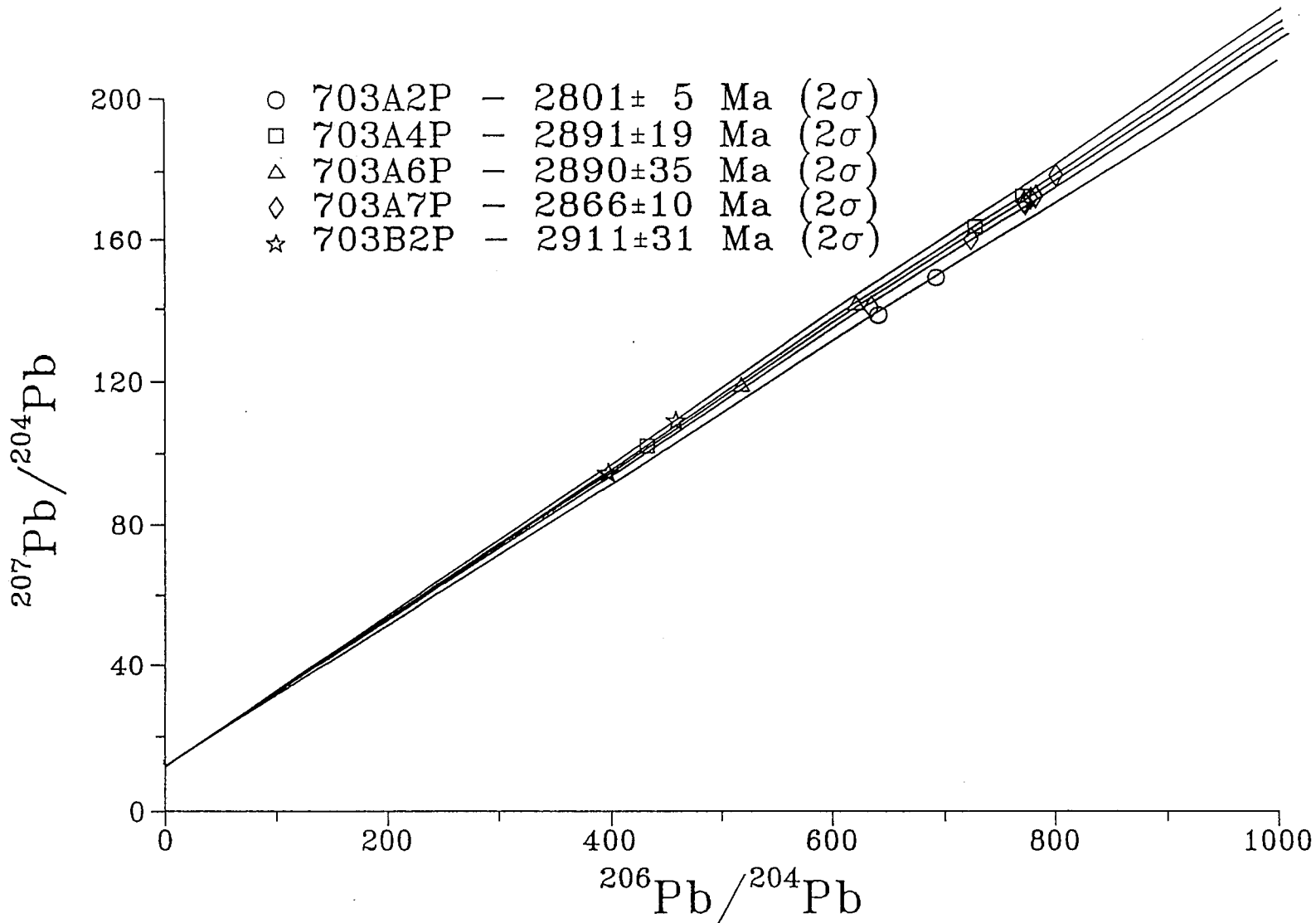
X-axis: $^{206}Pb/^{204}Pb$

Y-axis: $^{207}Pb/^{204}Pb$

138

Figure 4.18 York fit of ^{204}Pb/^{206}Pb vs. ^{207}Pb/^{206}Pb data from 703.
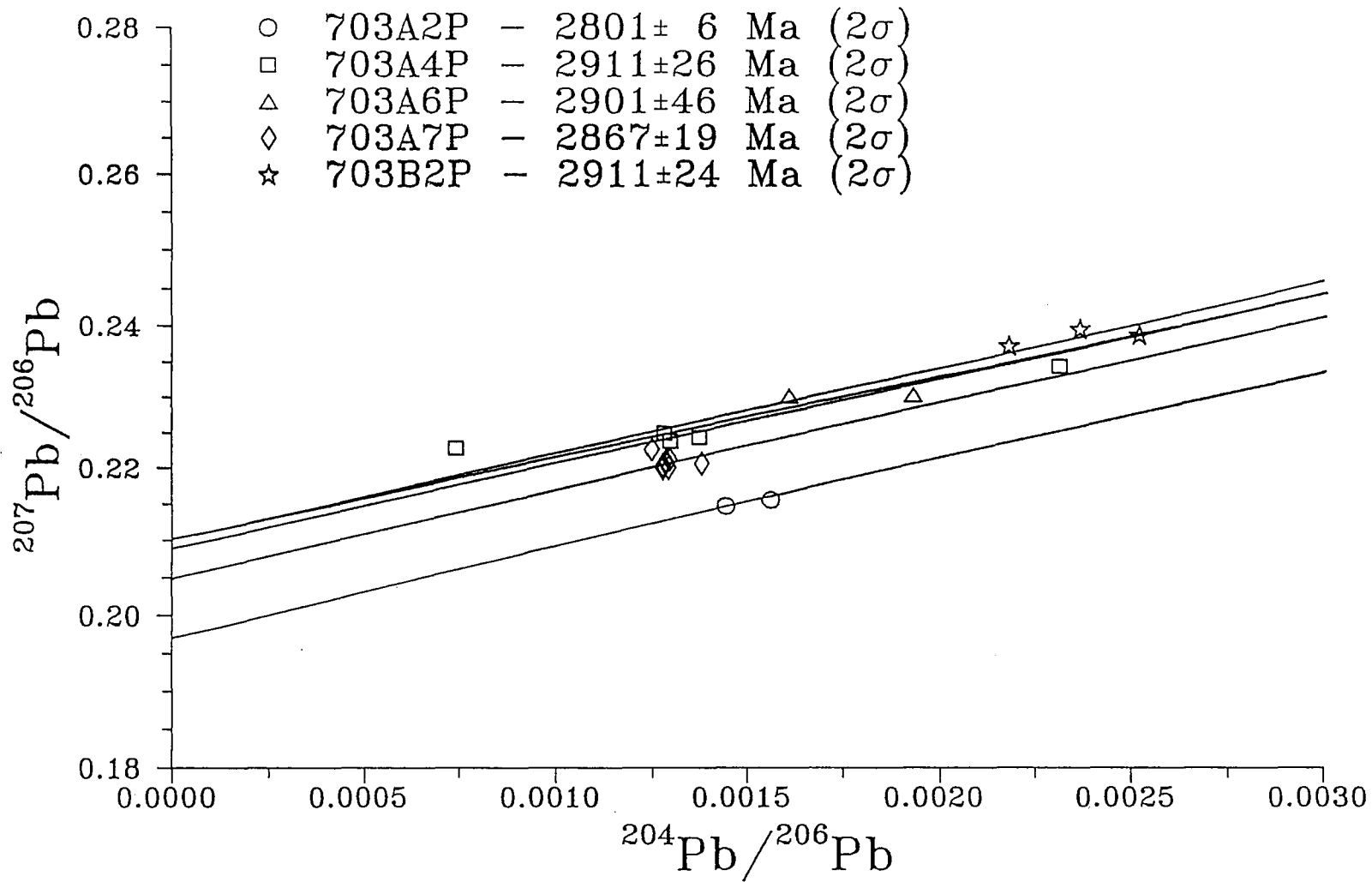
Figure 4.19   Age histogram of 703.
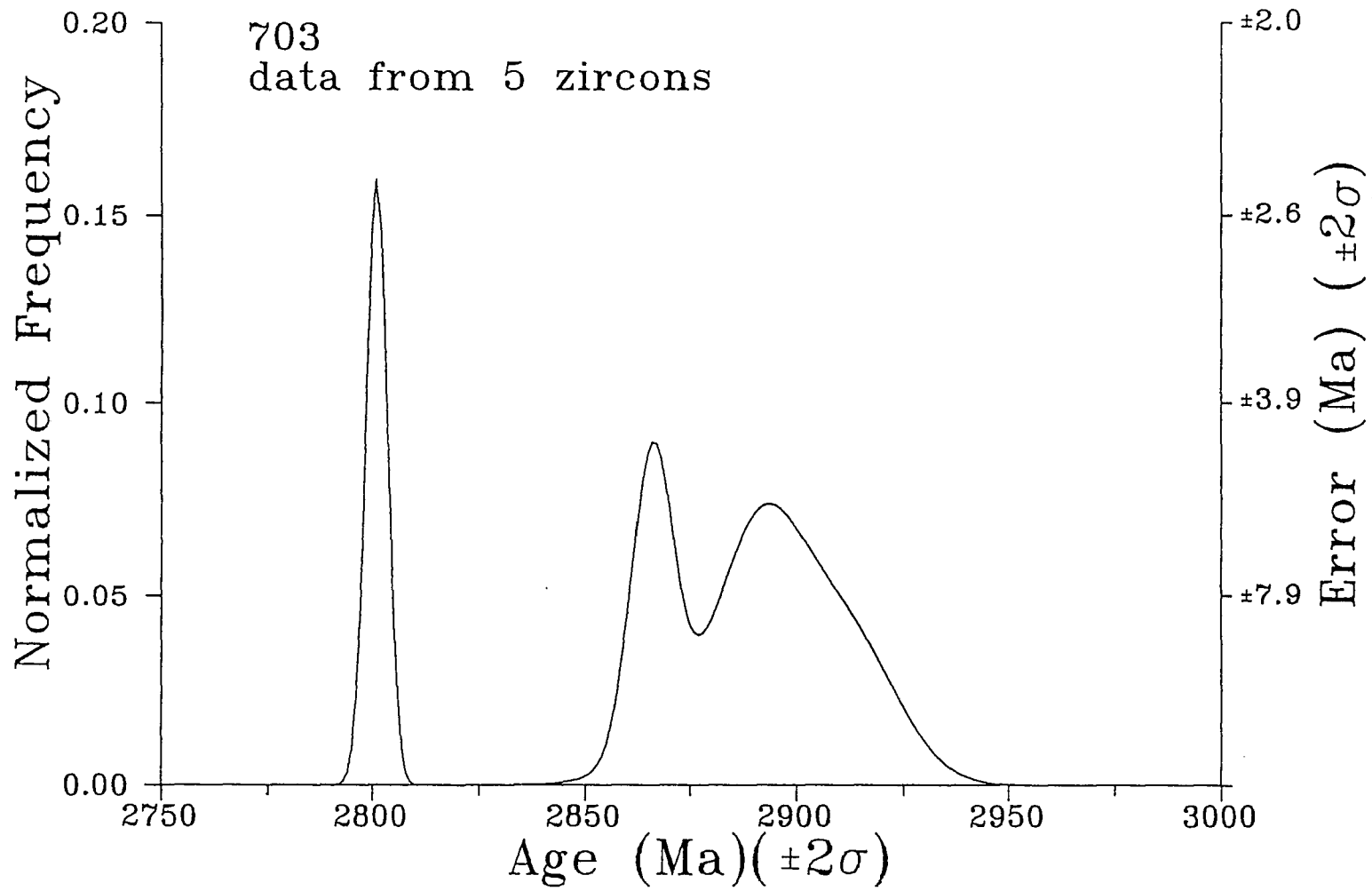
4.2.4 Conclusions

The results from the Cedar Lake gneiss samples (605,CED1,
CED6, and CED7) appear confusing due to the different range in
ages of each sample when examined separately. However, since
they are from the same tonalite, but different locations, the
data may be combined.

One method by which to examine the results is a
sequential order diagram (Figure 4.20) (Compston and Kröner,
1988). The zircons from one site, i.e. 605, are arranged in
order of increasing age. Thus, the youngest zircons is
designated #1, the next older zircon is #2, and so on. The
order is plotted versus the age. The horizontal bar through
each point represents the error in age of each zircon.

The purpose of this diagram is to visually group the
zircons. A stack of zircons of the same age can represent an
event such as a time of metamorphism or crystallization. If
many zircons, especially if they are from different sites,
have the same age then it is likely it is due to an event
rather than a result of mixing.

If the ages from one site spread over a range, i.e. a
sloped series of points, this is probably due to a mixing
between events. The upper and lower extrema are possible ages
for crystallization and metamorphic events.

Most sites have zircons that varied over a narrow range
of ages. The major exception is 605. The many and varied

141

Figure 4.20 Sequential order diagram for data from all four sites from the Cedar Lake tonalite. Horizontal bars indicate 2σ error in age.
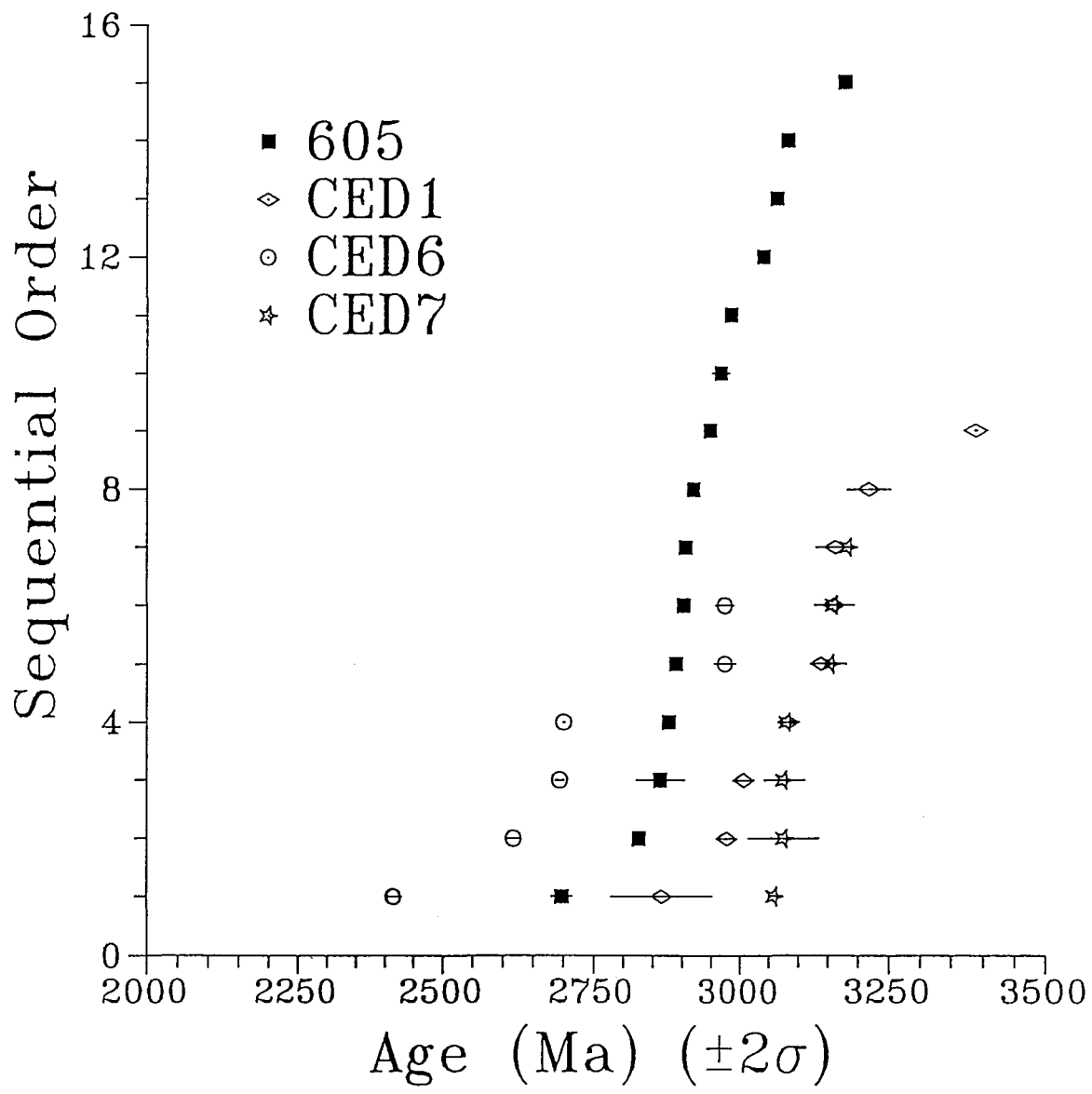
ages of this site makes it the key to the interpretation of the history of the Cedar Lake gneiss. From Figure 4.20 it can be seen that 605 represents a continuum of ages from 3190 Ma to 2700 Ma. The ages inbetween are the result of varying amounts of mixing between these two sources (3170 and 2700 Ma) with no major gaps in age between them.

The upper age (3183±2) corresponds well with the age of crystallization derived by Corfu (1988) (3170+20/-5 Ma) for the Cedar Lake gneiss. The zircon evaporation age in this study can more tightly constrain the age derived by Corfu (1988) from 3170+20/-5 Ma to 3183±2 Ma. The lower age of 2698±17 Ma corresponds with the time of Kenoran amphibolite metamorphism and the emplacement of the Lount Lake batholith (Beakhouse, 1983) which surrounds the tonalitic gneiss. The range in ages also reflect the highly metamorphosed field appearance of the 605 site (Dickin, pers. comm.). A review of the photographs and their derived ages show no major difference in age between the population of larger crystals used early in this study and the smaller, lighter coloured crystals used later. The long prismatic crystals (Plate 4.2 A,B,C,D, and E) gave a range of ages. The youngest age was derived from a crystal whose shape is blocky (l:w=1:1) (Plate 4.2 F).

The data from 605 can also be plotted on a pseudo-concordia diagram (Figure 4.21). A discordia intersects the concordia at 3170 and 2700 Ma. All samples from 605 are

143

Figure 4.21   Pseudo-concordia of data from 605.   Apparent $^{207}Pb/^{206}Pb$ ages are shown as varuing lines intersecting the concordia.   Dashed line between 2700 Ma and 3170 Ma represents the discordia (as derived by Corfu, 1988).

Cedar Lake - 605
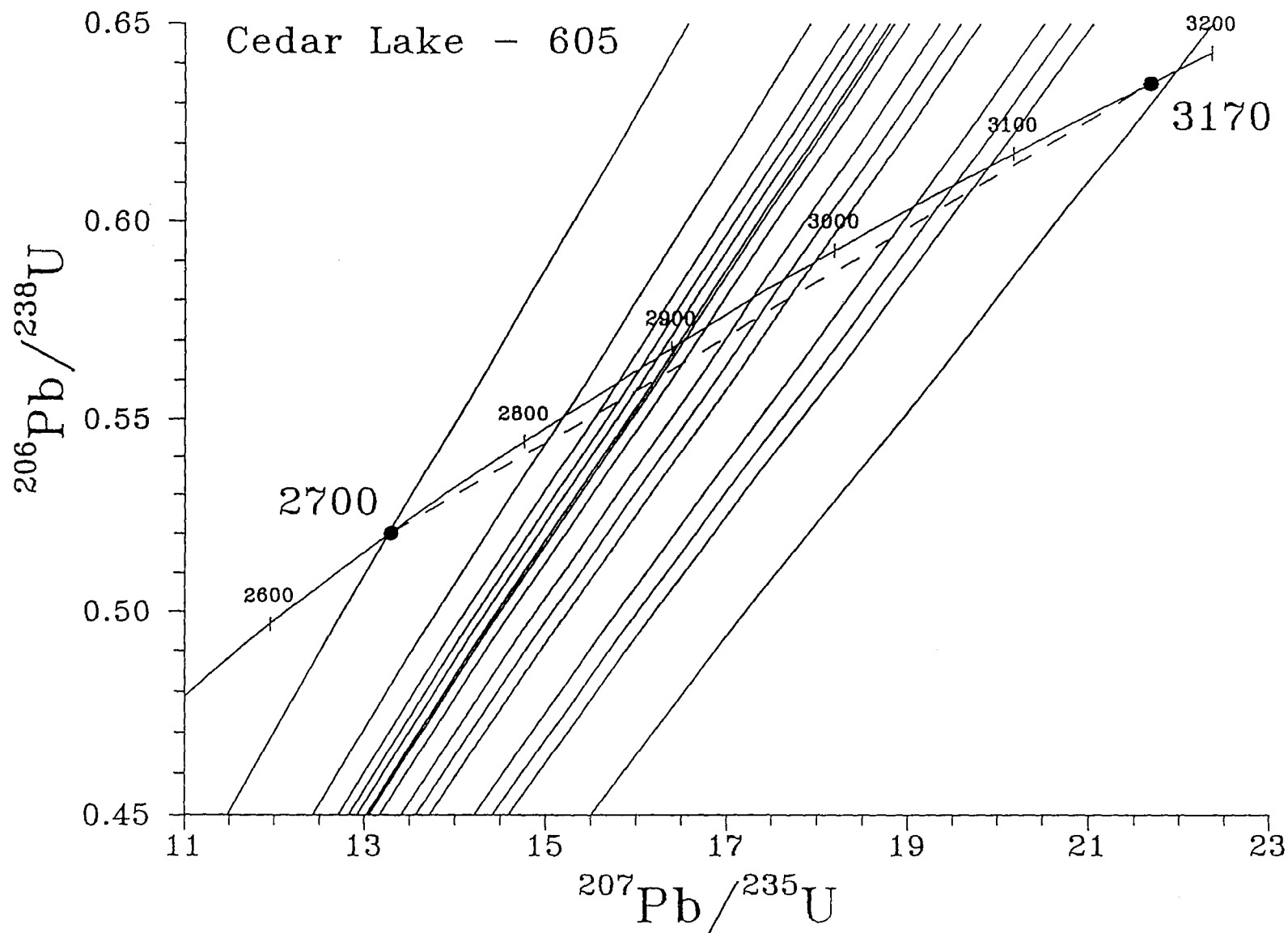
bounded (within error) by the discordia with most zircons tending to be 50%-50% mixes from both sources.

The younger 605 age (2700 Ma) corresponds (Figure 4.21) with two zircons from CED6. The older age correspond with two zircons from CED1 and one from CED7. Thus, the upper and lower ages are substantiated with data from other sites.

The two unusually low ages of CED6 can be explained by Pb loss. The zircon with the age of 2408±9 Ma is the most anhedral crystal studied (Plate 4.6 D). These ages could also be the result of a low grade metamorphic event which occurred between 2640 and 2520 Ma age (Corfu, 1988). Other zircons from CED6 (at ≈2950 Ma) are probably the result of a mix between 2700 Ma and 3186 Ma. Thus, from CED6 the upper age of 3170 could not be found due to Pb loss (continual Pb loss or mixing between sources) or the small number of zircons samples from this site.

CED1 and CED7 zircons form a continuum of ages from approx. 2900 Ma to the upper age of 3170 Ma. The lower age of 2700 Ma does not appear. These sites were probably not as strongly affected by Pb loss due to metamorphism as those from 605 and CED6.

CED1 has one zircon whose age is anomalous. CED1B3 results in an age of 3391±2 Ma. The confidence in this age is supported by the long and stable beam it produced. The common Pb was low so the age could be directly derived by the average of ^{207}Pb/^{206}Pb and no common Pb correction was needed. Such old

ages have rarely been reported in the Winnipeg River Belt of the Superior Province (Hinton and Long, 1979, Card, 1990). Hinton and Long (1979) had found 2 zircons (from a suite of 29 zircons) from the Lac Seul gneiss with an age of 3300±100 Ma. The ages were derived from an ion microprobe. The age of the zircon CED1B3 does fall within these age limits. Nonetheless, this zircon (Plate 4.4 F) appears, both in shape, colour, and size, similar to other zircons in CED1. Thus, there are no physical differences that would indicate a separate population. This is probably a xenolithic zircons from a remnant of older crust. Supracrustal remnants in the Cedar Lake gneiss have been noted in field studies by Westerman (1977) and were presumed to be older than the Cedar Lake tonalite, itself. Since only one zircon was found at this age of 3391±2 Ma, this age should be considered a minimum age.

The data from all four sites within the Cedar Lake gneiss have been combined in an age histogram diagram (Figure 4.22). The zircons with small errors appear prominently. They form a continuum between 2698 and 3183 Ma with one zircon at 3391 Ma. The gap between the zircon at 3183 and 3391 is empty, i.e. no zircons have ages which fall within this range. This is probably due to the presence of two separate populations since there is no mix between them.

Nd model ages fo the four sites from the Cedar Lake gneiss imply that it was derived from a very old crustal component. All Nd model ages are older than the zircons found

146

Figure 4.22 Combined age histogram for all four sites from
Cedar Lake tonalite.
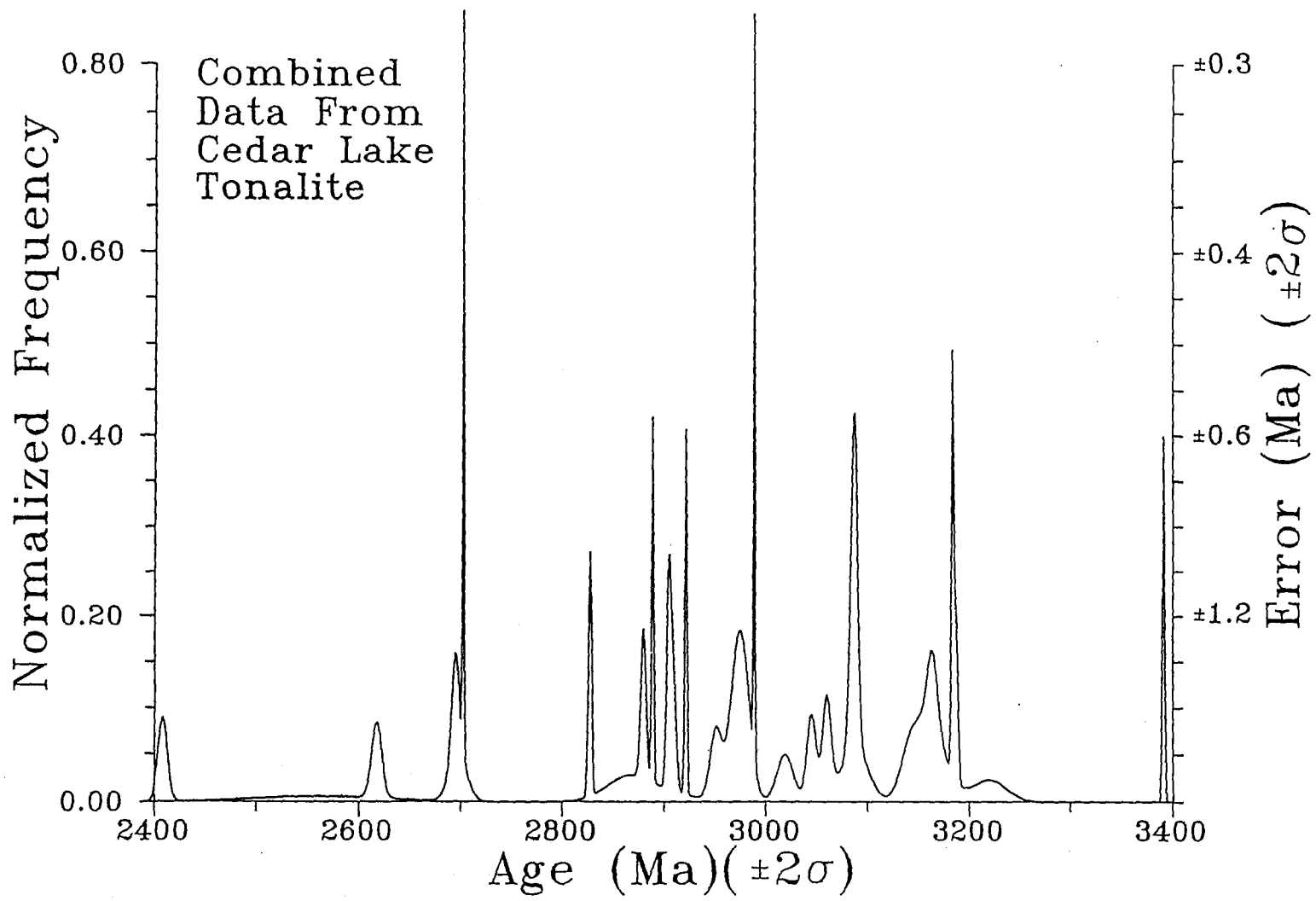
within them. Thus, other sites in the Cedar Lake gneiss may contain xenolithic zircons as well.

The zircons from the Lac Seul gneiss (703) varied from 2801±5 to 2911±24 Ma (Figure 4.19). This results in a minimum age of the gneiss to be 2911 Ma. Other reported ages in this area are older (3040±40 Ma, Krogh *et al.*, 1976). Thus, the ages found in this study are probably a mix between the Kenoran metamorphism and this older age. Another possibility is that these ages reflect the 2.9 Ga metamorphic event described by Hinton and Long (1979) from studies of cores in the Lac Seul gneiss. The polymetamorphic history of this gneiss makes it difficult to state with certainty to which event these zircons are associated.

Thus, the zircon evaporation technique has distinguished that the bulk of the Cedar Lake gneiss was crystallized at least 3183±2 Ma ago and affected by metamorphism at 2700 Ma. Also, the tonalite contains xenolithic zircons from an older crust source which is believed to be at least 3391 Ma.

The mix of ages between the age of crystallization and the age of metamorphism allows for a test of an assumption made by many authors (Kober, 1986, Kober, 1987, and Compston and Kröner, 1988) who use the zircon evaporation technique. The assumption is that step heating of the zircon crystal allows for age determination of various growth stages in the same zircon. For most cases in this study there was only one temperature at which the zircon was evaporated. However, in

one case of a zircon from sample 605 from the Cedar Lake gneiss, a repeated evaporation at 4.5 and 4.8 Amps was achieved. The resultant ages were identical within error. Many zircons from 605 were studied and evaporated at different temperatures and resulted in ages varying from 2698±17 Ma and 3183±2 Ma. No correlation was seen between the resultant age and evaporation temperature (Figure 4.23). The oldest zircon was actually derived from the lowest evaporation temperature. SEM photographs taken by O'Hanley *et al.* (1991) show that Si (and Pb) is released from the rim of the zircon first and then gradually, towards its centre. This evidence would dismiss this assumption made by Kober (1986). Therefore, it must be assumed that the Pb from the zircon is released all at once and is mixed upon the ionization filament. The interpretation of multiple events within one zircon must be looked upon with some scepticism.

Figure 4.23 Apparent ages from 605 as derived from different evaporation ages.
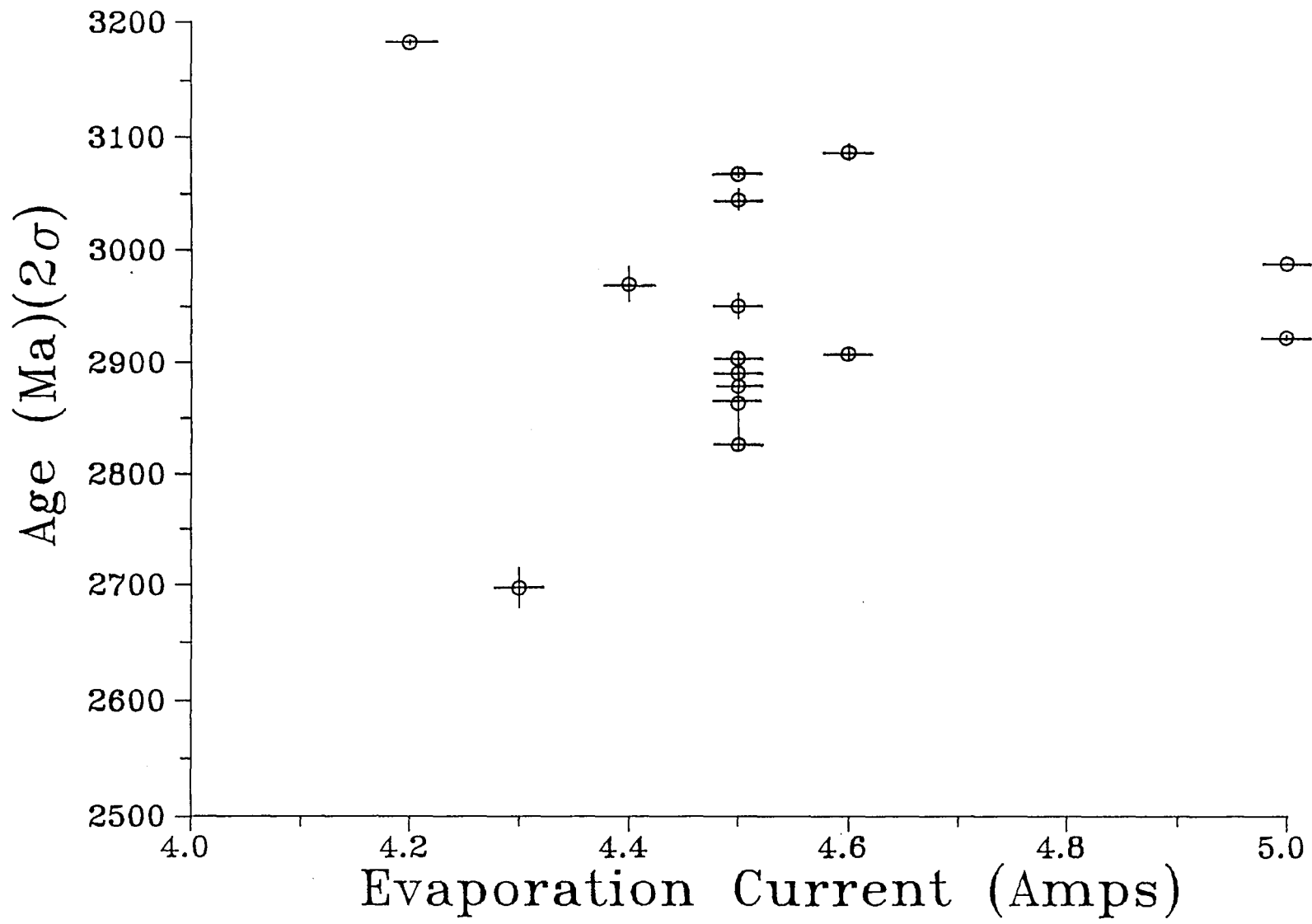
Chapter 5

Conclusion

The aim of this study was to determine whether the zircon evaporation technique of Kober (1986, 1987) is a valid method of age determination in a variety of geological situations. Rock types varied from granites, orthogneisses, paragneisses, and orthoquartzites. The grade of metamorphism is all samples tended to be high (amphibolite facies). The zircons, themselves, varied in character from magmatic crystals (Battersea Pluton) to multi-growth metamorphic crystals (Cedar Lake and Lac Seul samples).

The age of the magmatic zircons from the Battersea granite is consistent with ages determined by conventional U-Pb dating (Marcantonio, 1989). This positive result lent confidence to this method.

From the Britt Domain, PE10.2, a granitoid pluton, was found to be cogenetic with that of the Britt Pluton (PSK0.6). The age of the Pine Cove Pluton (min. age = 1331±15 Ma) constrains the time of last movement of the French River suture line. A sample of the quartzofeldspathic gneiss, PE11.3, surrounding the plutons gives expected Grenvillian ages. A nearby orthoquarzite, CBQ, contains small rounded detrital zircons. Provenance is determined to be from two distinct terrains, Archean (2.7 Ga) and Proterozoic (1.9 Ga)

in age. This result agrees with work by Dickin and McNutt (1989). Their Sm-Nd study of the French River area in the Britt Domain proposes evidence for a 1.9 Ga accreted terrain.

Zircons from the Cedar Lake and Lac Seul tonalitic gneiss from the Winnipeg River Belt in the Superior Province were studied to determine how well the evaporation method would work with metamorphic zircons. Would the results be completely overprinted by the metamorphic event due to a high degree of discordance? The resultant ages span between the last major metamorphic event, the Kenoran orogeny at 2700 Ma, to the age of crystallization at 3170 Ma. This upper limit agrees with U-Pb results by Corfu *et al.* (1988). The spread of ages is due to various amounts of mixing between younger metamorphic rims and older cores. These rims and cores are not obvious in thin section of these zircons.

One zircon from the Cedar Lake tonalite results an age of 3391±2 Ma. This may be a xenocryst from older crust mixed into the tonalite. Supracrustal remanents of older crust is recognized in field studies of this area (Westerman, 1977) and by Nd model ages (Dickin, unpublished data).

Previous work using the zircon evaporation method (Kober, 1986, Kober, 1987, Compston and Kröner, 1987, Kröner and Todt, 1988, and Ansdell, 1991 pers. comm.) has manipulated the raw data differently than in this study. Some of these authors accepted only data that has no measurable common Pb, i.e. $^{206}Pb/^{204}Pb \geq 40,000$. Their age results are solely based upon

the average of ^{207}Pb/^{206}Pb ratios. Many zircons in this study contain inclusions so that no pristine samples could be chosen. These zircons contain measurable amounts of common Pb, but their data was usable by plotting it upon standard ^{206}Pb/^{204}Pb vs. ^{207}Pb/^{204}Pb isochron diagram or a ^{204}Pb/^{206}Pb vs. ^{207}Pb/^{206}Pb diagram. A York fit linear regression (York, 1969) is preformed on the data and the resultant slope and intercept, respectively, is used to determine the age. Therefore, the data from zircons with or without common Pb is usable.

The zircon evaporation technique is ideal for reconnaissance work due to the ease of sample preparation and the large number of zircons that can be tested quickly. Thus, it is ideal for detrital zircons, especially if their source terrains are widely spaced in time, i.e. 100 Ma. If the sources differ little in age, i.e. 10 Ma, then errors in age and small amounts of Pb loss in the zircons will blur the distinction between the sources.

Another advantage of the evaporation method is that its ease of use allows more zircons to be tested than is usually conducted in a U-Pb zircon analysis. The greater amount of sampling increases the chances of finding anomalously aged zircons as in the case of the 3.4 Ga zircon from CED1.

All zircons in this study were exposed to amphibolite grade metamorphism. In many cases, i.e. the Battersea Pluton, this resulted in little or no noticeable Pb loss. Presumably,

this method would be even more reliable for zircons that had undergone a lesser degree of metamorphism.

The main disadvantage is the lack of accuracy, especially for metamorphic zircons, inherent in this method. Since the amount of discordance is not directly measurable, the resultant ages will represent a minimum age. The ages should perhaps be known as "Pb model ages", analogous to Nd model ages, since they are a mix between a crystallization age and a metamorphic age (or a fictious age due to continual Pb loss). This inaccuracy due to discordance can be overcome by sampling a wide variety of zircons from the same rock. Each zircon will have varying degrees of Pb loss or Pb mixing. The extrema of oldest and youngest ages have been shown to be successful in determining the age of crystallization and age of metamorphism. A change in zircon preparation, i.e. air abrasion, could help in determining the age of only the cores. Such a reduction is sample size would create a problem in loading the zircons in the filament and the smaller amount of Pb will be more difficult to measure.

References

Barovich, K. M., Patchett, P. J., Peterman, Z. E., and Sims, P. K. (1989) Nd isotopes and the origin of 1.9-1.7 Ga Penokean continental crust of the Lake Superior region. Geol. Soc. Amer. Bull., 101, 333-338.

Beakhouse, G. P. (1977) A subdivision of the western English River Subprovince. Can. J. Earth Sci., 14, 1481-1489.

Beakhouse, G. P. (1983) Geological, geochemical and Rb-Sr and U-Pb zircon geochronological investigations of granitoid rocks from the Winnipeg River belt, northwestern Ontario and southeastern Manitoba. Ph. D. Thesis, McMaster Univ., Hamilton, Ont., 376 p.

Beakhouse, G. P. (1985) The relationships of supracrustal sequences to a basement complex in the western English River Subprovince in: Evolution of Archean Supracrustal sequences, ed. Ayres, L. D., Thurston, P. C., Card, K. D., and Weber, W. Geol. Assoc. Can. Special paper 28, 169-178.

Blatt, H., Middleton, G., and Murray, R. (1980) Origin of sedimentary rocks, second edition. Prentice-Hall Inc, 782 p.

Box, G. E. P., Hunter, W. G., and Hunter, J. S. (1978) Statistics for experimenters: an introduction to design, data analysis, and model building. Wiley, 635 p.

Card, K. D. (1990) A review of the Superior Province of the Canadian Shield, a product of Archean accretion. Precam. Res., 48, 99-156.

Chukhonin, A. P. (1979) A mass-spectrometric study of the forms taken by lead in zircon. Geochem. Internat., 15, 186-189.

Compston, W. and Kröner, A. (1988) Multiple zircon growth within early Archaean tonalitic gneiss from the Ancient Gneiss Complex, Swaziland. Earth Planet. Sci. Lett., 87, 13-28.

Condie, K. C. (1989) Plate tectonics & Crustal Evolution, third edition. Pergamon Press, 476 p.

Corfu, F. (1988) Differential response of U-Pb systems in coexisting accessory mineral, Winnipeg River Subprovince, Canadian Shield: implications for Archean crustal growth and stabilization. Contrib. Mineral Petrol., 98, 312-325.

Davidson, A. (1986) New interpretations in the southwestern Grenville Province. in: The Grenville Province, eds. Moore, J. M., Davidson, A. and Baer, A. J., Geol. Assoc. Can. Special paper 31, 61-74.

Davidson, A. and Bethune, K. M. (1988) Geology of the north shore of Georgian Bay, Grenville Province of Ontario. Current Res., Part C, Geological Survey of Canada, Paper 88-1C, 135-144.

Davidson, A., Culshaw, N. G., and Nadeau, L. (1982) A tectono-metamorphic framework for part of the Grenville Province, Parry Sound, Ontario. Current Res., Part A, Geological Survey of Canada, Paper 82-1A, 175-190.

Davidson, A. and Morgan, W. C. (1980) Preliminary notes on the geology east of Georgian Bay, Grenville Structural Province, Ontario. Current Res., Part A, Geological Survey of Canada, Paper 81-1A, 291-298.

Dickin, A. P. and McNutt, R. H. (1989) Nd model age mapping of the SE margin of the Archean Foreland in the Grenville Province of Ontario. Geology, 17, 299-302.

Dickin, A. P., McNutt, R. H., and Clifford, P. M. (1990) A neodymium isotope study of plutons near the Grenville Front in Ontario, Canada. Chem. Geol., 83, 315-324.

Douglas, R. J. W. and Price, A. (1979) Nature and significance of variations in tectonic styles in Canada in: Variations in tectonic styles in Canada, eds. Price R. A. and Douglas, R. J. W. Geol. Assoc. Can. Special paper 11, 625-688.

Fairbairn, H. W., Hurley, P. M., Card, K. D., and Knight, C. J. (1969) Correlation of radiometric ages of Nipissing Diaabase and Huronian metasediments with Proterozoic orogenic events in Ontario. Can. J. Earth Sci., 6, 489-497.

Gentry, R. V. (1984) Lead retention in zircons. Science, 223, 835.

Goodwin, A. M., Ambrose, J. W., Ayres, L. D., Clifford, P. M., Currie, K. L., Ermanovics, I. M., Fahrig, W. F., Gibb, R. A., Hall, D. H., Innes, M. J. S., Irving, T. N., MacLaren, A. S., and Pettijohn, F. J. (1979) The Superior Province in: Variations in tectonic styles in Canada, eds. Price R. A. and Douglas, R. J. W. Geol. Assoc. Can. Special paper 11, 527-623.

Hinton, R. W. and Long, J. V. P. (1979) High-resolution ion-microprobe measurement of lead isotopes: variations within single zircons from Lac Seul, northwestern Ontario. Earth Planet. Sci. Lett., 45, 309-325.

Kober, B. (1986) Whole-grain evaporation for $^{207}Pb/^{206}Pb$-age-investigations on single zircons using a double-filament thermal ion source. Contrib. Mineral Petrol., 93, 482-490.

Kober, B. (1987) Single-zircon evaporation combined with Pb^{+} emitter bedding for $^{207}Pb/^{206}Pb$-age investigations using thermal ion mass spectrometry, and implications to zirconology. Contrib. Mineral Petrol., 96, 63-71.

Kober, B., Pidgeon, R. T., and Lippolt, H. J. (1989) Single-zircon dating by stepwise Pb-evaporation constrains the Archean history of detrital zircons from the Jack Hills, Western Australia. Earth Planet. Sci. Lett., 91, 286-296.

Krogh, T. E. (1982) Improved accuracy of U-Pb zircon dating by selection of more concordant fractions using a high gradient magnetic separation technique. Geochim. et Cosmochim. Acta, 46, 631-635.

Krogh, T. E., Harris, N. B. W., and Davis, G. L. (1976) Archean rocks form the Lac Seul region of the English River Gneiss Belt, northwestern Ontario, Part 2. Geochronology. Can. J. Earth Sci., 13, 1212-1215.

Kröner, A. (1990) Single zircon evaporation as a tool in understanding early Archaean crustal evolution: the Barberton-Swaziland terrain. Seventh Inter. Conf. on Geochron., Cosmochron. and Isotope Geol., Geol. Soc. of Australia, 27, 44.

Kröner, A., Compston, W., and Williams, I. S. (1989) Growth of early Archaean crust in the ancient gneiss complex of Swaziland as revealed by single zircon dating. Tectonophys., 161, 271-298.

Li, W.-X., Lundberg, J., Dickin, A. P., Ford, D. C., Schwarcz, H. P., McNutt, R. H., and Williams, D. (1989) High precision mass-spectrometric uranium-series dating of cave deposits and implications for paleoclimate studies. Nature, 339, 534-536.

Lumbers, S. B. (1975) Geology of the Burwash area, districts of Nipissing, Parry Sound and Sudbury. Ontario Division of Mines Geological Report 116, 160 p.

Marcantonio, F. (1989) Isotopic studies of plutonic and metamorphic rocks from the Frontenac Arch, Grenville Province of Ontario and from Islay, in the southern Inner Hebrides of Scotland. M. Sc. Thesis, McMaster Univ., Hamilton, Ont., 97 p.

Marcantonio, F., McNutt, R. H., Dickin, A. P., and Heaman, L. M. (1990) Isotopic evidence for the crustal evolution of the Frontenac Arch in the Grenville Province of Ontario, Canada. Chem. Geol., 83, 297-314.

O'Hanley, D. S. (1991) The age of the auriferous granites and mesothermal gold mineralization, Goldfields area, Saskatchewan in: Program with abstracts. Geol. Assoc. Can., 16, A92.

Parrish, R. and Roddick, J. C. (1985) Geochronology and isotope geology for the geologist and explorationist. Geol. Assoc. Can.(Cordilleran Section) Short Course #4.

Parrish, R. (1990) Guidelines for 1990-1991 special awards for Abitibi-Grenville geochronology. memo from Geol. Survey of Canada, geochronology section, 1-5.

Poldervaart, A. (1955) Zircons in rocks. 1. Sedimentary rocks. Amer. J. Sci., 253, 433-461.

Roscoe, S. M. (1973) The Huronian Supergroup, a paleoaphebian sucession showing evidence of atmospheric evolution in: Huronian stratigraphy and sedimentation, ed. Young, G. M., Geol Assoc. Can. Special Paper 12, 31-47.

Roubault, M., Coppens, R., and Kosztolanyi, Ch. (1967) Determination de l'age individuel des zircons des roches granitiques par la mesure du rapport $^{207}Pb/^{206}Pb$. in: Radioactive Dating and Methods of Low-Level Counting, Int. Atomic Energy Agency, 359-370.

Stacey, J. S. and Kramers, J. D. (1975) Approximation of terrestrial lead isotope evolution by a two-stage model. Earth Planet. Sci. Lett., 26, 207-221.

Van Breemen, O., Davidson, A., Loveridge, W. D., and
Sullivan, R. W. (1986)   U-Pb zircon geochronology of
        Grenville tectonics, granulites and igneous precursors,
        Parry Sound, Ontario. in: The Grenville Province,
        eds. Moore, J. M., Davidson, A. and Baer, A. J., Geol.
        Assoc. Can. Special Paper 31, 191-207.

Westerman, C. J. (1977) Tectonic evolution of a part of the
        English River Subprovince, northwestern Ontario. Ph. D.
        Thesis, McMaster Univ., Hamilton, Ont., 292 p.

Wynne-Edwards, H. R. (1972) The Grenville Province in:
        Variations in tectonic styles in Canada, eds. Price R.
        A. and Douglas, R. J. W. Geol. Assoc. Can. Special
        Paper 11, 263-334.

York, D. (1969) Least squares fitting of a straight line
        with correlated errors. Earth Planet. Sci. Lett., 5,
        320-324.